

THE UNIVERSITY OF CHICAGO

INTERBANK RUNS: A NETWORK MODEL OF SYSTEMIC LIQUIDITY CRUNCHES

A DISSERTATION SUBMITTED TO
THE FACULTY OF THE DIVISION OF THE SOCIAL SCIENCES
KENNETH C. GRIFFIN DEPARTMENT OF ECONOMICS
AND
THE FACULTY OF THE UNIVERSITY OF CHICAGO
BOOTH SCHOOL OF BUSINESS
IN CANDIDACY FOR THE DEGREE OF
DOCTOR OF PHILOSOPHY

BY
YINAN SU

CHICAGO, ILLINOIS

AUGUST 2018

Copyright © 2018 by Yinan Su

All Rights Reserved

To my parents

有鸟将来，张罗而待之。得鸟者，罗之一目也。今为一目之罗，则无时得鸟矣。

《淮南子》

A net is hung in expectation of the coming birds.

It takes one hole of the net to catch a bird.

But, if one makes a net with only one hole, never a bird can be captured.

– Liu An, king of Huainan, *the Huainanzi* (second century BCE)

TABLE OF CONTENTS

LIST OF FIGURES	vii
ACKNOWLEDGMENTS	viii
ABSTRACT	ix
1 INTRODUCTION	1
2 LITERATURE REVIEW	8
3 MODEL	12
3.1 Big Picture	12
3.2 Timing	12
3.3 Bank Balance Sheet at Time 0	13
3.4 Asset Returns and Liquidation Costs	15
3.5 Depositor Run at Time 1	17
3.6 Bank’s Problem at Time 0	18
3.7 Interbank Lending Equilibrium	22
3.8 Multiple Equilibria and Comparisons with Other Games on Network	24
3.9 Example: Circle Network	27
4 SYSTEMIC BEHAVIOR IN NETWORK GAMES	31
4.1 Mean-Field Approximation	32
4.2 Systemic Equilibrium	34
4.3 A Random Network Model	36
4.4 Definitions of Equilibrium Concepts	41
4.5 Intermediate Results	43
4.6 Equilibrium Asymptotics	45
4.7 Numerical Verification with Observed Networks	49
4.8 Shape of f^* and Number of Equilibria	52
5 APPLICATIONS	59
5.1 Financial Fragility Measure	59
5.2 The Systemic Effects of Local Insolvency Shocks	61
5.3 Optimal Bailout Plans	66
5.4 The Effects of Restraining Too-Interconnected-to-Fail Banks	70
6 CONCLUSION	75
A PROOFS AND ADDITIONAL ALGEBRAIC DETAILS	77
A.1 Verifying the Conditional Expectation of Degrees	77
A.2 Proof of Proposition 1	77
A.3 Proof of Proposition 2	78
A.4 Proof of Lemma 1	78

A.5	Proof of Proposition 3	80
A.6	Proof of Lemma 2	82
A.7	Proof of Proposition 4	82
A.8	Proof of Proposition 5	83
A.9	Proof of Proposition 6	86
A.10	Proof of Proposition 7	89
A.11	Proof of Lemma 3	89
A.12	Proof of Proposition 8	90
A.13	Proof of Proposition 9	91
A.14	Proof of Proposition 10	91
A.15	Proof of Proposition 11	92
A.16	Proof of Proposition 12	92
A.17	Optimized Bank Profit Function	93
B	ADDITIONAL FIGURES	94
	REFERENCES	97

LIST OF FIGURES

1.1	A Graphical Representation of the Systemic Liquidity Equilibrium	4
3.1	Configuration of the Financial System	13
3.2	Bank balance sheet at time 0	14
3.3	Optimal time-0 asset portfolio	20
3.4	Circle Network	27
3.5	Circle Network Equilibria and Comparative Statics	29
4.1	Observed Networks Visualization	50
4.2	Exact and Approximated Equilibrium Comparison	51
4.3	Graphical Representation of $h^*(x)$	55
4.4	An Example Network with Three Equilibria	58
5.1	Comparative Statics: Proportional Connection Contraction	60
5.2	System-wide Stress Testing	63
5.3	W^* Approximation of Stress Testing	65
5.4	f^* after W^* -Preserving In-Degree Contractions	73
B.1	Weighted non-assortative matching in the federal funds market	94
B.2	Numerical Individual Response Function used in Subsection 4.7	94
B.3	Numerical Comparative Statics with respect to β	95
B.4	Degree Distributions of 3Eqm40 in Figure 4.4	95
B.5	Systemic Response Function f^* of 3Eqm40 as in Figure 4.4	96
B.6	μ and equilibrium systemic liquidity in Stress Testing	96

ACKNOWLEDGMENTS

I am extremely grateful to the dissertation committee co-chairs, Professors Lars Peter Hansen and Zhiguo He, as well as the committee members, Professors Douglas Diamond and Bryan Kelly. They are the best advisors I could imagine. They provide invaluable knowledge, guidance, support, and incentive. Meeting their expectations will be my lifelong endeavor. I feel deeply blessed and indebted to study at the University of Chicago for interacting with these and several other great minds.

The dissertation also benefited from the helpful discussion and comments from Moritz Lenel, Robert Shimer, Larry Schmidt, Lin William Cong, Michael Weber, Fernando Alvarez, Itay Goldstein, Alireza Tahbaz-Salehi, Brian Rogers, Vasco Carvalho, Yunzhi Hu, Hyunsoo Doh, Paymon Khorrami, Yiyao Wang, Qi Li and participants at the Economic Dynamics Working Group, the Finance Brownbag, the Capital Theory Working Group, and the Finance Seminar at the University of Chicago. I thank Enghin Atalay, Kamil Yılmaz, Francis Diebold, and Mert Demirer for helping with the interbank network data.

I would like to thank my fellow students, especially Rui Cui, Hanzhe Zhang, Yuan Mei, Xiao Zhang, Cong Zhang, and Yan Xu, for friendship and support during the PhD program.

At the end of the student career, I would like to thank all my teachers, in addition to the ones at Chicago. I am lucky and privileged to receive the best education in both the Chinese and American systems.

Above all, I would like to express my sincere gratitude to my parents, Jun Su and Dan Li, for my pampered life and upbringing, for their unconditional love and care.

ABSTRACT

I study how interbank lending network structures affect financial fragility. Interbank lending is beneficial but subject to coordination failure. With interbank wholesale funding, banks' balance sheets become inflated, which give the retail depositors a sense of safety to allow the bank to have more illiquid investments. In interbank runs, banks run on banks as they mutually reinforce each other to withdraw interbank lending. Banks' individually precautionary liquidity hoarding strategies are connected by the pairwise lending relationships. Mean-field analysis extracts the systemic behavior from the network of strategic interactions. I show such dispersed and indirectly linked interactions also lead to discontinuous and system-wide liquidity crunches as if the interactions are centralized. Local insolvency shocks trigger the interbank run if the network is unraveled beyond a critical point. The model is applied to identify the optimal capital injection targets of government bailouts and study the systemic effects of the proposed regulations on restraining the highly connected banks.

CHAPTER 1

INTRODUCTION

During the 2007-08 financial crisis, a dramatic and system-wide decrease occurred in the funding liquidity of financial institutions (“banks” for short).¹ The defining feature is that *banks run on banks*. The bank-to-bank withdrawal of the wholesale funding is the prominent form of the liquidity crunch. Banks mutually reinforce each other to withdraw interbank lending among themselves – a scenario called an “interbank run” in this paper. In classical bank runs, the retail depositors coordinate with each other to run on a bank. In interbank runs, the strategic interactions are between banks linked by the pre-existing lender-borrower relationships, which form the interbank network. The connections are heterogeneous and not centralized, many banks are only indirectly linked. Yet the liquidity crisis is system-wide. How does the network connect the dispersed interactions into a systemic liquidity crunch? This paper focuses on this problem to study the effects of the network structure on fragility of the financial system.

Many argue the interconnectedness channels the contagion of bank failures and causes systemic risks. If a borrower bank cannot repay a lender bank, the lender bank may default on its lenders. However, banks do not passively follow the domino-style contagion mechanisms. They preemptively adjust interbank lending in expectation of the counterparties’ actions, and this endogenous adjustment depends on the network structure.

The strategic interactions on a complex interconnected structure can lead to sudden and dramatic systemic behavior, such as the interbank run. Understanding how systemic events emerge from the complex interbank network has important policy implications. For instance, at the onset of the 2008 crisis, the Treasury invested \$250 billion to inject liquidity to banks.² But how to determine which institutions are critical to bail out to prevent a

1. In this paper, I use “bank” in the broad sense, including not just depository institutions, but also shadow banks, investment banks, and so on.

2. Under the Capital Purchase Program, the Treasury injected capital to U.S. financial institutions

systemic meltdown, depending on their positions in the network? Moreover, when reckoning the crisis, many policies have been proposed to constrain the interconnectedness of the highly connected banks;³ but will such changes in the network structures reduce financial fragility?

To answer these questions, I build a model of the financial system with interbank lending interactions. Then I conduct a systemic analysis to extract the network-wide interbank run behavior. The model captures the benefits of interbank lending: it allows the financial system to convert retail deposits into illiquid real investments. But the desirable arrangement of mutually extending interbank liquidity is subject to coordination failure, and hence inherently unstable. I show dispersed bank-to-bank interactions aggregate into multiple equilibria of systemic liquidity. The discontinuous transition of systemic liquidity between the equilibria characterizes the interbank run.

The model can be summarized in three steps. First, I model a bank's individual response to interbank funding. On the liabilities side, a bank is funded by deposits and interbank funding. On the assets side, it chooses the portfolio of liquid assets (cash) and illiquid lending (a bundle of real investments and interbank lending). Asset liquidity is characterized by the liquidation value in the potential event of bankruptcy when depositors run: cash has one-to-one liquidation value while illiquid lending is less than one-to-one. *Liquidity hoarding* is the key features in a bank's individual strategy of choosing illiquid lending given the amount of interbank funding it receives.⁴

Specifically, I assume the deposits are senior to interbank debt, based on depositor-preference laws and unsecured interbank funding. Therefore, as long as assets' total liquidation value covers the amount of deposits, depositors will not panic and run. I also assume

through purchases of preferred stock. The fact that the first batch and most recapitalization targeted "healthy, viable" institutions faced public and political controversies. Details in Subsection 5.3.

3. For example, the proposed Single Counterparty Credit Exposure Limit (SCCL) as part of the Dodd-Frank Act. Details in Subsection 5.4.

4. The bank's individual liquidity management problem is similar to that in Ennis and Keister (2006). The possibility of retail depositor run leads bank to hold a more liquid portfolio, which limits the fund available for the profitable but illiquid investments. The difference here is that acquiring interbank funding can alleviate this constraint.

a bank cannot survive a depositor run. As a result, a bank would like to invest all funding in illiquid lending for the high return, but it has to maintain a certain asset liquidity composition to deter depositor runs. I show that if interbank funding is high, the bank can invest all assets into illiquid lending. In a certain interbank funding region, a bank is liquidity hoarding in response to interbank funding decrease: it has to not only scale down total assets, but also tilt the composition toward cash. That means a reduction of interbank funding leads to an *amplified* reduction of illiquid lending, and deposit funding is “locked up” in the form of cash instead of being invested. Eventually, with low interbank funding, the bank fails in the function of liquidity transformation.

Second, banks’ individual liquidity hoarding strategies are connected by the interbank lending network, giving a network-wide interbank lending game. For tractability, I make the following assumption. When a bank reduces illiquid lending, it reduces from its (interbank and real) borrowers proportionally. In another word, the ratio one bank lends to another per the lender’s total illiquid lending, is fixed. These ratios between all pairs of banks, called connection intensities, make up the exogenous interbank network. The network determines not only the flow of funds, but more importantly, the banks’ strategies. If a bank decreases illiquid lending, its direct borrower banks suffer funding liquidity shrinkages. The borrower bank in turn has incentive to withdrawal interbank lending from its borrowers. An interbank lending equilibrium is formed when every bank optimizes its illiquid lending taking others’ choices as given. The equilibrium is defined with respect to the strategy profile of all banks’ actions.

The equilibrium condition can be intractable if the network structure is complex. In the third step, I conduct a systemic analysis of the overall liquidity behavior in interbank lending equilibrium. The multidimensional equilibrium condition with respect to all banks liquidity level is approximated by a one-dimensional equilibrium condition with respect to a summarization of the overall funding liquidity level — systemic liquidity. The new condition can be understood as a transformed economy (Figure 1.1). In the original economy,

the strategic interactions are pairwise, heterogeneous, and dispersed. It is not obvious to deduce the system-wide equilibrium behavior. In the transformed economy, all banks are directly interacting via the constructed center node representing systemic liquidity. Each bank accesses interbank funding from systemic liquidity according to its total incoming connection intensities (in-degree), and then chooses illiquid lending according to the individual best response. A proportion of the illiquid lending is contributed back to systemic liquidity according to the bank’s total outgoing connection intensities (out-degree). This allows me to write the approximated equilibrium condition by aggregating all banks’ direct interactions with systemic liquidity, which becomes one-dimensional.

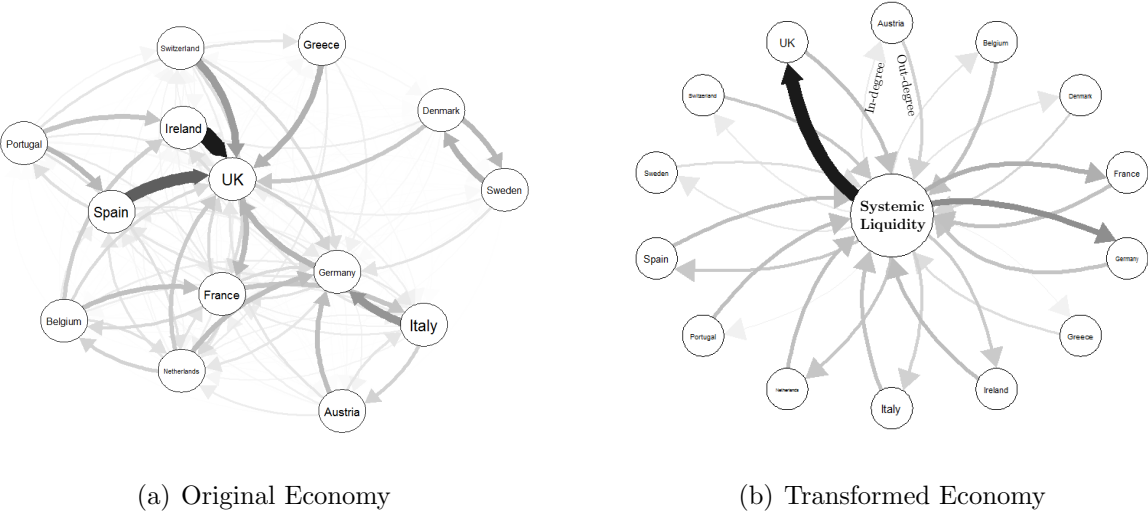


Figure 1.1: A Graphical Representation of the Systemic Liquidity Equilibrium

In (a), the arrows represent the pairwise connection intensities as well as the pairwise strategic interactions. In (b), the outward arrows represent in-degrees, which determine how much each bank accesses interbank funding from systemic liquidity. The inward arrows represent out-degrees, which determines how much each bank’s illiquid lending is contributed back to systemic liquidity. The in-degree (out-degree) of a node in (b) is the sum of the connection intensities flowing into (out of) that node in (a). The width and shade an arrow represents the values of that connection intensity. Details about the numerical construction are reported in Subsection 4.7.

The systemic analysis adopts the idea of mean-field approximation. The rationale is that every bank’s set of direct lenders is a subsample of all banks, and hence has roughly the same composition as the population. Specifically, the average interbank liquidity extended

by the bank's direct lenders is approximately the same as systemic liquidity, a network-wide average. The approximation would hold exactly if the heterogeneity of banks' interbank funding levels only came from the size of their direct lender sets (in-degrees).

I provide a formal justification of the systemic analysis with a random network model. I show that the approximation error of the systemic liquidity equilibrium compared to the original condition converges to zero in probability as the size of the network increases. The property of the random network distribution, the asymptotic analysis, and general applications of the systemic analysis method are discussed in Chapter 4. In addition, numerical exercises using observed interbank networks show the method is practically accurate in small networks.

The systemic analysis captures the main economic mechanism: interbank lending is beneficial, but interbank runs occur as coordination failure. The instability is embodied by the technical result that systemic liquidity has multiple equilibria. Depending on the network structure, an equilibrium with positive systemic liquidity exists. While zero systemic liquidity always constitutes another equilibrium – an autarky in which banks only hold cash.

The key assumption driving the multiplicity result is that interbank debt has lower seniority than deposits. In the positive equilibrium, banks coordinate on extending interbank liquidity. Although the aggregate amount of deposits flowing into the financial system is fixed, borrowing and lending among themselves make every bank's balance sheet bigger. The inflated balance sheet gives the bank's own depositors a "sense of safety", because the depositors know they are more senior than interbank creditors if they demand early withdrawal. The resulting lower propensity of depositor run allows the bank to allocate more funding into illiquid lending, part of which goes to other banks, contributing back to systemic liquidity. The positive equilibrium illustrates how the interbank coordination is efficient, with high illiquid lending comes high real investments at each bank.

To the opposite, the zero systemic liquidity equilibrium captures that interbank runs occur as coordination failure. Since interbank creditors have lower seniority during the

potential bankruptcy liquidation in the future, they might choose to not extend interbank lending *ex ante*.⁵ Importantly, this strategy profile is self-fulfilling. The amplifying effect in each bank's liquidity hoarding behavior can fuel a mutually reinforcing run on systemic liquidity across the network. That is why the dramatic interbank run can be triggered by small perturbations. At the zero equilibrium, without interbank funding, each bank essentially deters its own depositor run by hoarding cash entirely. The financial system fails in the function of transforming deposits into real investments.

Based on the analyses above, I study the systemic financial fragility of the interbank network. Specifically, I examine how exogenous changes in the network structure trigger interbank runs. An interbank run is triggered if network structure changes cause the non-existence of the positive systemic liquidity equilibrium. Around the critical condition where the positive equilibrium is barely sustained, a small change in the network structure can trigger a large system-wide behavior transition. Given a network that supports a positive equilibrium, financial fragility measures how close the interbank run is to being triggered, if the connection intensities decrease.

Local insolvency shocks, modeled as exogenous changes in the network structure, can trigger a systemic interbank run. For example, suppose some banks are found to be exposed to toxic mortgage-backed securities and become insolvent. Before the start of the global interbank lending game, other banks respond to the insolvency shock by cutting lending connections to the insolvent banks. In this counterfactual scenario, the shock changes the network structure as the shocked banks are removed. In approximation, a one-dimensional summary statistic of the networks called *effective connectedness* determines whether the positive systemic liquidity equilibrium exists (and the level of it if exists). Effective connectedness is increasing in the average degree, as well as the correlation of the in- and out-degree. Accumulating local insolvency shocks unravel the network, decreasing effective connectedness.

5. He and Xiong (2012) models the similar incentive of creditors to not roll over debt upfront in order to avoid being attacked by more senior creditors in potential future distresses.

For modest reductions in effective connectedness, the positive equilibrium decreases. If the reduction is beyond a cutoff level, which measures financial fragility, the positive equilibrium disappears, an interbank run is triggered.

I apply my model to address two policy questions regarding the connection of financial networks and fragility. At the onset of the crisis, governments injected capital into financial institutions to prevent systemic failure. Which banks in the network are crucial to bailout, given the limited budget of the injection plan? I find the banks that are constrained in liquidity in the status-quo equilibrium are not necessarily the top-priority targets. Banks that would be in the liquidity hoarding region if the network unravels to the critical condition, so that the financial system is on the brink of runs, are more effective targets. This results justifies the capital injection plan targeted the “healthy and viable” banks rather than the banks that are already liquidity constrained.

When reckoning the crisis, some policies have been proposed to address the “too-interconnected-to-fail” problem, especially in limiting the connectedness of highly connected banks. Will such a change of the network structures reduce financial fragility? I treat the change as a contraction of the distribution of funding connections (in-degrees), keeping the average connection level fixed. The implication is twofold. First, if in-degree and out-degree are uncorrelated, it decreases financial fragility. However, when in-degree and out-degree are positively correlated, which is arguably the reality, a countervailing force is present. Since the well funded banks also take up a greater share in the contribution to systemic liquidity, putting a constraint on them might outweigh giving support to the poorly funded banks.

CHAPTER 2

LITERATURE REVIEW

This paper analyzes the interbank run on network by combining the insights of the liquidity crises literature and the financial networks literature.

In the liquidity crises literature, the seminal paper by Diamond and Dybvig (1983) models retail depositors' run on a bank. The depositors display strategic complementarity among themselves to preemptively demand early withdrawal from a banks. The similar idea is subsequently applied to settings of creditors running on non-bank financial institutions (He and Xiong, 2012), investors running on currencies (Morris and Shin, 1998), investors running on a financial market (Bernardo and Welch, 2004), financial institutions running on the real-sector (Bebchuk and Goldstein, 2011). My paper's focus is banks running on banks.

Diamond and Rajan (2005), Brunnermeier and Pedersen (2009), Benmelech and Bergman (2012), and Liu (2016), among others, also analyze the bank-to-bank mutually reinforcing liquidity crises. In these papers, an interbank market serves as the centralized mechanism for the bank-to-bank interactions. All banks are directly connected via the market, and a one-dimensional equilibrium condition typically displays destabilizing dynamics.

I break the assumptions of atomistic agents directly interacting through a monolithic market mechanism. I show that even if the interactions are indirect and heterogeneous, the system is still subject to discontinuous and systemic liquidity crunches. The setting of dispersed interactions is transformed to a setting *as if* the banks are directly interacting. This bridges the gap between the financial networks literature and the liquidity crises models based on direct coordination problems.

The dispersed interactions and their interconnectedness structure are important considerations. The reduction of wholesale funding from institutional relationship lenders is a salient feature in the financial crisis.¹ In addition, this is more pertinent if the distressed

1. Notable examples include Northern Rock, Bear Stearns, and Lehman Brothers.

banks cannot access the centralized short-term funding market ex post. Moreover, the interconnectedness structure is also a major concern from a policy perspective.

A strand of literature studies the relationship between financial networks and systemic risks, for example Eisenberg and Noe (2001), Acemoglu, Ozdaglar, and Tahbaz-Salehi (2015b), and Elliott, Golub, and Jackson (2014). They model the cascading asset-value loss as an insolvent borrower bank default to its interbank lenders, the lenders' lenders, and so on. They define systemic risk as the event in which such cascading "contagion" process spreads to a significant proportion of the banking network. In comparison, I stress that banks are precautionary and strategic in managing liquidity. In my model, the direction of the strategy interaction is the opposite – from lender to borrower – the liquidity hoarding at a bank gives its interbank borrower incentives to follow suit.² Therefore, the nature of the systemic risk in my model is a liquidity crisis. In this view, not until the insolvency contagion cascades through the whole network, will it trigger a systemic liquidity crunch, due to banks' individually precautionary liquidity hoarding strategies.³

Allen and Gale (2000) and Nash (2016) study liquidity shortage contagion on stylized networks structures. Their models feature ex-post interbank liquidity risk sharing through deposit cross holdings or interbank credit commitments. In my model, depositor runs do not materialize in equilibrium. The focus is on banks' ex-ante coordination in interbank lending.

A major novelty of this research is tackling the class of network games with multiple equilibria caused by amplifying individual best-response functions. The result is the characterization of the network-wide discontinuous behavior transition. In the games on networks literature, Ballester, Calvó-Armengol, and Zenou (2006) feature linear strategic complementarity, which is applied to skill investment with positive externalities on social networks. Bramoullé, Kranton, and D'Amours (2014) study local public goods provision and free-riding

2. In this sense, Gai, Haldane, and Kapadia (2011) is close to mine. It investigates the contagion of a binomial liquidity-shortage state from lender to borrower with simulation.

3. The liquidity view of the systemic risk is expressed in the description of the past financial crisis, for example in Brunnermeier (2009), Shin (2009).

with strategic substitutability. Denbee, Julliard, Li, and Yuan (2017) empirically identifies that liquidity holding decisions between connected banks are complementary. The individual best response with liquidity hoarding behavior in my model implies that the complementarity is non-linear and amplifying. In such cases, the game played on network can admit multiple equilibria, which are necessary to characterize network-wide instability. However, intricate local network patterns can induce complicated multiplicity that is hard to analyze. I adopt mean-field approximation method to overcome this problem and extract the systemic behavior in equilibrium.

Mean-field approximation is widely applied to network analyses in the natural sciences. Gao, Barzel, and Barabási (2016) demonstrate the method in mutualistic networks in ecology and other networks in natural sciences. Haldane and May (2011) argue for drawing insights from ecology network techniques to study systemic risks. This paper is among the first to apply the method to network games.⁴ I deliver asymptotic analysis of the approximation method in random networks that is related to the Chung-Lu model (Chung and Lu, 2002), (Chung and Lu, 2006). Kelly, Lustig, and Nieuwerburgh (2013) share a similar idea with the mean-field approximation by using the population firm size dispersion to approximate the dispersion in every firm's customer set.

Some financial network papers, for example Gai and Kapadia (2010), Gai et al. (2011), and Gofman (2017), resort to simulation method to study the contagion of a binomial state on the network. My approach not only overcomes the numerical difficulties, but also affords succinct and interpretable analysis.

Jackson and Yariv (2007) and Galeotti, Goyal, Jackson, Vega-Redondo, and Yariv (2009) share similar ideas with the mean-field approximation method. In their model, agents make binomial decisions without knowing the identity of its connection. As a result, the Bayesian expectation of the counterparties' actions serves as the equilibrium object, which is similar to my one-dimensional systemic liquidity. My model works in a complete-information setting,

4. Another paper with related ideas is Sadler (2017).

with continuous actions and directed, weighted networks.

CHAPTER 3

MODEL

3.1 Big Picture

The economy has three periods (time 0, 1, 2). For simplicity, there is no time discount. The financial system consists of n banks. Banks lend and borrow with each other. Hence, they are linked by the lender-borrower relationships, which form the interbank lending network. The financial system as a whole interacts with the rest of the world in two aspects. It receives funding from retail depositors and invests the funding into a liquid storage asset (called cash) and the illiquid real investments (Figure 3.1).

Each bank serves a group of retail customers who deposit d dollars in total. The depositor requires a one-dollar return at time 2 for each dollar saved at time 0. However, the depositors of one bank might have a panic-driven run at time 1.¹ On the asset side, there are two physical assets. Each dollar invested in cash at time 0 can be returned at either time 1 or time 2 at the face value. The real investments return $R > 1$ if held to maturity, but only pay out $\beta < 1$ if liquidated early at time 1.

When the interbank lending network functions well, the financial system can convert most of the retail deposit funding (nd) into real investment, while avoiding a depositor run. Otherwise, if the coordination on the network fails, all banks hold cash to self-insure against the potential depositor run, leading to inefficient zero total real investments. The shift from the first scenario to the second would characterize interbank runs.

3.2 Timing

At time 0, banks make decisions on the quantity of interbank lending, real investments, and cash holding simultaneously. Time 0 is the focus of analysis because interbank runs are

1. Details in Subsection 3.5.

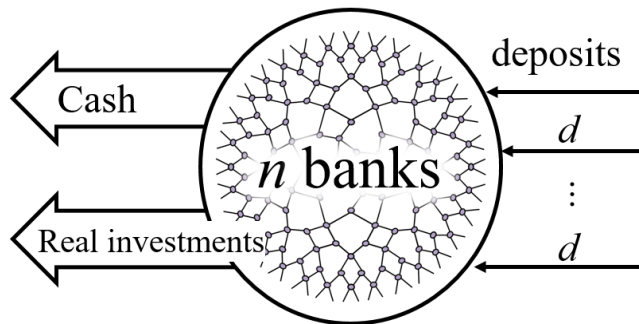


Figure 3.1: Configuration of the Financial System

The arrows represent time-0 flow of funds to and from the financial system. The financial system as a whole converts funding from retail deposits (nd) to cash and real investments. Within the financial system, n banks lend and borrow among themselves.

modeled as the equilibrium shift of the interbank lending game played at this period. At time 1, retail depositors of one bank might run depending on the bank’s condition. Time 1 does not necessarily represent a concrete sequential date in the real world. It represents an uncertain potential scenario of financial distress that banks are worrying about ex ante. Its existence gives banks incentive to preempt depositors by withdrawing lending and building up cash buffer at time 0.² At time 2, the survived assets mature and debts are cleared. Depositors fundamentally only value time-2 payoffs. Each bank also maximizes only time-2 payoff, provided it is safe at time 1.

3.3 Bank Balance Sheet at Time 0

A generic bank i ’s balance sheet at time 0 is illustrated in Figure 3.2. It is funded with d from its retail depositors and y_i from other banks through interbank borrowing. y_i is an endogenous variable depending on bank i ’s direct interbank lenders’ decisions. Given total

2. Documented in Shin (2009), Northern Rock’s liquidity crisis was triggered by the non-renewal of wholesale funding from sophisticated institutional investors. “Depositor run . . . was an event in the *aftermath* of the liquidity crisis at Northern Rock, rather than the event that triggered its liquidity crisis.” This justifies the sequence of the events in the model. Moreover, from the creditors’ perspective, “run on Northern Rock may be better seen as the tightening of constraints on the creditors of Northern Rock rather than as a coordination failure among them.” This justifies the concern of future liquidity need being the reason for the institutional lenders to retract lending preemptively.

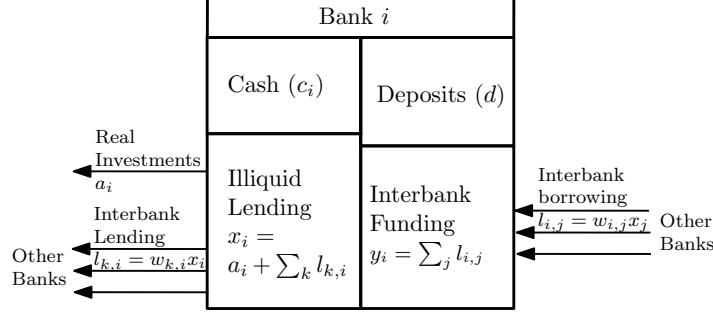


Figure 3.2: Bank balance sheet at time 0

Bank i is funded by retail depositors and interbank borrowing. The total funding is invested in cash and illiquid lending. For illiquid lending, a part goes to interbank borrowers, the rest goes to real investment. The items in the graph represent time-0 flow of funds, not valuation.

funding of $d + y_i$ dollars, bank i allocates c_i dollars into cash, and x_i dollars into *illiquid lending*. Illiquid lending is composed of a bundle of real investments and interbank lending to other banks. I assume when bank i changes its illiquid lending level, the proportion it allocates to the the real and interbank borrowers are fixed.

Specifically, I make the following assumptions about illiquid lending allocation. For any choice of x_i , at most $w_{k,i}$ proportion of x_i can be loaned to bank k .³ Exogenously $w_{k,i}$ is called the lending intensity from bank i to k . The collection of all pairwise lending intensities $\{w_{i,j}\}$ is arranged in the $n \times n$ *adjacency matrix* \mathbf{W} , which defines the weighted and directed *interbank lending network*. The rest of x_i that is not loaned to any other banks is invested in bank i 's real investments. This part of x_i flows outside the financial network, typically in the form of bank loans to the real sector. I make the following tie-breaking assumption, As long as bank k promises returns are not dominated by real investment, bank i is lends to interbank borrowers first, i.e. utilizing the full capacity of $w_{k,i}$.

The network structure is exogenously given. The underlying assumption is that, when a bank reduces illiquid lending, it decreases lending to real and interbank borrowers at fixed proportions. The original proportions are inherited from the lending positions at the

3. Indexing conventions: Letters i, j, k are reserved for the indexing of generic banks. For clarity, i is retained for the current object of discussion, j for i 's lender, and k for i 's borrower. As a result, connection intensity shall usually appear as $w_{i,j}, w_{k,i}$.

beginning of time 0. Effectively, I can calibrate the pre-existing interbank lending exposures as given, and study the counterfactual scenarios in which banks withdraws interbank liquidity proportionally from all borrowers. Therefore, in my model, the total illiquid lending of a bank is endogenous, but the proportional distribution is predetermined. This paper is not about network formation, although that would be an interesting extension. Instead I take the set of lending relationships as given, and study the induced equilibrium and its stability with respect to network shocks in a comparative statics sense.

Under the assumptions, suppose all banks deplete interbank lending capacity, then $l_{k,i} = w_{k,i}x_i$ is the amount bank i lends to k . *Interbank lending intensity* of bank i , expressed as $\delta_i^O = \sum_k w_{k,i}$, is the proportion of i 's illiquid lending that is allocated to interbank lending. It is the i 'th column sum of \mathbf{W} . In network terminology it is also call i 's *out-degree*. The rest of illiquid lending is real investments, $a_i = (1 - \delta_i^O)x_i$. Given other banks' illiquid lending choices, bank i 's interbank funding is $y_i = \sum_j w_{i,j}x_j$. This quantity will be endogenously determined in equilibrium later. Until then, let us take y_i as given and study bank i 's individual problem.

The adjacency matrix \mathbf{W} satisfies the following parameter conditions.

CONDITION 1 (Adjacency Matrix). *All entries are nonnegative: $w_{i,j} \geq 0, \forall i, j$; diagonal entries are all zero: $w_{i,i} = 0$; interbank lending intensities (out-degrees) are less than 1: $\sum_k w_{k,i} < 1, \forall i$.*

3.4 Asset Returns and Liquidation Costs

An asset's return structure is characterized by two numbers, hold-to-maturity value and early liquidation value. The two classes of assets, cash and illiquid landing, feature the trade-off between the long and short term payoffs.

The returns of cash and real investment are given exogenously by the physical constraints outside the financial system. For one dollar invested at time 0, cash returns one dollar at

either time 1 or time 2, whereas real investment returns either $\beta < 1$ at time 1 or $R > 1$ at time 2.

Interbank lending's return structure is assumed to be the same as that of the real investments: β at time 1 or R at time 2. The idea is that financial assets are equally illiquid as real assets. This is justified with the assumption that the borrower cannot promise more than the return of its real investments, due to unverifiable asset portfolio composition. At time 1, it cannot promise a higher liquidation value by demonstrating it has cash assets, which generates time 1 cash flow greater than β . The other way to micro-found is to assume the interbank debt is not retractable, whereas there will be a secondary market for interbank debt at the time of distress (time 1). All buyers in the market, however, have to maintain their asset portfolio composition, in order to deter their retail depositor run. They cannot arbitrage by buying interbank debt with cash holding at time 1. The only option is to liquidate their real investment to purchase secondary interbank debt. Assuming buyers in the distress market have full bargaining power, the amount raised by selling interbank debt early is only β per R dollar at time 2, limited by the return of the real investment.⁴

For time-2 returns, the rationale is similar. The borrower has full bargaining power ex post. As stated before, the lender chooses to deplete the maximum interbank lending intensities as long as the interbank borrower offers as high as the outside option of real investment. This tie-breaker assumption means the lender would not replace interbank lending with real investment as long as their returns are equal during the contraction of illiquid lending. As a result, the borrower promises just R at time 2 to attract interbank funding.

Therefore, a bank is indifferent between interbank lending to different banks as well as the bank's real investments, since they have same return structures. The lender treats them

4. Both of these ways of micro-foundation assumes some friction at time 1 to generate low market liquidity of the interbank debt at the interim period. The low market liquidity in turn causes funding liquidity problems upfront at time 0, as I will illustrate later. This channel is one of the two legs of the "liquidity spiral" in Brunnermeier and Pedersen (2009).

combined in a bundle as total illiquid lending (x_i) in its portfolio selection problem, which is declared soon.

In addition to the liquidation cost per dollar invested ($1 - \beta$), there is a fixed liquidation cost γ to withdraw any positive amount of illiquid lending (x_i) for a bank at time 1. This reflects a bank-level overhead during financial distress to initiate the costly liquidation process. If the payoff provided by liquidating x_i does not cover even the fixed cost, the bank can choose not to withdraw any x_i during the time-1 financial distress. As a result, the total time-1 liquidation value from x_i is $\max\{x_i\beta - \gamma, 0\}$.

3.5 Depositor Run at Time 1

Each bank serves a group of depositors who inelastically supply in total d dollars of deposits as long as it returns the face value at time 2. At time 1, the group of retail depositors at the same bank may experience a panic driven depositor run as in Diamond and Dybvig (1983). If such a depositor run happens to a bank, its interbank lenders will lose their early liquidation value and be placed to the residual claimant at period 2, according to depositor preference laws. Such an event would be so detrimental to interbank lenders that they want to avoid lending to such banks of depositor run tenancies ex ante. But first, I describe when will a depositor run will happen, assuming the bank somehow already attracted y_i interbank borrowing at time 0.

The panic-driven run will not materialize if the bank has prepared enough asset liquidation value to cover all the potential liquidity needs of the depositors at time 1. Specifically, each individual depositor considers the following problem. Depositors hold demand deposits that are senior to interbank borrowing. Suppose a ρ proportion of bank i 's depositors demand early withdrawal of ρd dollars at time 1. An individual atomistic depositor chooses the better of two alternatives: to withdraw early or to wait. If she joins the run, she is repaid at the face value if the bank can come up with at least ρd at time 1 from c_i and/or x_i liquidation. Otherwise, the bank is insolvent and all depositors are repaid pro rata. The

withdrawal can be stored for time-2 consumption with zero net return. If she does not join the run, and the bank is insolvent at time 1, nothing is left for her when she comes at time 2. However, if the bank is solvent, that is, if the time-1 asset value is not depleted by ρd , it must decline interbank debt if it would otherwise infringe the remaining depositor's savings balance $(1 - \rho)d$. Accordingly, when she joins the other $1 - \rho$ depositors for time-2 withdrawal, her savings will be intact.⁵

The depositor run is a strategy profile in which all depositors choose early withdrawal. A depositor run is an equilibrium if any depositor optimally chooses to withdraw early given that all other depositors run too. Given a bank's balance sheet, a depositor run equilibrium does *not* exist if and only if the time-1 asset value is enough to serve all depositors at time 1. Specifically, the depositor run-proof condition is

CONDITION 2 (Depositor Run Proof).

$$d \leq \max \{x_i \beta - \gamma, 0\} + c_i.$$

When the depositor-run-proof condition is satisfied, the only equilibrium in the time-1 depositor coordination game is all depositor choosing late withdrawal. Such a depositor run-proof bank is considered safe for interbank lenders.

3.6 Bank's Problem at Time 0

This subsection describes the bank's individual problem at time 0. Given deposit funding d and interbank funding y_i , bank i chooses asset portfolio (x_i, c_i) . For the moment, suppose all interbank counterparties are safe. In other words, all interbank creditors will not demand early withdrawal, and all interbank borrowers can return β or R at time 1 or 2.

A key concern of the bank is the possibility of a time-1 depositor run. I assume that the

5. Time-2 withdrawers might find their accounts shrunk if assets left over after paying ρd at time 1 is not enough. This scenario will not happen if the depositor-run-proof condition is met.

banks are extremely averse about even the slightest chance of a depositor run. Specifically, banks adopt maximin decision-making under the Knightian uncertainty of a depositor run. It is uncertain whether bank i 's depositors will see the sunspot to initiate a depositor run. The bank, being maximin, optimizes the asset portfolio assuming the worse case scenario in which the sunspot will arrive. In this case, if the bank's balance sheet is not depositor-run-proof, the bank is assumed to earn a negative payoff after the run. If the balance sheet is depositor-run-proof, the run equilibrium does not materialize, the bank survives to time 2 and earns the margin after paying off debts. Specifically, the bank's problem is

$$\begin{aligned} \max_{c_i \geq 0, x_i \geq 0} \min \left\{ x_i R + c_i - d - y_i R, \left\{ \begin{array}{ll} x_i R + c_i - d - y_i R & \text{if } d \leq \max \{x_i \beta - \gamma, 0\} + c_i \\ -\text{Run Punishment} & \text{if } d > \max \{x_i \beta - \gamma, 0\} + c_i \end{array} \right\} \right\} \\ \text{s.t.} \quad x_i + c_i \leq d_i + y_i. \end{aligned}$$

The solution should be an asset portfolio that is depositor run-proof, because the bank always has the option to avoid any possibility of depositor run by passing through the funding ($x_i = y_i, c_i = d$). This portfolio choice at least earns zero profit with no uncertainty.

Given that the bank always maintains a depositor-run-proof balance sheet, the problem is transformed to maximizing the time-2 profit, subject to depositor-run-proof condition and balance-sheet budget constraint:

$$\begin{aligned} \max_{c_i \geq 0, x_i \geq 0} \quad & x_i R + c_i - d - y_i R \\ \text{s.t.} \quad & x_i + c_i \leq d_i + y_i \\ & d \leq \max \{x_i \beta - \gamma, 0\} + c_i. \end{aligned}$$

Alternatively, the depositor-run-proof constraint can be interpreted as a regulation on asset liquidity. The banks are mandated to prepare enough time-1 liquidity to cover the amount of deposits. This assumption simplifies the micro-foundation, but it loses the inter-

pretation that interbank lending is a way for banks to provide the sense of safety for depositors while maintaining high illiquid investments. Regardless, being depositor-run-proof is a key constraint that shapes the banks optimal strategy.

The solution to program is the policy functions $f(y_i)$ and $g(y_i)$ for the optimal choices of illiquid lending and cash with respect to interbank liquidity y_i . Notice the policy functions are irrelevant of bank identity (no i subscript). Graphical representations are provided in Figure 3.3.

$$x_i = f(y_i) = \begin{cases} y_i & \\ \frac{y_i - \gamma}{1 - \beta} & \\ y_i + d & \end{cases}, \quad c_i = g(y_i) = \begin{cases} d & y_i \in \left[0, \frac{\gamma}{\beta}\right) \\ \frac{-\beta}{1 - \beta} y_i + \frac{1}{1 - \beta} \gamma + d & y_i \in \left[\frac{\gamma}{\beta}, \frac{1 - \beta}{\beta} d + \frac{\gamma}{\beta}\right) \\ 0 & y_i \in \left[\frac{1 - \beta}{\beta} d + \frac{\gamma}{\beta}, +\infty\right) \end{cases} \quad (3.1)$$

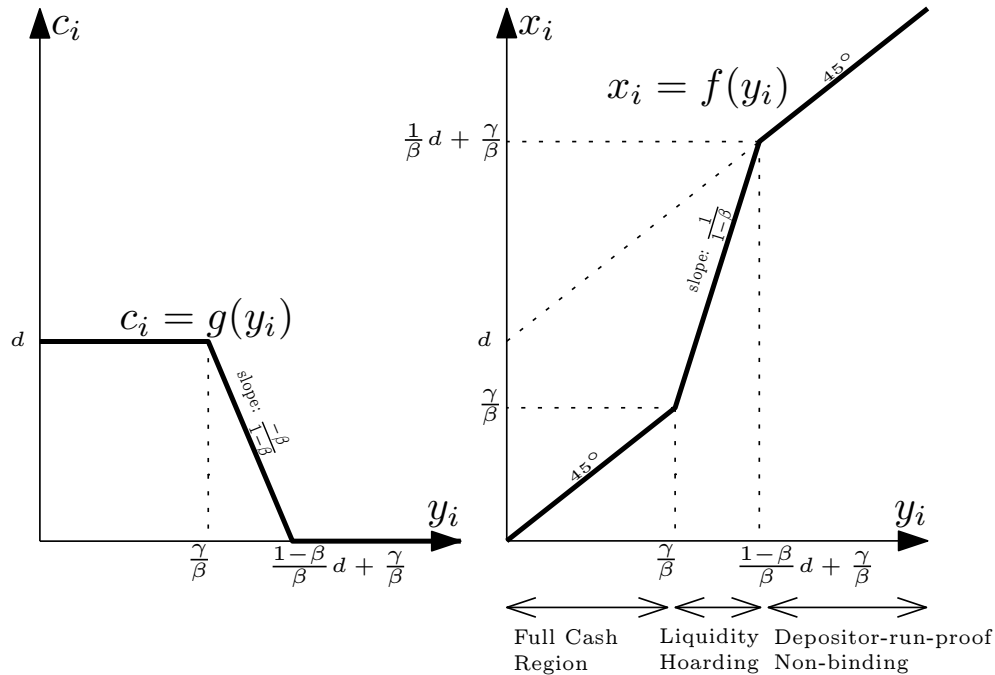


Figure 3.3: Optimal time-0 asset portfolio
Policy functions $x_i = f(y_i)$, $c_i = g(y_i)$.

The simple solution features the key economic mechanism—liquidity hoarding. Regard-

less of the liquidity pressure from depositors, the bank would always like to allocate all funding in high-return illiquid lending x_i . When interbank funding y_i is high, the depositor-run-proof constraint is not binding, even if all funding is loaned out to illiquid borrowers. Time-1 liquidity is ample just from x_i 's liquidation value ($x_i\beta - \gamma \geq d$). In this region, x_i changes one to one as y_i changes.

Then, as interbank liquidity decreases, the bank's balance sheet shrinks. Having a portfolio of all illiquid assets would not be depositor-run proof. The depositor-run-proof constraint becomes binding. Compared to the high y_i case, the bank has to not only decrease total assets, but also switch to a more liquid asset portfolio to maintain enough ($\geq d$) time-1 asset liquidation value. In detail, for a one-dollar decrease in interbank funding y_i , illiquid lending x_i has to be cut back by more than one dollar ($\frac{1}{1-\beta}$). The excess ($\frac{\beta}{1-\beta}$) is used to accumulate cash, whose time-1 return is greater than that of the illiquid asset ($1 > \beta$). This behavior is called liquidity hoarding. The change in interbank funding y_i causes an *amplified* change in illiquid lending x_i . Graphically, the best-response function f is steeper (slope > 1) in the middle interval, called the liquidity hoarding region. This individual amplification response plants the seed of systemic fragility, as will be illustrated in Proposition 1.

Finally, when x_i cannot cover even its fixed liquidation cost ($x_i\beta \leq \gamma$), its liquidation value is zero. All time-1 liquidity needs have to be prepared in the form of cash ($c_i = d$). All of the deposits are locked up as cash and cannot be invested into the high return asset. Again, in this full cash region, x_i changes one to one as y_i changes. At the extreme when $y_i = 0$, the bank has no meaningful business on either the lending or the borrowing sides. It simply passes through all deposits to cash.

Interbank funding helps the bank to earn profits, because it inflates the balance sheet, allowing the deposit to be invested in illiquid assets. Given the solution, it is easy to write the optimized bank profit function of y_i .⁶ In fact, at the optimal portfolio, $profit(y_i) = (R - 1)(d - c_i) = (R - 1)(x_i - y_i)$, because the balance sheet budget constraint is always

6. The exact expression of the optimal profit function is reported in Appendix A.17.

binding. These expressions show all profits are generated from the part of the deposits that are converted into illiquid lending, multiplied by the interest rate margin. Or in other words, interbank funding does not generate profit by itself, because its time-2 funding rate is as high as illiquid lending (R). It seems futile, but the purpose of borrowing and lending at the same rate is to create a “sense of safety” for the depositors by having a bigger balance sheet. The depositor’s claim is more senior than that of interbank borrowers. Therefore, should liquidity distress occur at time 1, the inflated balance sheet, with a greater asset side, will be able to provide more time-1 liquidity to the depositors. The “sense of safety” from a bigger balance sheet allows a higher proportion funding to be invested in the high return asset, even though the per unit liquidation value is lower. Consequently, interbank funding generates profits by freeing up deposits, which otherwise must be held as cash to prepare time-1 liquidity. From small to big y_i , this process starts when illiquid lending begins to cover its own time-1 fixed liquidation costs ($\beta x > \gamma$), and stops when all deposits have been freed up ($c = 0$). This is why the marginal profit of addition y_i is only positive in the liquidity-hoarding region of y_i .

3.7 Interbank Lending Equilibrium

The rest of the chapter discusses how interbank coordination can achieve the preferable arrangement of inflated balance sheets, and how the coordination is inherently unstable.

Banks’ portfolio-choice strategies are interlinked through the interbank lending network. At time-0, all banks in the network solve the same problem of balance sheet management simultaneously. Each bank’s individual problem is the same as described above, but its interbank funding opportunities are specific. How much a bank can acquire interbank funding depends on how it is connected to the interbank lenders and how the lenders’ make their lending decisions. Define the pure-strategy Nash equilibrium of the interbank lending game at time 0:

DEFINITION 1 (Interbank Lending Equilibrium). *Interbank lending equilibrium is the*

time-0 allocations—cash c_i , real investments a_i , and interbank lending $l_{i,j}$, such that each bank i

- chooses to utilize all the interbank borrowing extended by other banks: $y_i = \sum_j l_{i,j}$,
- chooses its optimal asset portfolios given interbank funding, subject to the depositor-run-proof condition: $x_i = f(y_i)$, $c_i = g(y_i)$,
- chooses to lend to other banks at its maximum proportional capacities: $l_{k,i} = x_i w_{k,i}, \forall k$, with the rest of x_i allocated to real investments: $a_i = x_i - \sum_k l_{k,i}$.

The first and third condition imply tie-breaker conditions for banks to engage in interbank business at the greatest extent. The first condition means each bank accepts all possible interbank funding, although the optimal profit function is only weakly increasing. The third condition means each bank withdraws liquidity from other banks at the fixed proportions, as long as the borrower is still safe.

In equilibrium, y_i is determined by the illiquid lending decisions of bank i 's direct lenders: $y_i = \sum_j w_{i,j} x_j$. In turn, y_i determines bank i 's illiquid lending (x_i). Also, x_i sufficiently describes bank i 's all other asset allocation actions. Specifically, $l_{k,i} = w_{k,i} x_i, \forall k$, $a_i = (1 - \delta_i^O) x_i$, and $c_i = g(f^{-1}(x_i))$. Therefore, the interbank lending network equilibrium can be characterized with respect to only the illiquid lending levels $\{x_i\}$:

CONDITION 3 (Interbank Lending Equilibrium Condition).

$$x_i = f \left(\sum_j w_{i,j} x_j \right), \quad \forall i.$$

Off the equilibrium, if a bank chooses not to maintain depositor-run-proof balance sheet, any other bank will avoid contact with it. Lending to an unsafe bank k would be undesirable. If bank k is run by its depositors, the interbank lending to it cannot be recovered. Bank i will not use the connection $w_{k,i}$. However, this does not alter i 's choice of asset

portfolio composition, because i can replace the $w_{k,i}$ proportion of interbank lending by real investment, whose return has no uncertainty. Borrowing from an unsafe bank would be undesirable too. The interbank funding provided is not stable. It would incur liquidation costs and provoke a depositor run if the unstable funding is retracted at time 1.

In summary, off-equilibrium depositor-run-prone banks would have neither interbank funding sources nor interbank lending opportunities. This is equivalent to removing the banks from the network. In Subsection 5.2, I explore this scenario and examine how the equilibrium changes with exogenous insolvency shocks in order to model the triggering of a systemic liquidity crunch. For the moment, I focus is on the equilibrium in which all banks are depositor-run proof.

3.8 Multiple Equilibria and Comparisons with Other Games on Network

Condition 3 is the typical form used in characterizing several games played on fixed network. In general, x_i represents agent i 's action. The connection intensity-weighted sum of neighboring agents' actions $\left(\sum_j w_{i,j}x_j\right)$ serves as the sufficient determinant of agent i 's best response. In the the Nash equilibrium, all agents choose action simultaneously taken others' actions as given. The equilibrium is characterized by the fixed-point condition with respect to the n -dimensional strategy profile $\{x_i\}$.

Different best-response functions (f) represent the various types of strategic interactions of previous research's interests. Ballester et al. (2006) study a model with an increasing and linear f , which is applied to skill investment with positive externalities on social networks. Bramoull  et al. (2014) study local public goods provision and free-riding with an f that is decreasing, linear, and bounded from below, representing strategic substitutabilities. Both attained closed-form solutions using eigen-analysis with interesting geometric interpretations

of the network topology.⁷

In the literature of financial networks and systemic risks, some papers also admit a similar fixed-point form as their core analysis.⁸ Eisenberg and Noe (2001), Elliott et al. (2014), and Acemoglu et al. (2015b) model the cascading asset default in the network. Their counterpart of the fixed-point condition represents the process of interbank debt repayments. In their analysis, x_i represents the total amount (or ratio) of bank i 's repayment to all interbank debts. The weighted sum ($\sum_j w_{i,j}x_j$) represents how much i can recover from its interbank borrowers. Given the interbank asset value, the amount bank i repays its creditors is determined by the debt contract payoff function, which is their counterpart of f .⁹

This model is different from the cascading-default models in several ways. First, the direction of risk propagation is the opposite. In my model, the lender bank's illiquid lending decision (x_i) affects that of the borrower banks, by changing the borrowers' funding liquidity. In contrast, asset default cascades from borrower to lender. Moreover, the systemic risk is characterized as the mutually reinforcement discontinuous behavior change, rather than the a passive asset-default propagation process. My model captures that the asset value loss can be the trigger of the systemic event. But the full-blown crisis is the systemic liquidity crunch. The interlinked precautionary behavior can induce an interbank run without the asset-loss process reaching a significant portion of the financial network.

To capture the discontinuous liquidity crunches, the important new technical feature of this paper is the multiple equilibria. The necessary condition to have multiple equilibria is that the strategic interaction has to be strong enough, so that action changes can be amplified down the chain of transmission. Otherwise, action changes dissipate along the

7. See Jackson and Zenou (2014) and Bramoullé and Kranton (2015) for more complete surveys on the topic of games played on fixed network.

8. See Glasserman and Young (2016) for more complete review of the financial network and systemic liquidity literature.

9. A difference is their f functions are heterogeneous. For example, let e_i be bank equity level, \bar{d}_i be debt face value, then debt repayment is $f_i(y_i) = \max\{y_i + e_i, \bar{d}_i\}$, where $y_i = \sum_j w_{i,j}x_j$. The intuition is the same without this realistic feature.

transmission chain, as in the cases of Eisenberg and Noe (2001) and Acemoglu et al. (2015b). In those cases, local shocks cannot trigger a discontinuous system-wide behavior change. Technically, the strong strategic interaction is represented by expansive individual best-response functions.

DEFINITION 2 (Expansive and Non-expansive Functions).

A function f is said to be non-expansive if $|f(y_1) - f(y_2)| \leq |y_1 - y_2|, \forall y_1, y_2$. Conversely, if there exist y_1, y_2 such that $|f(y_1) - f(y_2)| > |y_1 - y_2|$, f is said to be expansive.

For example, the specific f considered in this paper (equation 3.1) is expansive due to liquidity hoarding. As discussed in Subsection 3.6, in the liquidity hoarding region, f 's slope is greater than 1, and hence expansive.

PROPOSITION 1 (Expansive Best Response Function is Necessary for Multiple Equilibria).

Given \mathbf{W} satisfies Condition 1, if f is non-expansive then there is at most one equilibrium. I.e., there exist at most one $\{x_i\}$ that satisfies equilibrium condition 3.¹⁰

Proof. See Appendix A.2. □

As stated in the proposition, such strong interaction represented by expansive response function is necessary for multiple equilibria. Models with non-expansive f does not have multiple equilibria, and hence cannot capture systemic-wide discontinuous changes. Therefore, in this model liquidity hoarding is the source of system-wide instability. A major novelty of this research is tackling the class of games with multiple equilibria caused by expansive individual best-response functions.

For the specific f considered in this paper, $f(0) = 0$. Therefore, every bank choosing zero illiquid lending ($x_i = 0, \forall i$) always constitutes an equilibrium. As stated, expansive f is only the necessary condition. Depending on the connection structure (\mathbf{W}), equilibria with

10. A similar result is reported in Acemoglu, Ozdaglar, and Tahbaz-Salehi (2015a).

positive interbank lending levels might exist. The following analyses study with what shape of networks the positive equilibrium is sustained. The next subsection presents an example of circle network with symmetric connections, in which the equilibrium is easy to analyze. For general connections, complicated multiplicity might arise due to the intricate connection patterns. I adopt mean-field analysis to overcome the difficulties in Section 4.

3.9 Example: Circle Network

A circle network is presented in Figure 3.4. Each bank i allocates w proportion of illiquid lending (x_i) to the next bank $i + 1$ (bank n to bank 1). The equilibrium is easy to analyze in this particular symmetrical case. The results in this example build the foundation for analysis on general networks.

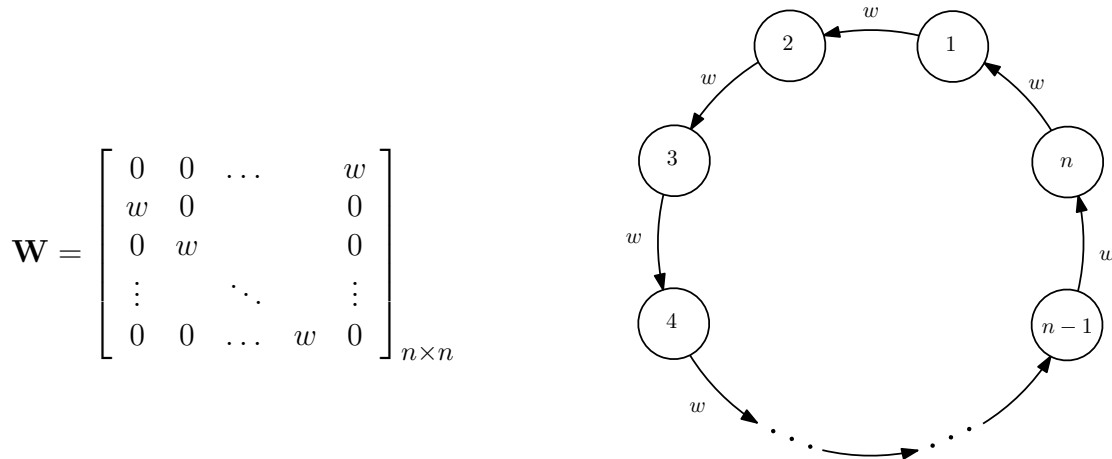


Figure 3.4: Circle Network

The adjacency matrix and the graphical representation of the circle network. Each bank i allocates w proportion of illiquid lending (x_i) to the next bank $i + 1$ (bank n to bank 1). The rest $(1 - w)$ is allocated to real investments. $w \in [0, 1]$.

Evaluate the equilibrium condition 3 at the circle network:

$$x_{i+1} = f(y_{i+1}) = f(wx_i), \quad \forall i \quad (n + 1 \text{ treated as } 1). \quad (3.2)$$

Because f is increasing, the solution must be symmetric. Let x denote the symmetric

equilibrium action. The equilibrium condition is reduced to the simple univariate equation $x = f(wx)$.

PROPOSITION 2 (Circle Network Equilibrium).

In the circle network, $x_i = \frac{d}{1-w}$ and $x_i = 0, \forall i$ are both equilibrium, if $w \geq 1 - \frac{\beta}{1+\gamma d}$. Otherwise, $x_i = 0, \forall i$ is the unique equilibrium.

Proof. See Appendix A.3. □

The symmetric equilibria are represented in Figure 3.5 as the crossing points of the $f(wx)$ curve and the 45° line. The graph of $f(wx)$ is the S-shaped piecewise linear curve, a horizontally stretched version of the individual best-response function $f(y)$ in Figure 3.3. When w is big, there are three equilibria.¹¹ At the highest equilibrium, all banks are in the depositor-run-proof non-binding region (as discussed in Subsection 3.6, Figure 3.3). $c_i = 0, \forall i$. As a result, the financial system converts all deposits (nd) to real investments. The highest possible efficiency level is achieved. In contrast, at the zero equilibrium, interbank lending and real investments are all zero. All deposit funding is held in the form of cash.

Figure 3.5 panel (a) illustrates that as w decreases, the $f(wx)$ curve stretches to the right. At first, the highest equilibrium x decreases. Interbank lending level decreases but total social real investments stays the the full level. As w drops below the critical value given in Proposition 2, the positive equilibria disappear. Every bank playing $x_i = 0$ becomes the unique equilibrium. For an economy that were at the high equilibrium, a small change of w across the critical value can cause a discontinuous change in the equilibrium interbank lending level. Every bank suddenly stops extending interbank lending and hoards cash. Total real investments evaporates as well.

This comparative statics reveals that the positive interbank lending equilibrium requires cooperation. Higher w means a greater proportion of illiquid lending is contributed to the borrower bank, which gives the borrower bank a higher incentive to pass on the high

11. The middle equilibrium is locally unstable. As defined in the next section, I only focus on the locally stable equilibria.

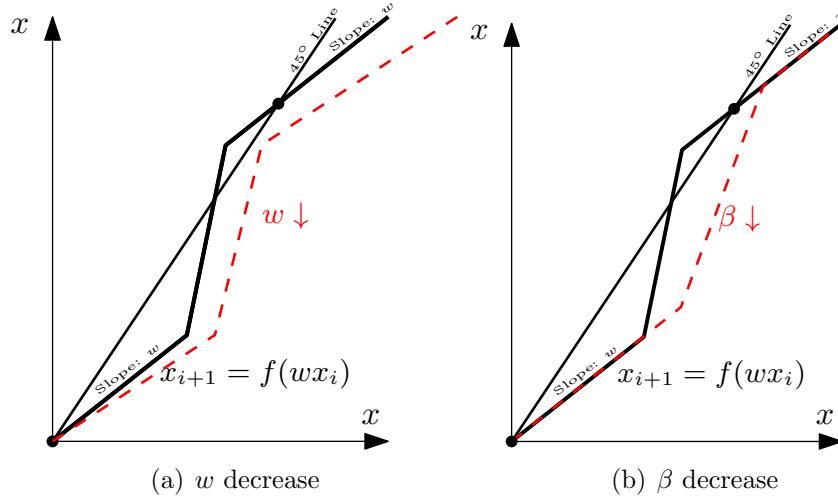


Figure 3.5: Circle Network Equilibria and Comparative Statics

The crossing points of $f(wx)$ and the 45° line represent the symmetric equilibria. The red dashed line represents the curves of $f(wx)$ when w or β are reduced.

lending action to its borrower. Therefore, high interbank connection intensities help sustain the cooperation. Moreover, the coordination can experience a dramatic failure. As the funding levels fall into the liquidity hoarding region, the withdrawal of funding at one bank is amplified at its borrower, resulting in a mutually reinforcing liquidity crunch to the extreme level of full cash hoarding and zero interbank lending. This process represents the triggering of an interbank run.

Figure 3.5 panel (b) depicts another comparative statics with respect to the time-1 return of the illiquid assets (β). When β decreases, both kinks in the f curve move to the upper right. Intuitively, if the early liquidation value of the illiquid assets decreases, the time-1 liquidity provided by a full illiquid asset portfolio decreases. The depositor-run-proof condition becomes binding at a higher interbank funding level (y_i). The banks require a higher level of interbank funding to stay away from hoarding liquidity. Therefore, as illustrated in the graph, if β decreases beyond a critical value, the highest equilibrium is no longer sustained, and an interbank run is triggered in a similar fashion.

Brunnermeier and Pedersen (2009) discuss a similar effect. If market liquidity (β) decreases, the ex ante funding liquidity of the borrower banks decreases, because the lender

banks are more constrained. However, in my model, around the critical value, a small change in market liquidity can trigger a discontinuous collapse in the funding network due to the instability in the interbank funding liquidity coordination. Both the models feature a discontinuous liquidity dry-out from a small exogenous change of market liquidity. But my model is driven by the mutually-reinforcing interactions of funding liquidity in the interbank network, while theirs is due to the feedback loop between funding liquidity and market liquidity.

The circle network is easy to study because the equilibrium collapses to a one-dimension condition under symmetricity. The next sections study the financial fragility in generalized network structures. The complex interconnectedness can be also reduced to a one-dimensional analysis of the systemic liquidity under mean-field approximation.

CHAPTER 4

SYSTEMIC BEHAVIOR IN NETWORK GAMES

This chapter introduces systemic equilibrium. The concept provides an intuitive and convenient way to study the system-wide discontinuous behavior of network games. I apply it to interbank lending games, and model interbank runs as a discontinuous shift of the systemic equilibrium.

The first two subsections give an intuitive introduction in the context of interbank lending games. First I introduce the mean-field approximation. Based on that, I define the new equilibrium construction — systemic equilibrium. The systemic equilibrium is an reduced-dimension approximation of the original equilibrium (condition 3). It reduces the original equilibrium condition with respect to the n -dimensional strategy profile into a new condition with respect to only one number, the systemic liquidity. The new characterization focuses on the relationship between the aggregate network properties and the systemic equilibrium behavior, and avoids the complexity in the original equilibrium condition caused by local peculiarities in the network.

Then, I provide formal justifications for applying the systemic equilibrium in general settings. First, I construct a random network model and analyze the original and systemic equilibria on it respectively. The validity of using systemic equilibrium to approximate the original equilibrium is established by showing the two converge to each other in large random networks as n goes to infinity. The random network model also helps to discuss what statistical properties of the network drive the approximation accuracy. Second, I conduct numerical verifications with observed interbank networks. It is shown that the approximation errors are practically small in finite networks as well. Third, I focus back to the specific strategic interaction in the setting interbank runs, and characterize the conditions of the network shape that determine the number of systemic equilibria. The result is also verified against the numbers of original equilibria numerically solved in simulated networks.

4.1 Mean-Field Approximation

Before starting, I declare some notations for network analyses. Given a directed and weighted interbank network represented by adjacency matrix \mathbf{W} , $\delta_i^O = \sum_k w_{k,i}$ is the *out-degree* of node i . In the context interbank network, it represents the *interbank lending intensity*, i.e., the proportion of bank i 's illiquid lending that is lent to other banks instead of real investments. $\delta_i^I = \sum_j w_{i,j}$ is node i 's *in-degree*. In interbank networks, it measures *interbank funding connection*, that is how much access bank i has to interbank funding sources. Bank i 's *direct lenders* are those that have positive connections to i , i.e. the set $\{j \mid w_{i,j} > 0\}$. μ is either the average in-degree or the average out-degree, noticing the basic fact that total in-degree equals total out-degree, $\mu = \frac{1}{n} \sum_i \delta_i^I = \frac{1}{n} \sum_i \delta_i^O = \frac{1}{n} \sum_{ij} w_{i,j}$.

Bank i 's interbank liquidity depends on the illiquid lending decisions of its direct lenders: $y_i = \sum_j w_{i,j} x_j$. The idea of mean-field approximation is to express the effect of the direct lenders on a given bank by a single systemic mean effect, which is the same across all banks. The direct lenders consist of a subset of all banks. Their aggregate effect on bank i can be decomposed into two parts: the total interbank funding connections of bank i multiplied by the connection-intensity weighted average x_j of the direct lender,

$$y_i = \sum_j w_{i,j} x_j = \delta_i^I \sum_j \frac{w_{i,j}}{\delta_i^I} x_j, \quad \forall i. \quad (4.1)$$

Loosely speaking, the composition of every bank's direct lender set is roughly the same. They are all drawn from the population of the whole network. Given this intuition, the mean-field approximation says, for each bank i , its direct lenders' average x_j approximately equals the system-wide average of x_j 's:

$$\sum_j \frac{w_{i,j}}{\delta_i^I} x_j \approx \sum_j \frac{\delta_j^O}{n\mu} x_j, \quad \forall i. \quad (4.2)$$

Both sides are weighted averages of \mathbf{x} . The left hand side is weighted by the connection

intensities to bank i . The right-hand side is weighted by out-degrees, which is a nodal property irrelevant the borrower's identity (i). It represents a system-wide summarization of the supply of interbank liquidity, defined as systemic liquidity: Define systemic liquidity as the out-degree weighted average of banks' illiquid lending,

$$x^* = \sum_j \frac{\delta_j^O}{n\mu} x_j. \quad (4.3)$$

Substitute x^* back into equation (4.1), the mean-field approximation says bank i 's interbank funding is approximated as

$$y_i \approx \delta_i^I x^*, \quad \forall i.$$

Under this approximation, the heterogeneity of banks' interbank funding levels only comes from the sizes of their incoming pools of direct lenders, measured by the interbank funding connections (in-degrees). Each bank i 's direct lender set's average action is approximated by systemic liquidity, which is the same for all i .

Notice in calculating the systemic liquidity (x^*), the banks with higher interbank lending intensity ($\tilde{\delta}^O$) are assigned with higher weights. Intuitively speaking, this is because the banks with high interbank lending intensities (δ^O) are more likely to become bank i 's direct lenders, or have a higher connection intensity to i . On the other hand, the banks with low interbank lending intensities direct more of their lending outside the system to real investments. Therefore, interbank lending intensity ($\tilde{\delta}^O$) is related a banks weight in contributing to the systemic liquidity (x^*).

A somewhat different interpretation of the approximation is that x^* is the systemic average interbank lending distributed per unit of connection. Total interbank liquidity extended on the network across all pairs of banks is $\sum_{k,i} l_{k,i} = \sum_i \delta_i^O x_i$. The total liquidity is distributed among $\sum_{k,i} w_{k,i} = n\mu$ units of total connections. Accordingly, $x^* = \frac{\sum_i \delta_i^O x_i}{n\mu}$ can be interpreted as the average interbank liquidity distributed per unit of connection. Suppose

the distribution of interbank liquidity is equal among all units of connections. Then bank i as a borrower has access to funding liquidity according to its total units of interbank borrowing connections (in-degree: δ_i^I). Thus, its interbank funding can be approximated as $y_i \approx \delta_i^I x^*$.

The intuition of the mean-field approximation is formalized in Proposition 3 in Subsection 4.5, after introducing the random network model.

4.2 Systemic Equilibrium

Condition 3 says the interbank lending equilibrium is characterized by the set of n equations,

$$x_i = f \left(\sum_j w_{i,j} x_j \right), \quad \forall i. \quad (4.4)$$

Evaluate the mean-field approximation at the interbank lending equilibrium. Effectively, substituting the approximation of interbank funding (equation 4.2) into the equilibrium condition (equation 4.4), we arrive at the approximated equilibrium condition,

$$x_i \approx f(\delta_i^I x^*), \quad \forall i.$$

At the original equilibrium, the above condition holds approximately. On the other hand, the exact solution of this condition should provide a close description of the original equilibrium. Hence, we define a new equilibrium concept that exactly solves the above approximated equation set:

DEFINITION 3 (Systemic Liquidity Equilibrium).

The systemic liquidity equilibrium is the vector of banks' illiquid lending $\{x_i\}$ and the associated systemic liquidity x^ , such that*

$$x_i = f(\delta_i^I x^*), \quad \forall i. \quad (4.5)$$

Taking the δ^{O} -weighted average of the above equilibrium conditions across i , we arrive at the equilibrium condition with respect to systemic liquidity x^* :

$$x^* = \sum_i \frac{\delta_i^{\text{O}}}{n\mu} f(\delta_j^{\text{I}} x^*). \quad (4.6)$$

The systemic liquidity equilibrium is characterized by a single equation with respect to one object x^* only. As long as x^* is solved, the individual x_i 's can be recovered as in (4.5). Equilibrium systemic liquidity becomes the single key object of analysis. This characterization reduces the dimensionality of the original equilibrium condition (Condition 3) from n to 1. As a result, it is much simpler to analyze.

The systemic liquidity equilibrium can be understood as a transformed structure of interbank interactions. The transformation is illustrated in Figure 1.1. In the original equilibrium, pairwise strategic interactions are dispersed on the decentralized interbank lending network. Each bank is directly interacting with a limited number of counterparties. The financial system is indirectly linked through the network.

In the transformed structure, each bank is directly interacting with systemic liquidity (x^*). Bank i accesses systemic liquidity according to its in-degree (δ_i^{I}), obtaining interbank funding of $\delta_i^{\text{I}} x^*$. The bank applies individual optimal response function f to the interbank funding level, and chooses its illiquid lending level as $f(\delta_i^{\text{I}} x^*)$. δ_i^{O} portion of the illiquid lending is contributed back to the interbank system. Combined, the equilibrium condition is determined by the aggregate effect of all banks' direct interactions with system liquidity. The aggregate effect is the out-degree weighted average of the individual optimal response function (f) evaluated at each bank's interbank funding level ($\delta_i^{\text{I}} x^*$). Intuitively, the dispersed interactions are transformed to a structure *as if* all banks are directly interacting with the constructed object of systemic liquidity. Hence, the dimension reduction of the equilibrium characterization is achieved.

4.3 A Random Network Model

From now, I provide formal justifications for applying the systemic equilibrium in general settings. This subsection provides a random network model and study the limiting behavior of the original and systemic equilibrium. The goal is to argue that the dimension-reduction technique of using systemic equilibrium to approximate the original equilibrium is accurate, by showing the approximation error converges to zero in the probability limit of large networks ($n \rightarrow \infty$). The intuition of the mean-field approximation, as introduced in the previous chapter, is laws of large numbers. But for random networks, degrees and the equilibrium actions are dependent across nodes due to network interconnections. This makes the general versions of laws of large numbers not directly applicable. I overcome the problem by building an ad hoc law of large numbers for random networks in order to pinpoint the probability limit of the systemic equilibrium. Then I use fixed point arguments to show the existence of an original equilibrium within an infinitesimal neighborhood of that limit. Combined, the conclusion is that for any systemic equilibrium, there is a original equilibrium whose systemic average is arbitrarily close at arbitrarily high probability, as long as n is large enough.

The other benefit of studying this random network model is to discuss the conditions of the network shape that drive the asymptotic accuracy of the systemic equilibrium. This subsection defines the random network generating process. It identifies weighted non-assortative connection the key distributional condition that drives the asymptotic accuracy of the systemic equilibrium. I provide both the formal definition and intuitive explanation of the condition below. Other than this condition, the network generating process is deliberately constructed general, so that it incorporates the various statistical properties of the observed financial and social networks, in order to demonstrate the application of systemic equilibrium is versatile.

DEFINITION 4 (Random Network Generating Process).

Let the $n \times n$ adjacency matrix \mathbf{W} , representing the directed weighted network, be constructed as:

$$w_{i,j} = \begin{cases} \frac{1}{(n-1)\tilde{\mu}} \lambda_{i,j} \tilde{\delta}_i^{\text{I}} \tilde{\delta}_j^{\text{O}}, & i \neq j \\ 0 & i = j \end{cases},$$

where

- the underlying in- and out-degree $\{\tilde{\delta}_i^{\text{I}}, \tilde{\delta}_i^{\text{O}}\}_{i=1}^n$ are a sequence of i.i.d. random variable from the joint degree distribution $\Pi(\tilde{\delta}^{\text{I}}, \tilde{\delta}^{\text{O}})$, which has the same marginal expectations ($\mathbb{E}\tilde{\delta}^{\text{I}} = \mathbb{E}\tilde{\delta}^{\text{O}} = \tilde{\mu}$), and
- for each directed pair of nodes (i, j) , the connection parameter $\lambda_{i,j}$ follows $\Lambda(\tilde{\delta}_i^{\text{I}}, \tilde{\delta}_j^{\text{O}})$, a distribution parameterized by $\{\tilde{\delta}_i^{\text{I}}, \tilde{\delta}_j^{\text{O}}\}$, and is independent of everything else.

The key statistical property driving the asymptotic results about the accuracy of mean-field approximation is weighted non-assortativeness:

CONDITION 4 (Weighted Non-assortative Network).

The random network is weighted non-assortative, which says the connection parameter $\lambda_{i,j}$ is uncorrelated with $\{\tilde{\delta}_i^{\text{I}}, \tilde{\delta}_j^{\text{O}}\}$, specifically,

$$\mathbb{E}(\lambda_{i,j} | \tilde{\delta}_i^{\text{I}}, \tilde{\delta}_j^{\text{O}}) = 1, \quad \forall \{\tilde{\delta}_i^{\text{I}}, \tilde{\delta}_j^{\text{O}}\}.$$

In addition, I impose the following restrictions on distributions Π and Λ that are required for the asymptotic results:

CONDITION 5 (Distribution Regularity Conditions).

The support of the underlying in- and out-degree distribution Π are non-negative. Π 's marginal expectations are the same: $\mathbb{E}\tilde{\delta}^{\text{I}} = \mathbb{E}\tilde{\delta}^{\text{O}} = \tilde{\mu}$.

The support of $\Lambda(\tilde{\delta}_i^{\text{I}}, \tilde{\delta}_j^{\text{O}})$ is non-negative for any $\tilde{\delta}_i^{\text{I}}, \tilde{\delta}_j^{\text{O}}$. There is a uniform bound B across any $\tilde{\delta}_i^{\text{I}}, \tilde{\delta}_j^{\text{O}}$, such that $\text{Var}[\lambda_{i,j} \tilde{\delta}_j^{\text{O}} | \tilde{\delta}_i^{\text{I}}] < B$ and $\text{Var}[\lambda_{i,j} \tilde{\delta}_i^{\text{I}} | \tilde{\delta}_j^{\text{O}}] < B$.

For each node, its underlying property is given by the underlying degrees $\{\tilde{\delta}_i^I, \tilde{\delta}_i^O\}$. Because the network is directed, two numbers, the underlying in- and out-degrees, *jointly* describe a node. The positive correlation of the in- and out-degree is observed in financial networks.¹ More importantly, the correlation is a key determinant of the systemic response function and hence the equilibrium systemic liquidity.² The model captures this feature of the network structure by the *joint* underlying degree distribution Π .

Notice the realized degrees $\{\delta_i^I, \delta_i^O\}$ are different from the underlying degrees $\{\tilde{\delta}_i^I, \tilde{\delta}_i^O\}$. By definition $\delta_i^I = \sum_j w_{i,j}$ and $\delta_i^O = \sum_k w_{k,i}$. But, under Condition 4, It is easy to verify that the conditional expectations of the realized degrees are the underlying degrees:³

$$\begin{aligned}\mathbb{E} \left[\delta_i^I \mid \tilde{\delta}_i^I \right] &= \tilde{\delta}_i^I, \\ \mathbb{E} \left[\delta_i^O \mid \tilde{\delta}_i^O \right] &= \tilde{\delta}_i^O.\end{aligned}$$

An edge's $(w_{i,j})$ distribution is controlled by $\tilde{\delta}_i^I, \tilde{\delta}_j^O$, which are the underlying degrees of the nodes that the edge connects, because $\Lambda(\tilde{\delta}_i^I, \tilde{\delta}_j^O)$ is parameterized by $\tilde{\delta}_i^I, \tilde{\delta}_j^O$. This setup serves two purposes. First, it identifies the weighted non-assortative matching property as the key property that guarantees the asymptotic results. At the same time, it is deliberately constructed to be flexible to incorporate the various statistical properties of the observed networks.

In the context of the interbank network, weighted non-assortative matching means a bank j with high underlying out-degree has a proportionally high expectation of lending connection to any other bank i , and vice versa:

$$\mathbb{E}(w_{i,j} \mid \tilde{\delta}_i^I, \tilde{\delta}_j^O) \propto \tilde{\delta}_i^I \tilde{\delta}_j^O, \quad \forall \{\tilde{\delta}_i^I, \tilde{\delta}_j^O\}. \quad (4.7)$$

1. Reported in Bech and Atalay (2010).

2. This feature about the directed networks is a new relative to Jackson and Yariv (2007).

3. A verification is provided in Appendix A.1.

From a borrower bank i 's perspective, if its underlying in-degree is larger, the bank has a higher expectation of forming a borrowing connection with any other bank. Importantly, no matter how high or low the borrower bank's $\tilde{\delta}_i^{\text{I}}$ is, in expectation, its borrowing connection intensities are always proportionally greater with high- $\tilde{\delta}_j^{\text{O}}$ lenders.

This weighted non-assortativeness property is the key for the mean-field approximation. Loosely speaking, the property implies that regardless of the borrower's identity, its set of direct lenders is always the same weighted random sampling of the population. The total size of the sample might be different, but those high- $\tilde{\delta}_j^{\text{O}}$ lenders always take up greater expected weights in the random sample, and vice versa. Intuitively this means that the borrower's identity is uncorrelated with the ($\tilde{\delta}_j^{\text{O}}$ -weighted) average property of the lenders. This intuition is formalized as Proposition 3.

Next, I discuss how this random network is general. In equation (4.7), the underlying degrees ($\tilde{\delta}_i^{\text{I}}, \tilde{\delta}_j^{\text{O}}$) only control the conditional *expectation* of $w_{i,j}$, while allowing its conditional distribution to vary with $\{\tilde{\delta}_i^{\text{I}}, \tilde{\delta}_j^{\text{O}}\}$. From any node i 's perspective, a high- $\tilde{\delta}_j^{\text{O}}$ node has either high connecting probability, or high connection intensity conditional on being connected, or mixture of the two. This creates flexibility in generating the networks of different shapes, or statistical properties.

To illustrate, study the following examples:

- $\lambda_{i,j} = 1$ deterministically.

The network is complete. $w_{i,j}$ is proportional to $\tilde{\delta}_i^{\text{I}}\tilde{\delta}_j^{\text{O}}, \forall \{i, j\}$. The mean-field approximation (equation 4.2) is exact even in finite samples.⁴

- $\lambda_{i,j} = 1/p$ with probability p ; otherwise, $\lambda_{i,j} = 0, \forall \{i, j\}$.

The connection probabilities between banks are fixed. Then, the skeleton of \mathbf{W} is an Erdős-Rényi random graphs.⁵ Conditional on being connected, the connection

4. Ignoring the convenience manipulation to zero out the diagonal of \mathbf{W} .

5. A skeleton of a network \mathbf{W} is a network \mathbf{W}' with $w'_{i,j} = \mathbb{1}\{w_{i,j} > 0\}$.

intensity is proportional to $\tilde{\delta}_i^I \tilde{\delta}_j^O$. The first example is a special case when $p = 1$.

- For some fixed ξ , $\lambda_{i,j} = \frac{1}{\xi \tilde{\delta}_i^I \tilde{\delta}_j^O}$ with probability $\xi \tilde{\delta}_i^I \tilde{\delta}_j^O$; otherwise, $\lambda_{i,j} = 0, \forall \{i, j\}$.⁶

Here, the connection probabilities are proportional to $\tilde{\delta}_i^I \tilde{\delta}_j^O$. Conditional on being connected, all connection intensities are the same. This degenerates to an unweighted network similar to the Chung-Lu Model (Chung and Lu, 2002) (Chung and Lu, 2006).⁷ In that model, the random graph is unweighted, and the connection probabilities are proportional to the pre-specified underlying degrees of the nodes at the two ends of each edge. The core-peripheral example (3Eqm40) in subsection 4.8 is simulated from a random network process of this type.

As illustrated by the examples, connection probability $\Pr(w_{i,j} > 0 | \tilde{\delta}_i^I, \tilde{\delta}_j^O)$ is not restricted. By varying distribution $\Lambda(\tilde{\delta}_i^I, \tilde{\delta}_j^O)$, different connection structures can be admitted. Beyond the examples given above, $\lambda_{i,j}$ does not need to take binomial values, and $\Pr(\lambda_{i,j} > 0 | \tilde{\delta}_i^I, \tilde{\delta}_j^O)$ does not need to take the product form. This flexibility allows for the various statistical properties of the observed unweighted connection structures, including the core-peripheral structure that is reported to describe several financial networks.⁸

A few empirical works investigate the assortativeness of financial networks. For example, Bech and Atalay (2010) examine the federal funds network. It documents that the borrower bank’s degree is uncorrelated with the average degree of the lender *weighted* by connection value.⁹ This fact justifies the weighted non-assortativeness condition. For unweighted degrees (the skeleton’s degree, i.e. the cardinal number of direct lenders), the paper

6. ξ must be chosen to guarantee $\xi \tilde{\delta}_i^I \tilde{\delta}_j^O \in [0, 1], \forall \{i, j\}$.

7. The Chung-Lu model is a family of unweighted and undirected random graphs with given “expected degree” of nodes (like the underlying degrees here). Their studies are not about games played on the network. Rather, they focus on power law random graphs (with power law degree distribution) and examine the large number properties of the measures of the graph structure itself, for example the average distance, diameter, and size of the dense subgraph.

8. Bech and Rørdam (2008), Bech and Atalay (2010), and Craig and von Peter (2014) report core-peripheral financial network structures.

9. Figure B.1 in Appendix B copies the correlation plot reported in their paper.

documents that the network is disassortative, in the sense that the unweighted degree of a bank is negatively related with the average degrees of its lenders.¹⁰ The disassortative relationships are most pronounced for small-degree banks, which connect to large-degree banks disproportionately more often.¹¹

4.4 Definitions of Equilibrium Concepts

Given a network realization \mathbf{W} and a uniformly continuous individual best response function f , define the following equilibrium concepts:

DEFINITION 5 (Original Equilibrium).

The original equilibrium is the vector of actions \mathbf{x} , such that

$$x_i = f \left(\sum_j w_{i,j} x_j \right), \quad \forall i. \quad (4.8)$$

Alternatively, the equilibrium condition in vector format is $\mathbf{x} = \mathbf{f}(\mathbf{W}\mathbf{x})$.

DEFINITION 6 (Systemic Average).

For any vector \mathbf{x} , define the associated systemic average x^ as the out-degree-weighted average:*

$$x^* = \sum_j \frac{\delta_j^O}{n\mu} x_j.$$

Notice the systemic average, like the two equilibrium concepts, is defined with respect to the network realization, hence a random variable.

10. A similar result is reported in Soramäki, Bech, Arnold, Glass, and Beyeler (2006) for the interbank payment flows network.

11. A conjecture is this is due to truncation bias. Some small-to-small connections' intensities are too small to be identified as a connection. As a result, in a large-degree bank's direct lender set, the equal-weighted average overweights the contribution of small banks, causing the negative correlations. If this is true, the matching is still non-assortative if weighted by connection intensity.

DEFINITION 7 (Systemic Equilibrium).

The systemic equilibrium is the vector of actions $\hat{\mathbf{x}}$, such that

$$\hat{x}_i = f(\delta_i^I \hat{x}^*), \quad \forall i,$$

where \hat{x}^* is the systemic average associated with $\hat{\mathbf{x}}$ as defined in Definition 6.

Taking the out-degree-weighted average of the above equilibrium conditions across i , we arrive at the equilibrium condition with respect to systemic average \hat{x}^* :

CONDITION 6 (Systemic Equilibrium Condition).

$$\hat{x}^* = \sum_i \frac{\delta_i^O}{n\mu} f(\delta_i^I \hat{x}^*).$$

DEFINITION 8 (Systemic Response Function).

Define systemic response function as $f^*(x) = \sum_i \frac{\delta_i^O}{n\mu} f(\delta_i^I x)$.

I will refine the focus on systemic equilibria that are locally stable. A equilibrium can be not locally stable, in the sense that small perturbations in x^* cause the system to move away from the equilibrium.¹²

DEFINITION 9 (Local Stability).

An one dimensional fixed point x of any function f is locally stable if there exist $\epsilon > 0$ such that

$$\begin{aligned} f(x) &> x, & \forall x \in (x - \epsilon, x) \cap [0, \infty), \text{ and} \\ f(x) &< x, & \forall x \in (x, x + \epsilon) \cap [0, \infty). \end{aligned}$$

If f^* is locally differentiable, the refined condition for locally stable systemic liquidity equi-

12. Jackson and Yariv (2007) provides a similar refinement.

librium is

$$x^* = f^*(x^*), f^{*'}(x^*) < 1.$$

4.5 Intermediate Results

This subsection provides intermediate results in the style of laws of large number on the random network, which is later used in showing the main statements. The essence of the analysis of the systemic behavior is studying the (properly weighted) averages on large random networks. Meanwhile, non-assortative matching (Condition 4) regulates the expectation the network \mathbf{W} . Hence, it is intuitive to expect that the averages should converge to the corresponding expectations. However, the degrees and equilibrium actions are not independently distributed across nodes, making the existing laws of large number not suitable. That is why I first build the versions of law of large numbers catered for random networks.

Sample degrees (δ_i^I, δ_i^O) are identically but *dependently* distributed, although the underlying degrees $(\tilde{\delta}_i^I, \tilde{\delta}_i^O)$ are i.i.d. To see this, suppose in a sample, all else equal, node i draws a higher underlying in-degree $(\tilde{\delta}_i^I)$. This leads to a higher propensity of the sample in-degree (δ_i^I) obviously. And it also leads to higher sample out-degrees for any other node j , because its connection to i ($w_{i,j}$) is now expected to be higher as well. On top of this, the dependency can soon become complicated due the degree correlations and network connections.

But we still have the following law of large number of sample degrees:

LEMMA 1 (Law of Large Numbers of Sample Degrees).

Suppose the random network is generated as in Definition 4, and satisfies the weighted non-assortativeness and distributional conditions (Conditions 4 and 5). Let $\phi(\delta_i^I, \delta_i^O)$ be a uniformly continuous function. Then, the weak law of large number holds for the sample degrees

upon mapping ϕ ,

$$\text{plim}_{n \rightarrow \infty} \frac{1}{n} \sum_i \phi(\delta_i^{\text{I}}, \delta_i^{\text{O}}) = \mathbb{E}\phi(\tilde{\delta}_i^{\text{I}}, \tilde{\delta}_i^{\text{O}}).$$

Proof. See Appendix A.4. □

To prove the lemma, first, it is straightforward that $\text{plim}_{n \rightarrow \infty} \frac{1}{n} \sum_i \phi(\tilde{\delta}_i^{\text{I}}, \tilde{\delta}_i^{\text{O}}) = \mathbb{E}\phi(\tilde{\delta}_i^{\text{I}}, \tilde{\delta}_i^{\text{O}})$, since the underlying degrees are i.i.d. It remains to show that the sample degrees converges to the underlying degrees uniformly across nodes. That is $\forall \psi > 0$,

$$\Pr\left(\left|\delta_i^{\text{O}} - \tilde{\delta}_i^{\text{O}}\right| < \psi, \forall i\right) \rightarrow 1, \quad \Pr\left(\left|\delta_i^{\text{I}} - \tilde{\delta}_i^{\text{I}}\right| < \psi, \forall i\right) \rightarrow 1, \quad n \rightarrow \infty.$$

The original equilibrium actions are also not independently distributed, making studying its mean-field approximation hard. To prepare for that analysis, I first show the mean-field approximations error (as in equation 4.2) of any independent nodal random variable \tilde{x}_i converges to zero in probability in large networks. \tilde{x}_i is introduced as an generic nodal property besides $\tilde{\delta}_i^{\text{I}}, \tilde{\delta}_i^{\text{O}}$, put in place for the original equilibrium action x_i .

Specifically, let $\tilde{\mathbf{x}}$ be an vector of i.i.d. nodal property. We allow it to be dependent of $\{\tilde{\delta}_i^{\text{I}}, \tilde{\delta}_i^{\text{O}}\}$, but independent of $\lambda_{i,j}$. Then it is shown that the systemic average of $\tilde{\mathbf{x}}$ and the connection-weighted average of $\tilde{\mathbf{x}}$ for each node's in-neighbors are asymptotically close:

PROPOSITION 3 (Mean-Field Approximation for any Independent Nodal Property).

Suppose the random network is generated as in Definition 4, both Conditions 4 and 5 are satisfied. Let $\{\tilde{\delta}_i^{\text{I}}, \tilde{\delta}_i^{\text{O}}, \tilde{x}_i\}_{i=1}^n$ be independently generated from the joint distribution $\Pi^J(\tilde{\delta}^{\text{I}}, \tilde{\delta}^{\text{O}}, \tilde{x})$, of which $\Pi(\tilde{\delta}^{\text{I}}, \tilde{\delta}^{\text{O}})$ is the marginal distribution, Then, the mean-field approximation error (as in equation 4.2) convergences in probability to zero as the number of nodes (n) increases:

$$\text{plim}_{n \rightarrow \infty} \sum_j \frac{w_{i,j} \tilde{x}_j}{\delta_i^{\text{I}}} - \tilde{x}^* = 0, \quad \forall i,$$

where $\tilde{x}^* = \sum_j \frac{\delta_j^O}{n\mu} \tilde{x}_j$ is the systemic average of $\tilde{\mathbf{x}}$ as defined in Definition 6.

Proof. See Appendix A.5. □

The lemma confirms the main intuition of the mean-field approximation discussed in Subsection 4.1. The loose discussion there is based on the assumption that the distributions of nodal properties $\tilde{\mathbf{x}}$ are the same in the whole network and each node's in-neighborhood. That is the case here: \tilde{x}_j is independent of $w_{i,j}$ conditional on $\tilde{\delta}_j^I, \tilde{\delta}_j^O, \forall i$. But that is not the case for the original equilibrium \mathbf{x} , which is a dependent of \mathbf{W} . It could be the case that $w_{i,j}$ and x_j are correlated across j for some i , rendering the random sampling intuition not applicable. Therefore, it is not rigorous to directly apply this intuition in analyzing the probability limit of an original equilibrium. The problem is dealt with next in the proof of Propositions 5 and 6.

4.6 Equilibrium Asymptotics

This subsection derives the main result that any systemic equilibrium is close to an original equilibrium in large random networks. More precisely, the result is for any systemic equilibrium, there is an original equilibrium, whose systemic average is arbitrarily close to that of the systemic equilibrium (at arbitrarily high probability, for large n). The overall logic leading to that result is both the equilibrium constructions converge to the same deterministic probability limit. First, Lemma 2 and Proposition 4 show the convergence of the systemic equilibrium and establish the probability limit. Then, Propositions 5 and 6 use Brouwer's fixed-point theorem to show the existence of an original equilibrium within an infinitesimal neighborhood of that limit. Finally, Proposition 7 combines the convergence result of the two equilibrium constructions to reach the main result.

LEMMA 2 (Systemic Response Function Convergence).

Suppose the random network is generated as in Definition 4, and both Conditions 4 and 5 are

satisfied. The systemic response function $f^{*[n]}(x) = \sum_i \frac{\delta_i^O}{n\mu} f(\delta_i^I x)$ converges in probability to a function \tilde{f}^* called the underlying systemic response function.

$$f^{*[n]}(x) \xrightarrow{p} \frac{1}{\tilde{\mu}} \mathbb{E} \left[\tilde{\delta}^O f(\tilde{\delta}^I x) \right] := \tilde{f}^*(x), \quad n \rightarrow \infty, \forall x. \quad (4.9)$$

This lemma is a direct application of the convergence of the sample degrees (Lemma 1). The proof is in Appendix A.6.

Given the underlying systemic response function \tilde{f}^* , define the *underlying systemic average* \tilde{x}^* as any locally stable fixed point (Condition 9) of \tilde{f}^* . Although there can be multiple \tilde{x}^* , each one is deterministic just like \tilde{f}^* . \tilde{x}^* is an important construction. It is the probability limit of both the systemic and original equilibrium, as respectively shown in Proposition 4 and Proposition 6 next. It

The underlying systemic response function \tilde{f}^* is determines the underlying systemic average. It contains all information about the dynamics of systemic equilibrium in large networks. Given the importance of \tilde{f}^* , the following analyses revolve around characterizing it. Its shape and number of associated \tilde{x}^* is studied in Subsection 4.8. Chapter 5 explores how \tilde{f}^* and its fixed points change when the network structure is changed exogenously.

Notice as shown by lemma 2, \tilde{f}^* is determined by only the joint distribution of the underlying in- and out-degrees Π and the individual best response function f . The underlying degree distribution Π sufficiently summarizes the network structure (\mathbf{W}) in determining \tilde{f}^* . The pairwise connection distribution Λ , which determines the edge realizations $w_{i,j}$, is irrelevant, as long as it is non-assortative. That is to say, neglecting the pairwise information does not hurt studying the systemic behavior. Only degree distribution matters, which is a nodal property. This formalizes the discussion in Subsection 4.2 that the local connection structure is irrelevant to how individual responses are aggregated into the systemic behavior. Empirically, in financial networks, bank-to-bank or other pairwise information is scarcely available. However, the in- and out-degrees can be constructed from just bank-level information, which

is more feasible. This shall provide new insights for empirical exercises and system-wide risk monitoring.

PROPOSITION 4 (Systemic Equilibrium Convergence).

Let $\hat{\mathbf{x}}^{[n]}$ be any sequence of systemic equilibria. $\forall \epsilon > 0$, there exists an underlying systemic average $\tilde{x}^{*[n]} \in \{\tilde{x}^*\}$ which is within distance ϵ to $\hat{\mathbf{x}}^{[n]}$'s systemic average $\hat{x}^{*[n]}$, with converging probability:¹³

$$\Pr \left(\left| \hat{x}^{*[n]} - \tilde{x}^{*[n]} \right| < \epsilon \right) \rightarrow 1, \quad n \rightarrow \infty.$$

Proof. See Appendix A.7. □

Having established the probability limit of the systemic equilibrium, now we turn the attention to the asymptotics of the original equilibrium.

I rely on Brouwer's fixed-point theorem to look for an original equilibrium. Define mapping $\mathcal{M} : \mathbb{R}^n \rightarrow \mathbb{R}^n$ as $\mathcal{M} = \mathbf{f}(\mathbf{W}\mathbf{x})$. Construct a random sequence of vectors $\tilde{\mathbf{x}}^{[n]}$ as $\tilde{x}_i^{[n]} = f \left(\tilde{\delta}_i^{\mathbf{I}} \tilde{x}^* \right)$. $\tilde{\mathbf{x}}^{[n]}$ will serve as the benchmark to look for an original equilibrium. I want to show that there is an infinitesimal compact and convex neighborhood \mathbb{S} around $\tilde{\mathbf{x}}^{[n]}$, such that $\mathcal{M}(\mathbb{S}) \subseteq \mathbb{S}$ in order to apply the fixed point theorem.

The argument has two steps. First, Proposition 5 shows that $\mathcal{M}(\tilde{\mathbf{x}}^{[n]}) - \tilde{\mathbf{x}}^{[n]} \xrightarrow{p} 0$. That is to say the benchmark's image can be arbitrarily close to itself as n increases. Then, in the proof of Proposition 6, I construct an \mathbb{S} around $\tilde{\mathbf{x}}^{[n]}$ such that the probability limit of $\mathcal{M}(\mathbb{S})$ is a proper subset of \mathbb{S} with a positive margin. Therefore, even adding the limiting errors, we still have $\mathcal{M}(\mathbb{S}) \subseteq \mathbb{S}$.

PROPOSITION 5 (Probability Limit of the Original Equilibrium Condition).

Suppose the random network is generated as in Definition 4, and both Conditions 4 and 5 are satisfied. Then sequence $\tilde{\mathbf{x}}^{[n]}$, defined as $\tilde{x}_i^{[n]} = f \left(\tilde{\delta}_i^{\mathbf{I}} \tilde{x}^* \right), \forall i$, satisfies the original

13. $\{\tilde{x}^*\}$ denotes the set of all \tilde{x}^* 's.

equilibrium condition in the probability limit:

$$\text{plim}_{n \rightarrow \infty} \tilde{x}_i^{[n]} - f \left(\sum_j w_{i,j} \tilde{x}_j^{[n]} \right) = 0, \quad \forall i.$$

Proof. See Appendix A.8. □

Proposition 5 directly applies the mean-field approximation result of Proposition 3. Because $\tilde{x}_j^{[n]} = f(\tilde{\delta}_j^I \tilde{x}^*)$ is independent across j , $\tilde{\mathbf{x}}^{[n]}$ satisfies the precondition of Proposition 3. Therefore, the proposition can be applied to calculate the limit of $\sum_j w_{i,j} \tilde{x}_j^{[n]}$.

PROPOSITION 6 (Original Equilibrium Convergence).

Given any underlying systemic average \tilde{x}^ , $\forall \epsilon > 0$, the probability that there exists an original equilibrium whose systemic average is within $\tilde{x}^* \pm \epsilon$ converges to one as n goes to infinity. That is to say, for any underlying systemic average \tilde{x}^* , there is a sequence of original equilibrium $\mathbf{x}^{[n]}$ with systemic average $x^{*[n]}$, s.t.*

$$x^{*[n]} \xrightarrow{P} \tilde{x}^*, \quad n \rightarrow \infty.$$

Proof. See Appendix A.9. □

The key of the proof is to construct an infinitesimal compact and convex set \mathbb{S} around $\tilde{\mathbf{x}}^{[n]}$, such that $\mathcal{M}(\mathbb{S}) \subseteq \mathbb{S}$. The idea of the construction is as follows. For any $\mathbf{x} \in \mathbb{S}$, consider its offset relative to the benchmark $\mathbf{e} = \mathbf{x} - \tilde{\mathbf{x}}^{[n]}$. \mathbf{e} can be decomposed into two components, one parallel and another orthogonal to $\tilde{\delta}^O$ respectively. Only the parallel component affects the systemic average of \mathbf{x} . Loosely speaking, the probability limit of \mathcal{M} is \tilde{f}^* . Hence, only the offset component that affects the systemic average (x^*) has effects on the image. Moreover, notice this is a contraction mapping, because \tilde{f}^* is a contraction mapping in the neighborhood of its locally stable fixed point \tilde{x}^* . The change of $\mathcal{M}(\mathbf{x})$'s systemic average must be smaller than the change of \mathbf{x} 's, by a positive margin parallel offset must be smaller

than that of \mathbf{x} by a positive margin. That is to say, $\mathcal{M}(\mathbf{x})$'s parallel offset is smaller than that of \mathbf{x} by a positive margin.

Given these observations, \mathbb{S} is constructed according to the decomposition. On the parallel direction, select \mathbf{x} such that $x^* - \tilde{x}^*$ within $\pm\epsilon$. On the orthogonal direction, choose the convex hull of the projection image of such $\mathcal{M}(\mathbf{x})$.

PROPOSITION 7 (Systemic Equilibrium Approximates the Original Equilibrium).

$\forall \epsilon, \psi > 0$ there exists an N , such that for any systemic equilibrium $\hat{\mathbf{x}}^{[n]}$ in large networks of $n > N$, there exist an original equilibrium $\mathbf{x}^{[n]}$ whose systemic average is within ϵ distance to that of $\hat{\mathbf{x}}^{[n]}$ at a probability greater than $1 - \psi$. In other words, $\forall \hat{\mathbf{x}}^{[n]}, \exists \mathbf{x}^{[n]}$ s.t.

$$\hat{x}^{*[n]} - x^{*[n]} \xrightarrow{p} 0, \quad n \rightarrow \infty.$$

Proof. See Appendix A.10. □

4.7 Numerical Verification with Observed Networks

This subsection presents numerical exercises with real-world observed financial networks. In addition to justifying the accuracy of the systemic equilibrium by studying its asymptotic properties, this section shows it is practically accurate in small networks. The idea for the verification exercises is very simple: numerically compute both the original and systemic equilibria in observed networks and examine whether their differences are small.

The inputs of the verification exercise are the individual response function f and the observed network \mathbf{W} . For f , I use the interbank lending one in Chapter 3. The primitive values (β, γ, d) and the shape of f are reported in Figure B.2 in Appendix B.

Two data sources provide two observed networks (\mathbf{W}) to conduct the exercise with. The first one, coded `Diebold13`, is the estimated interconnectedness among 13 major U.S. financial institutions by Diebold and Yilmaz (2011). They use variance decomposition of the high-frequency realized volatility data of the financial institutions to measure the directed

and weighted pairwise connectedness. I treat the estimated volatility shock exposure of a bank to another as the interbank lending intensity specified in my model. The second observed network, coded `Europe14`, is 14 European country consolidated bank cross-holdings, reported by the Bank for International Settlements “The International Banking Market” report.¹⁴ The interbank lending intensities are observed from the cross-holding shares directly, treating each country as a bank node. The same dataset is used in Elliott et al. (2014) to illustrate their model.¹⁵ The visualization of the two networks are shown in Figure 4.1.

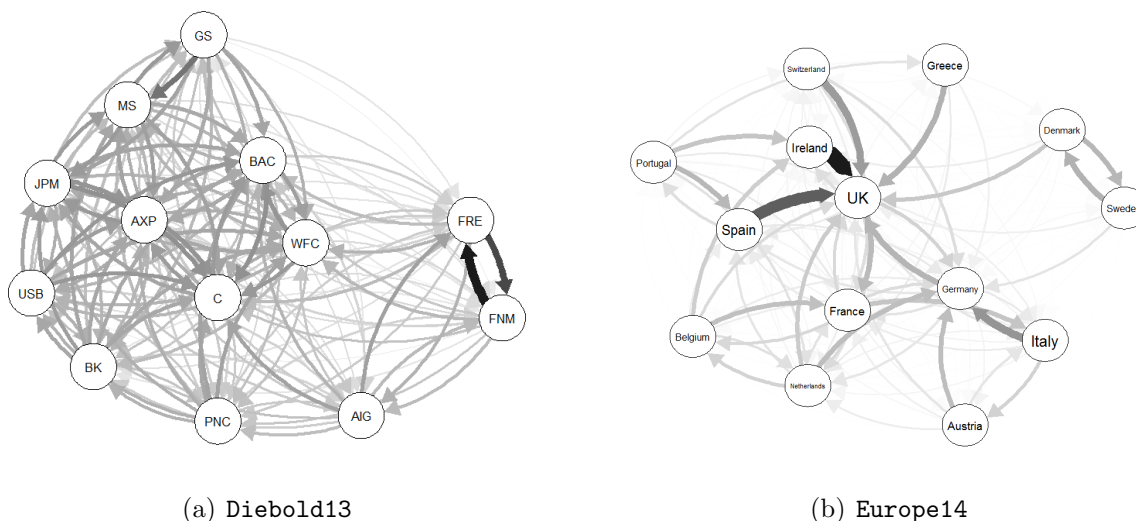


Figure 4.1: Observed Networks Visualization

The width and shade of the arrows represents connection intensity ($w_{i,j}$). The layout of the nodes is given by an algorithm such that more connected nodes are closer. The graphs are produced with R package `qgraph`.

For each configuration, I conduct the same numerical experiment. First calculate the original equilibrium by solving equation (4.8) in Definition 5.¹⁶ To compare, I also report the systemic average of original equilibrium. Then I calculate the systemic equilibrium by

14. Table 9B, “Consolidated claims of reporting banks on individual countries: foreign claims by nationality of reporting banks, immediate borrower basis”.

15. They picked 6 European countries, whereas I reconstructed the data for all 14 European countries with observable international lending and borrowing. Using the sub-graph of the 6 countries they pick does not change the results.

16. The numerical algorithm looks for the positive stable equilibrium by iterating the fixed point condition from a very large vector $\{x_i\}$ until numerical convergence.

solving Condition 6. I report the positive locally stable systemic equilibrium. From that, the equilibrium actions $\{x_i\}$ are backed out as in equation (4.6). The results are plotted in Figure 4.2.

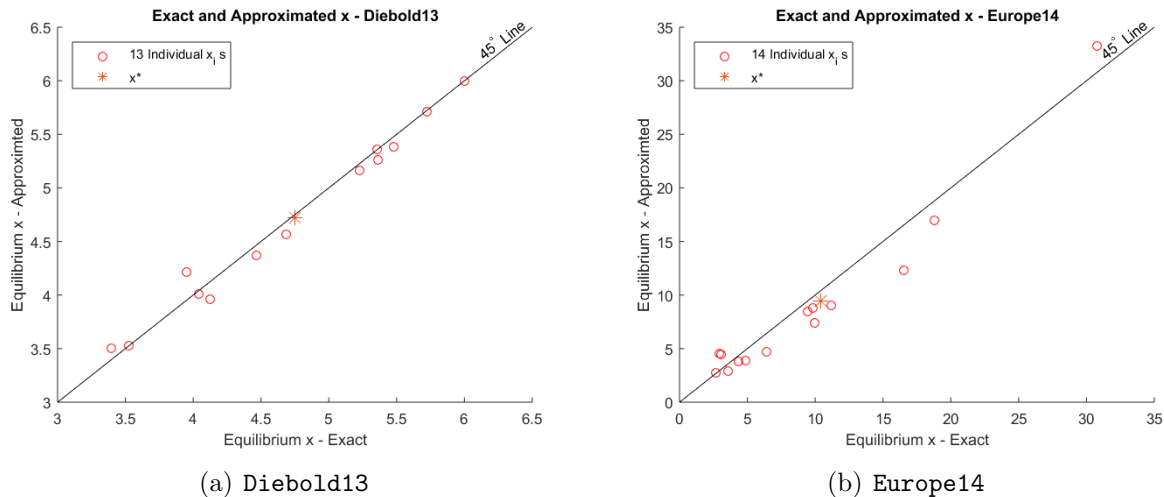


Figure 4.2: Exact and Approximated Equilibrium Comparison

Each circle represents the equilibrium illiquid lending (x_i) for a bank in the network. The star marker shows the out-degree weighted average of x_i , the systemic liquidity (x^*). Their horizontal coordinates are the exact original equilibrium levels. The vertical coordinates are the approximated systemic equilibrium levels. The vertical offsets of the markers from the 45° show the approximation error relative to the original equilibrium.

Figure 4.2 shows the systemic equilibrium is accurate in comparison to the numerically solved original equilibrium. As shown in the plots, both individual x_i and x^* align with the 45° line well. In detail, the approximation errors are generated in two layers. First, the x^* solved from the systemic liquidity approximation does not exactly reproduce the x^* associated with the exact equilibrium. In the plots, the star markers representing x^* are slightly off the 45° line slightly. On top of that, the individual equilibrium play (x_i) is approximated by the bank's in-degree as in equation (4.2). Even if x^* were recovered accurately, there is mean-field approximation error, which only disappears in large samples, as analyzed in Subsection 4.6. However, even with the overlapping sources of error, the systemic equilibrium is fairly close. More importantly, the research interest focuses on the systemic behavior. The fact that x^* is accurate justifies the application of mean-field analysis

to studying systemic liquidity crunches. The accuracy of the individual illiquid lending level is of secondary importance in this application.

The robustness of the numerical verification is established by varying the two inputs f and \mathbf{W} . First, I experiment with the different configurations of the individual response function. Figure B.3 in Appendix B compares the equilibrium x^* in the two equilibrium constructions with varying β . It shows the systemic liquidity equilibrium is constantly close to the exact equilibrium with different f . This comparative statics exercise shows the decrease in β can trigger a discontinuous crunch in systemic liquidity. The plot shows if β is below a certain threshold level, the cooperative systemic liquidity equilibrium can no longer be sustained. The intuition is similar to the β comparative statics conducted with the circle example network in Subsection 3.9.

The following analyses involves several other numerical exercises with different \mathbf{W} . Section 5.2 shows a series of networks as perturbed version of the two presented here, with a subset of nodes removed. Section 4.8 shows an example of simulated network. The systemic equilibrium is shown to be close to the original equilibrium in these scenarios as well.

4.8 Shape of f^* and Number of Equilibria

This subsection specializes to the network games of the interbank lending scenarios (with an f as in equation 3.1). I analyze the relationship between the network shape and the shape of the systemic response function f^* , which is the key to study the systemic behavior. I put particular emphasis on the conditions of the degree distribution such that f^* implies at most two locally stable systemic equilibria.

I find in normal situations, f^* displays the S-shape similar to the individual best-response function (f) depicted in Figure 3.3 or Figure 3.5. Yet f^* 's S-shape is more rounded, because it is the weighted average of individual f , which is kinked. Consequently, there are typically either one or two locally stable systemic equilibria, depending on the general attitude of the S-shape. However, if the in-degree distribution is multi-modal, f^* might have more than

one inflection point, forming a curve of two or more connected S-shapes, resulting in the possibility of more than two equilibria.¹⁷

First define effective connectedness, a one-dimensional statistic of \mathbf{W} , which will arise as the center quantity connecting the network structure to the general attitude of the f^* curve.

DEFINITION 10 (Effective Connectedness).

Effective connectedness of a network \mathbf{W} is the out-degree weighted in-degree $W^ = \sum_i \frac{\delta_i^O}{n\mu} \delta_i^I$.*

Start analyzing from the definition of f^* (Definition 8), $f^*(x) = \sum_i \frac{\delta_i^O}{n\mu} f(\delta_i^I x)$. Define $h(x) = f(x) - x$, $h^*(x) = f^*(x) - W^*x$, which are the counterparts of f and f^* after removing the linear general trends:

$$\begin{aligned} f^*(x) &= \sum_i \frac{\delta_i^O}{n\mu} h(\delta_i^I x) + W^*x, \\ h^*(x) &= \sum_i \frac{\delta_i^O}{n\mu} h(\delta_i^I x). \end{aligned}$$

It is suffice to analyze the shape of h^* . From policy function (equation 3.1), h is the piecewise linear function:

$$h(x) = \begin{cases} 0 & x \in [0, y_l) \\ u(x - y_l) & x \in [y_l, y_h) \\ d & x \in [y_h, +\infty). \end{cases}$$

where the shorthands are $u = \frac{\beta}{1-\beta}$, $y_l = \frac{\gamma}{\beta}$, $y_h = \frac{1-\beta}{\beta}d + \frac{\gamma}{\beta}$. y_l, y_h cut the domain of interbank funding into the three regions: full cash, liquidity hoarding, and depositor-run-proof non-binding, as discussed in Subsection 3.6.

For small $x \leq y_l/\delta_{max}^I$, $h^*(x) = 0$. This means $f^*(x) = W^*x, \forall x \in [0, y_l/\delta_{max}^I)$, the lowest systemic liquidity interval in which even the bank with the highest funding connection

17. Again, I am only counting locally stable systemic liquidity approximation equilibria as defined in Definition 9.

(δ^I) is in the full cash region.¹⁸ It is easily verified that $W^* < 1$ under Condition 1. Combined, this implies that $x^* = 0$ always constitutes a locally stable equilibrium.

For $x \geq y_h/\delta_{min}^I$, $h^*(x) = d$. That is $f^*(x) = W^*x + d$. In the highest (potentially off-equilibrium) systemic liquidity level, even the lowest δ^I bank is depositor-run-proof non-binding. The system-wide cash-hoarding would be zero in this highest efficiency allocation.

In the more relevant middle interval, h^* is continuous, piece-wise linear, and non-decreasing. But what about its convexity? How many inflection points? These properties affect the number of equilibria. If a single inflection point separates the the middle section of h^* into a convex region and a concave intervals, then f^* is S-shaped, and there are at most two locally stable equilibria. Otherwise, if h^* has more “waves”, there might be more than two.

Take derivative of the piece-wise linear h^* ,¹⁹

$$\begin{aligned} h^{*'}(x) &= \sum_i \frac{\delta_i^O \delta_i^I}{n\mu} h'(\delta_i^I x) \\ &= uW^* \sum_i \frac{\delta_i^O \delta_i^I}{n\mu W^*} \mathbb{1}_{[\frac{y_l}{x}, \frac{y_h}{x})}(\delta_i^I) \end{aligned} \quad (4.10)$$

The summation can be interpreted as the $(\delta_i^O \delta_i^I)$ -weighted number of banks that are in the liquidity hoarding region, if systemic liquidity is x . Notice the weights (the first term in the summation) are normalized.

$f^{*'}(x) = h^{*'}(x) + W^*$ is the marginal systemic response, which is the aggregate of each bank’s individual liquidity response policies. If a bank is in the liquidity hoarding region, its marginal supply f' is more sensitive. Therefore $h^{*'}$ counts the number of banks that are in the liquidity hoarding region. However, the sum must be weighted by $\delta_i^O \delta_i^I$, since a bank that has greater access of interbank funding (high δ^I) and/or contributes more back to the

18. δ_{max}^I stands for the largest in-degree in the network. Similarly, δ_{min}^I represents the smallest positive in-degree. Including banks with zero in-degree is trivial, since those banks always play zero lending, and has no effect on others.

19. Here, I assign the derivatives at the kink points such the the derivative step function is right continuous. Therefore, $h'(y) = \mathbb{1}_{[y_l, y_h)}(y)$. $\mathbb{1}_{\mathbf{A}}(x)$ represents the indicator function, valued one if $x \in \mathbf{A}$ and zero otherwise.

system (high δ^O) plays a greater role in the aggregate systemic response of the marginal increase in systemic liquidity.

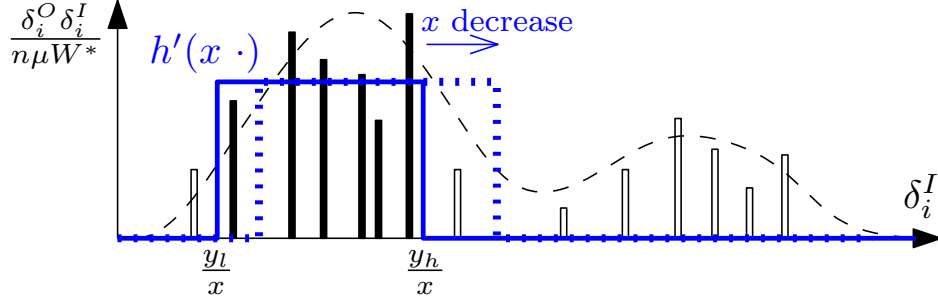


Figure 4.3: Graphical Representation of $h^{*I}(x)$

The summation expression $\sum_i \frac{\delta_i^O \delta_i^I}{n \mu W^*} \mathbb{1}_{[\frac{y_l}{x}, \frac{y_h}{x}]}(\delta_i^I)$ as in equation (4.10) can be interpreted as the $(\delta_i^O \delta_i^I)$ -weighted number of banks that are in the liquidity hoarding region. The vertical bars represent $(\delta_i^O \delta_i^I)$ -weights for each bank. Each bar's horizontal position is δ_i^I . The blue boxcar function maps δ^I to $h'(x \delta^I)$, or equivalently expressed as $\mathbb{1}_{[\frac{y_l}{x}, \frac{y_h}{x}]}(\delta_i^I)$. The solid bars represent the banks that are in the liquidity hoarding region given current x . The sum of the solid bars represents the summation in equation (4.10). The dashed curve represents the underlying probability density $\pi^t(\delta^I)$. The area under it within the interval $(\frac{y_l}{x}, \frac{y_h}{x})$ is the population counterpart \tilde{h}^{*I} shown as the integral in equation (4.11).

As in Figure 4.3, due to the discrete distribution of δ_i^I , little can be asserted about the properties of $h^{*I}(x)$ besides it is a non-negative step function. It can be locally rugged due to the discrete inclusions and exclusions of δ_i^I 's as x moves. Therefore, we study the population counterpart of the degree distribution. Let $\pi(\tilde{\delta}^I)$ be the marginal distributions associated with Π .

LEMMA 3 (Population Counterpart of $h^{*I}(x)$).

*Suppose the random network is generated as in Definition 4, and both Conditions 4 and 5 are satisfied. Then $h^{*I}(x)$ converges in probability to its population counterpart denoted as \tilde{h}^{*I} ,*

$$\text{plim}_{n \rightarrow \infty} h^{*I}(x) = \tilde{W}^* \int_0^{+\infty} h'(\tilde{\delta}^I x) \pi^t(\tilde{\delta}^I) d\tilde{\delta}^I := \tilde{h}^{*I}(x) \quad (4.11)$$

where $\tilde{W}^* = \frac{\mathbb{E}[\tilde{\delta}^O \tilde{\delta}^I]}{\tilde{\mu}}$ is the population counterpart of W^* ,

and $\pi^t(\tilde{\delta}^I)$ is a transformed marginal probability density function of $\tilde{\delta}^I$ such that the Radon-Nikodym derivative with respect to the natural probability $\pi(\tilde{\delta}^I)$ is proportional to $\tilde{\delta}^I \mathbb{E}[\tilde{\delta}^O | \tilde{\delta}^I]$,

$$\pi^t(\tilde{\delta}^I) = \frac{\tilde{\delta}^I \mathbb{E}[\tilde{\delta}^O | \tilde{\delta}^I]}{\mathbb{E}[\tilde{\delta}^O \tilde{\delta}^I]} \pi(\tilde{\delta}^I). \quad (4.12)$$

Proof. See Appendix A.11. □

DEFINITION 11 (Unimodal Function and Distribution).

A univariate function $\pi(x)$ is said to be unimodal if $\exists m$, s.t. $\pi(x)$ is weakly increasing for $x \leq m$ and weakly decreasing for $x \geq m$. A univariate distribution is said to be unimodal if its density function is unimodal. m is called mode.

It is desirable to know under what conditions $\tilde{h}^{*'} is a unimodal function, because when $\tilde{h}^{*'} is unimodal, \tilde{h}^* is composed of a convex interval followed by a concave interval, or S-shaped. In that case, there can be at most two equilibria.$$

PROPOSITION 8 (Sufficient Condition for at Most Two Equilibria).

If $\mathbb{E}[\tilde{\delta}^O | \tilde{\delta}^I] \pi(\tilde{\delta}^I)$ is unimodal, then \tilde{f}^* is composed of a convex interval followed by a concave interval, separated by an inflection point. Consequently, there can be at most two locally stable equilibria for $x^* = \tilde{f}^*(x^*)$.

Proof. See Appendix A.12. □

As x^* changes from high to low, banks with low in-degree are the first to exit from the liquidity hoarding region and reach full cash hoarding region. This generally causes the system-wide liquidity hoarding to subside, as $\tilde{h}^{*'} decreases. However, consider the case where there is another mode that is significantly distinct from the first one. When x^* further decreases, these bank with high in-degrees just begin to shift into the liquidity hoarding region. This causes a second wave of system-wide liquidity hoarding, characterized by another mode in $\tilde{h}^{*'} , or equivalently another S-shape in \tilde{h}^* .$$

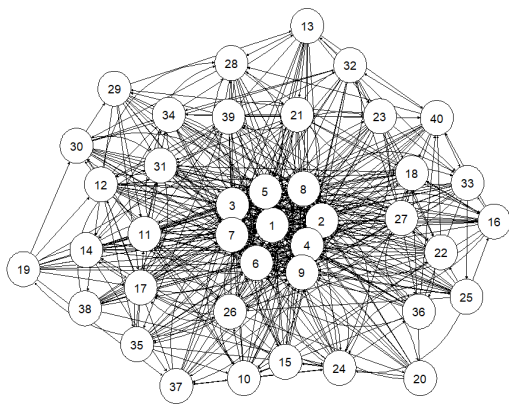
Taken together, if the in-degree distribution is K -modal, \tilde{h}^* might have at most K waves, and equivalently \tilde{f}^* has at most K consecutive S-shaped regions. Then there could be at most $K+1$ equilibria (along with the zero-equilibrium) if the \tilde{f}^* curve happens to be crossing the 45° line back and forth for every S-shaped regions.

Nonetheless, this is the only form of more than two equilibria. Proposition 8 provides a *sufficient* condition that unimodality implies at most two equilibria.

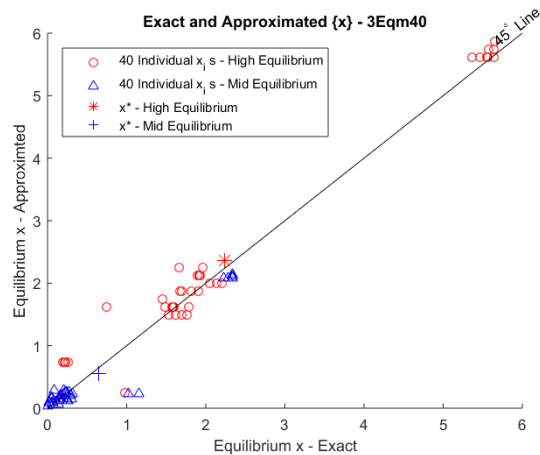
Bi-modal in-degrees could be plausible in real interbank networks if there is distinct dichotomy of the core and peripheral banks. Hence I provide a simulated network example to better demonstrate the intuition gained in the above analysis.

The simulation follows the random network generating process in Definition 4. For degree distribution Π , I specifying two kinds of underlying in-degrees. The core banks have higher underlying in-degrees than the peripheral. This dichotomy structure gives the bi-modal in-degree distribution, satisfying the necessary condition to obtain more than two equilibria. Every node has the same underlying out-degree. The connection intensity distribution Λ follows the third case in the examples in Section 4.3. That is, the probability of having a connection between node i, j is proportional to $\tilde{\delta}_i^I \tilde{\delta}_j^O$, while conditional on connected, all connections have the same intensity (w). The connection intensity is then numerically chosen so that f^* has the right attitude to give three locally stable equilibria. The simulated network is presented in Figure 4.4 Panel (a), and the realized in and out-degree distribution are reported in Appendix B Figure B.4.

As shown in panel (b), in the highest systemic equilibrium, both the core and the peripheral banks enjoy positive interbank funding and choose positive actions. The core banks choose discontinuously high x_i because they are connected to much more lenders. In the middle equilibrium, systemic liquidity (the blue cross marker) is lower. The peripheral bank suffers liquidity hoarding and choose x_i close to zero. The core banks manage to sustain cooperation just within themselves. Yet, their actions are lower than those in the highest equilibrium. Finally, the third and worst case is the market collapse equilibrium, in which



(a) Example Network Visualization: 3Eqm40



(b) Exact and Approximation Equilibria: 3Eqm40

Figure 4.4: An Example Network with Three Equilibria

The network consists of 40 banks (9 core and 31 peripheral). Panel (b) reports the high and middle equilibria induced by this network in the same fashion as in Figure 4.2.

all banks hoard liquidity and choose zero illiquid lending.

CHAPTER 5

APPLICATIONS

5.1 Financial Fragility Measure

This section studies how changes in the network structure affect the systemic response function and the equilibrium systemic behavior. I first define the financial fragility measure by studying the situation when the network connections contract proportionally.

PROPOSITION 9 (Proportional Connection Contraction).

Let $f^(x; \mathbf{W})$ denote the systemic response function given an adjacency matrix \mathbf{W} . If all pairs of connection decrease proportionally at rate θ , i.e. $w_{i,j}$ change to $\theta w_{i,j}, \forall i, j$, then the systemic response function changes as.*

$$f^*(x; \theta \mathbf{W}) = f^*(\theta x; \mathbf{W}).$$

Proof. See Appendix A.13. □

As shown in Figure 5.1, if the whole network decreases proportionally at the rate of θ , then the f^* curve stretches to the right by $\frac{1}{\theta}$. Because f^* is an increasing function, the transformation decreases f^* at every point. If the contraction is modest (θ close to 1), the positive equilibrium systemic liquidity decreases, as shown in panel (a). With more severer contraction (θ significantly small), the cooperative equilibrium is not sustained. Zero systemic liquidity is the only equilibrium. A critical θ level separates these two scenarios. At this borderline case, the positive equilibrium is barely sustained, as depicted in panel (b). The critical θ , defines the measure of financial fragility.

DEFINITION 12 (Financial Fragility Measure).

Suppose the conditions of Proposition 8 are satisfied (i.e. at most two equilibria), and the cooperative equilibrium exist. The financial fragility of the cooperative equilibrium is measured

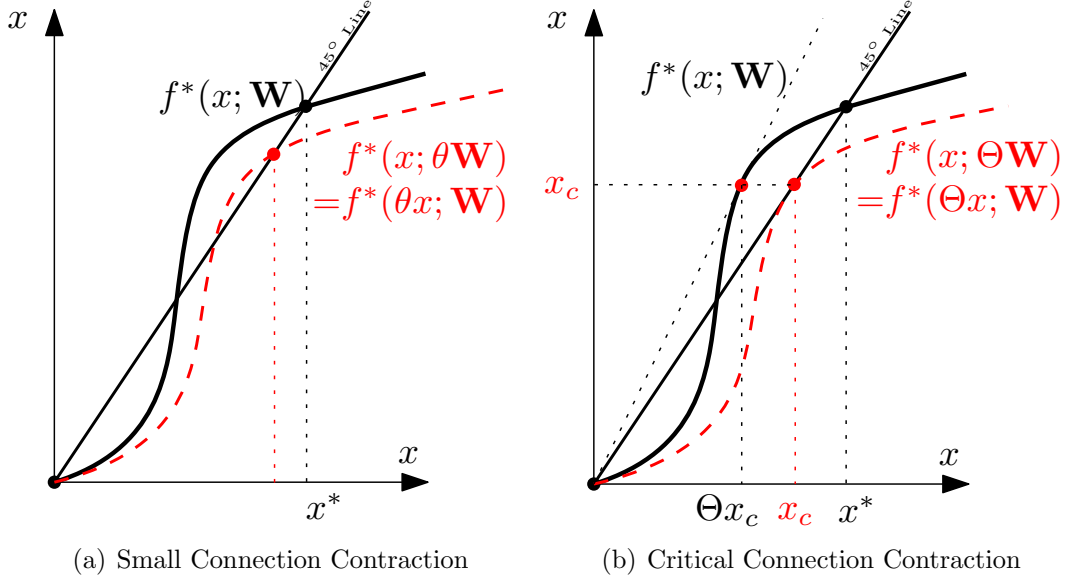


Figure 5.1: Comparative Statics: Proportional Connection Contraction
 Under a universal proportional connection contraction, the systemic response function stretches to the right and away from the vertical axis.

as

$$\Theta = \min \{ \theta \text{ s.t. } \exists x > 0, x = f^*(\theta x) \}.$$

Financial fragility is defined as the minimum proportion of connection intensities that must be retained to sustain the positive systemic liquidity equilibrium. Conversely, $1 - \Theta$ is the ratio of connection loss that the system can tolerate before the interbank market collapses, which measures stability of the financial system.

Also denote the *systemic liquidity at the critical condition* as x_c . Specifically, x_c solves $x_c = f^*(\Theta x_c)$. It is the equilibrium systemic liquidity at the borderline connection contraction level $\theta = \Theta$. The marginal change to the system response function f^* around point $(\Theta x_c, x_c)$ informs about fragility, which will be a focus in the following analysis. These constructions are illustrated in Figure 5.1.

In addition, define efficiency of the financial system as the quantity of total real investments.

DEFINITION 13 (Efficiency Measure).

The efficiency of a equilibrium $\{x_i\}$ is measured as the total quantity of real asset investment,

$$\mathcal{E} = \sum_i (1 - \delta_i^O) x_i.$$

It is noted that under a universal proportional connection contraction, efficiency decreases. Recall that the financial system converts the fixed amount of total deposits (nd) into either real investment or cash. Therefore, $\mathcal{E} = nd - \sum_i g(y_i)$. In systemic liquidity approximation, that is $y_i = \delta_i^I x^*$. For small proportional connection contraction, both δ_i^I and equilibrium x^* decreases. Since the policy function of cash ($g(y_i)$) is weakly decreasing, the banks that are in the liquidity hoarding region hoards more cash. As a result, real investments, which measures social efficiency, decreases.

5.2 The Systemic Effects of Local Insolvency Shocks

This subsection considers how bank level insolvency events trigger a systemic liquidity crunch. I show the effects of local lending-borrowing connection losses are similar to that of a universal proportional connection contraction.

Consider a counterfactual scenario, in which a subset \mathcal{S} of banks experience local insolvency shocks. Before the start of the time-0, the banks' real investments are learned to be not safe. For example, the market finds out these banks are exposed to the toxic subprime mortgages. The complement set of the remaining banks (\mathcal{R}) respond to the shock, by cutting lending connections to the shocked banks in the time-0 interbank lending game. They redirect the proportion of illiquid lending (x_i) that loans to the \mathcal{S} banks to their own real investments. The \mathcal{R} banks out-degrees decreases correspondingly. For \mathcal{S} banks, since their incoming connections are severed, their interbank funding liquidity decreases to zero, and hence their outgoing illiquid lending also becomes zero. Effectively, the scenario of insolvency shocks on \mathcal{S} is a change on the network structure: shocked banks \mathcal{S} are removed from

the network. The remaining interbank connections among the safe banks ($w_{i,j}, \forall i, j \in \mathcal{R}$) constitute the unraveled network, which is denoted as $\mathbf{W}_{\mathcal{R}}$.

An equivalent interpretation of the counter-factual scenario is a subset \mathcal{S} of banks leave the interbank business out of panic. Suppose, the shocked banks choose to reject interbank funding and self-insure by having a full-cash portfolio exogenously, for reasons outside of the current model. Then the interbank lending game is played on the remaining network $\mathbf{W}_{\mathcal{R}}$.

Notice the counterfactual scenario is not about asset loss contagion from failed borrowers to their lenders, because the remaining banks are quarantined from the asset loss contagion. They can sever the lending exposures to \mathcal{S} banks before the start of the interbank lending game. Instead of asset losses, \mathcal{R} banks suffer decreases in funding opportunities: the \mathcal{R} banks who used to borrow from \mathcal{S} banks experience decreases in interbank funding connections (δ^I). I examine how much of such funding connection decreases will trigger a systemic liquidity crunch.

I conduct a system-wide stress testing by studying what happens to the systemic liquidity in the counter-factual scenarios in which a subset of banks are stressed. We are interested in how the initial local panics trigger a systemic liquidity crunch. To infer about the fragility of the financial system, I experiment with different shocked sets \mathcal{S} and examine in which cases the positive systemic liquidity equilibrium is no longer sustained. For each generated \mathcal{S} , I numerically solve the highest equilibrium systemic liquidity in the corresponding remaining network $\mathbf{W}_{\mathcal{R}}$.

I report the system-wide stress testing results with the two observed networks in Figure 5.2. Specifically, a series of \mathcal{S} 's are generated by adding banks to it one by one in a random sequence, in order to capture the expanding range insolvency shocks. Each broken line in Figure 5.2 plots the highest equilibrium systemic liquidity quantities for each random sequence. This process is repeated for different random sequences.

It is observed that as more banks are shocked and the network unravels, the equilibrium systemic liquidity decreases at first. After a significant amount of banks are shocked, an

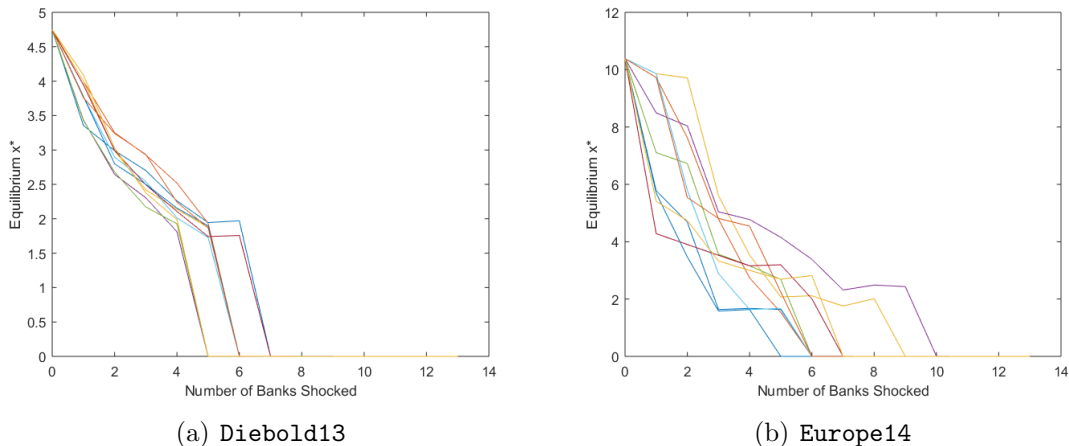


Figure 5.2: System-wide Stress Testing

Stress test developed by sequentially removing banks from the two observed financial networks. Each path correspond to a sequence of expanding \mathcal{S} . The horizontal axis is the number of shocked banks (size of \mathcal{S}). The vertical axis is the positive systemic liquidity equilibrium associated with $\mathbf{W}_{\mathcal{R}}$, calculated by solving Condition 3 numerically. I plot 10 random sequences for each network.

interbank run is triggered as the positive equilibrium collapses to zero. An important feature is that the systemic behavior is different in different sequences of insolvency shocks. In some sequences, the interbank run is triggered after only a few banks being shocked, while some others last longer. Especially in the case of **Europe14**, in which the heterogeneity across banks is greater. This should be an expected phenomenon, since different banks are of different importance. Merely knowing the number of the shocked banks provides inadequate information about the equilibrium outcome of the system. This situation calls for a summary statistic of the remaining network that better summarizes its systemic behavior.

I demonstrate a method to that uses effective connectedness (W^*) to summarize the effects of local insolvency shocks on the systemic response and infer about the critical value when an interbank run will be trigger. As defined in Subsection 4.8, W^* is the out-degree weighted first moment of in-degree. It controls the general attitude of the systemic response function f^* , while the higher moments control its curvature. The one dimensional summary statistics W^* provides a rather close one-to-one mapping of the systemic response function.

In approximation,

$$f^*(x; \mathbf{W}_{\mathcal{R}}) \approx f^*\left(\frac{W_{\mathcal{R}}^*}{W^*}x; \mathbf{W}\right) \quad (5.1)$$

Given this approximation, effective connectedness of the remaining set of banks ($W_{\mathcal{R}}^*$) is an approximated statistic of the systemic response function $f^*(\cdot; \mathbf{W}_{\mathcal{R}})$, which contains all the information about whether the positive equilibrium still exists and its level if it exists. For each $W_{\mathcal{R}}^*$, approximated equilibrium systemic liquidity is the solution of $x = f^*\left(\frac{W_{\mathcal{R}}^*}{W^*}x\right)$. Therefore, the one-dimensional statistic $W_{\mathcal{R}}^*$ maps the network structure into the equilibrium systemic liquidity.

The mapping provides an framework to analyze the stress testing results. For an observed interbank network, one can infer when the systemic liquidity crunch is to be triggered by monitoring the decrease of W^* . To verify that the approximation methods provides a close description, I rearrange the disorganized dots in Figure 5.2 according $W_{\mathcal{R}}^*$ and produce Figure 5.3. The result shows the effective connectedness of the remaining network $W_{\mathcal{R}}^*$, provides accurate prediction of the equilibrium systemic liquidity. And there exist a critical level effective connectedness that marks a discontinuous transition of the equilibrium systemic liquidity. For modest reductions in effective connectedness, the systemic liquidity decreases continuously. If the reduction is beyond the critical level, the positive equilibrium disappears. Around the critical level, small and local losses of interbank connections can trigger a large and system-wide liquidity crunch.

I contrast W^* with μ , the equal-weighted degree average, in order to show the virtue of the W^* approximation in depicting the equilibrium. Figure B.6 in Appendix plots the same set of stress testing results. But the horizontal coordinates are further changed to the average degrees (μ) of the remaining networks. In general, μ is much less informative in describing the system-wide equilibrium behavior of the network. Each μ corresponds to a wide range of equilibrium systemic behavior, sometimes ranging from market collapse to

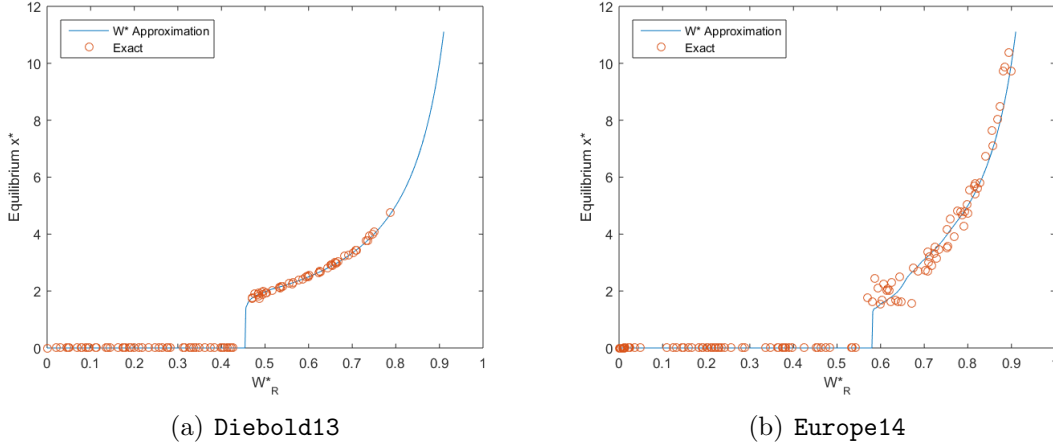


Figure 5.3: W^* Approximation of Stress Testing

The blue curve plots the positive systemic liquidity equilibrium under W^* approximation, i.e. the solution of $x = f^*(\frac{W^*_{\mathcal{R}}}{W^*}x)$ as a function of $W^*_{\mathcal{R}}$. The red circles plot the same set of stressed scenarios as in Figure 5.2. But, the horizontal coordinates are the corresponding $W^*_{\mathcal{R}}$, rather than the numbers of the shocked banks. As in Figure 5.2, the vertical coordinate of a red circle is the positive systemic liquidity equilibrium in $\mathbf{W}_{\mathcal{R}}$, calculated by solving Condition 3 numerically.

high systemic liquidity.

To understand why W^* is an informative summarization of the network structure, I decompose W^* into two parts,¹

$$W^* = \mu \cdot \left(1 + \frac{\text{Cov}(\delta^O, \delta^I)}{\mu^2} \right) = \mu \cdot \left(1 + \text{corr}(\delta^O, \delta^I) c_v(\delta^I) c_v(\delta^O) \right) \quad (5.2)$$

The first term μ is the equally weighted average degrees. It measure the *density* of the connections. Local shocks that decreases the density of the network structure increases the financial fragility of interbank lending. The second part is the unit-less terms after controlling for μ . A network structure is said to be more *symmetric* if the in-degrees and out-degrees are more correlated. If the network structure becomes less symmetric, W^* decreases, and the systemic liquidity equilibrium becomes more fragile.

The symmetricity result implies that mismatch between short-term interbank funding

1. c_v denotes the coefficient of variation.

and lending contributes to the fragility of the system. This is an intuitive result featured in several analyses of liquidity crises. Ideally, the tension between liquid funding and illiquid investments distribute evenly across the network. However, in less symmetric networks, the tension is accumulated at certain “pinch points” of the network. For example, according to Shin (2009), Northern Rock heavily relied on nonretail funding to finance long-term illiquidity. When the system reduces assets and paying down debt, tension is manifested at the asymmetrical point. Paddrik, Park, and Wang (2016) reports that the National Banking Acts led to a concentrated and pyramid-shaped interbank deposits network: Rural banks in Pennsylvania lent to local hubs, which in turn lent to core banks in New York. The core banks have illiquid lending concentrated on real investments, and have low contribution back to the interbank system (low- δ^O). Such asymmetric structure contributed to magnifying the frequency and extent of banking crises.

The result attained here provide a formal rationale for the intuitive observations, and deduce a quantitative measure of symmetricity that is linked to the fragility of the equilibrium.

5.3 Optimal Bailout Plans

During the financial crisis, governments carried out bailout programs by injecting liquidity to financial institutions. In the U.S., the core of the bailout plan was the Capital Purchase Program (CPP) as part of the Troubled Asset Relief Program (TARP). Primarily, the Treasury invested in preferred stocks of the “healthy, viable” financial institutions.

In an October 2008 speech², Bernanke said: “Government assistance should be provided with the greatest reluctance and only when the stability of the financial system, and thus the health of the broader economy, is at risk.” The purpose of the Treasury was to “promote financial stability, maintain confidence in the financial system, and permit institutions to

2. Ben S. Bernanke, “Stabilizing the Financial Markets and the Economy” (Speech, New York, October 15, 2008) <https://www.federalreserve.gov/newsevents/speech/bernanke20081015a.htm>

continue meeting the credit needs of American consumers and businesses.”³ The policymakers’ focus is on preventing systemic failure, rather than saving individual banks or improving the current situation. However, preventing systemic failure given complex financial networks is not always straightforward. One debatable aspect is the injection targets — which banks should receive more liquidity? In practice, nine “systemically important” financial institutions received half of the total CPP investments, in the first round in October 2008. Later, smaller banks were enlisted mostly because it was “not politically feasible” to only favor large financial institutions.⁴

This paper’s insights about systemic behavior on the interbank network can address this problem. I study the government’s problem of minimizing financial fragility by choosing an optimal liquidity injection plan. The government is constrained by a limited total budget on the program. I assume the government can observe the status quo network structure, or at least its joint degree distribution, in order to infer the systemic response function. Yet the decisions are made without knowing the local insolvency shock realization. Therefore, the government’s goal is to reduce financial fragility, so that when local insolvency shocks hit, the system has a greater capacity to avoid a systemic failure.

Suppose the government lends z_i dollar to bank i at the same term as interbank lending. Then, bank i ’s interbank funding becomes $y_i = \delta_i^I x^* + z_i$. Given a liquidity injection plan represented by the vector $\{z_i\}$, the systemic response function is

$$f^*(x; \{z_i\}) = \sum_i \frac{\delta_i^O}{n\mu} f(\delta_i^I x + z_i)$$

The government’s problem is to minimize the systemic fragility associated with this systemic response function by choosing injection plan $\{z_i\}$.

The systemic response function is increasing in z_i at every point. So liquidity injection

3. Office of the Special Inspector General for the Troubled Asset Relief Program. “Quarterly Report to Congress, Second Quarter 2009,” Quarterly Report to Congress (April 21, 2009).

4. See Scott (2016).

always increases the equilibrium systemic liquidity, reduces financial fragility, and improves efficiency. However, targeting different banks has different implications for financial fragility and efficiency.

Suppose the government's budget constraint is

$$\sum_i (z_i + \zeta(\frac{z_i}{Z})) = Z$$

Z is the total budget of the program. $\zeta(\frac{z_i}{Z})$ is the convex function of the additional costs of spending z_i on bank i . This is a technical assumption to avoid too concentrated liquidity injection targets. In practice, the cost can be associated with the external pressure when the program is concentrated on a few banks.

PROPOSITION 10. *Suppose injection plan $\{z_i\}$ solves the government's problem. At the limit of small budget ($Z \rightarrow 0^+$), the share of bank i 's liquidity in the total budget, $\frac{z_i}{Z}$, is a (weakly) increasing function of $\delta_i^O f'(\delta_i^I \Theta x_c)$.*

Proof. See Appendix A.14 □

The bailout plan should target more on the banks with a high measure of $\delta_i^O f'(\delta_i^I \Theta x_c)$. The interpretation can be understood from the aspects of the in- and out-degrees.

First, liquidity injection to the high- δ^O banks is more effective in increasing the overall level of f^* . Given a fixed amount of marginal increase in illiquid lending (x_i) induced by the injection, δ_i^O proportion will be contributed back to the interbank system, which ripples through the network to boost systemic liquidity. Therefore, all else equal, targeting the capital injection at high- δ^O banks is more cost effective.

On the second layer, the in-degree determines the marginal effect of liquidity injection (z_i) on illiquid lending (x_i). For a individual bank's response to injection, $\frac{\partial}{\partial z_i} f(\delta_i^I x + z_i) = \frac{1}{1-\beta}$ if $\delta_i^I x + z_i \in (y_l, y_h)$, or 1 elsewhere. That is, the bank's lending decision is more sensitive to liquidity injection if its funding level in the liquidity hoarding region. Injecting liquidity

to a bank in this region would “leverage” a greater-than-one marginal effect, as the bank would release some cash that is otherwise hoarded to defend depositor runs. Different banks are in this region at different systemic liquidity levels depending on their in-degrees. High- δ_i^I banks that are ample with liquidity at the status quo equilibrium only find them in the liquidity hoarding region with a significant systemic liquidity reduction. Meanwhile, altering f^* at different systemic liquidity domain has different implications for the system. Financial fragility is determined by f^* around its critical systemic liquidity level $x = \Theta x_c$, shown in Figure 5.1 (b) as the tangent point $(\Theta x_c, x_c)$. So the optimal plan should put more weights on banks with a high calculation of $f'(\delta_i^I \Theta x_c)$. Therefore, to increase fragility, it is justified for the government to take precautions by targeting the banks that *would be* in the liquidity hoarding region in the critical situation when connection intensities decrease by Θ and x^* decreases to x_c .

In comparison, suppose the policymaker’s focus is the efficiency of the status quo equilibrium, instead of the fragility with respect to a systemic liquidity crunches. Then, f^* around $x = x^*$ ought to be maximized in order to increase the current equilibrium systemic liquidity level. As a result, the optimal injection z_i is (weakly) increasing in $\delta_i^O f'(\delta_i^I x^*)$. The banks that *currently are* in the liquidity hoarding region are the optimal targets. In contrast, these banks are not necessarily the targets under the fragility goal. Their funding liquidity levels are already binding in the depositor-run-proof constraint at the current systemic liquidity level. Should the effective connection unravels to the critical level, these banks could further fall into the full cash-hoarding region (the lowest interval in Figure 3.3). In that case, the external capital injection is not as effective. These banks are too poorly funded to exert the leveraging effect of liquidity injection. The government should save the limited resource on better-connected banks that would amplify the injected amount under the critical conditions.

5.4 The Effects of Restraining Too-Interconnected-to-Fail Banks

As shown in subsection 5.2, local insolvency can trigger systemic liquidity crunches in the interconnected financial system. Reckoning this mechanism of the 2008 financial crisis, it has been argued that the too-interconnected-to-fail financial institutions must be limited to alleviate financial fragility and avoid the necessity of government intervention during potential crises. Bernanke (2010) states that *“if the crisis has a single lesson, it is that the too-big-to-fail problem must be solved.”* Volcker (2012) argues that the risk of failure of large, interconnected firms must be reduced, *“whether by reducing their size, curtailing their interconnections, or limiting their activities.”* In my model, in-degree connectedness determines the bank balance sheet size. In this sense, too-interconnected-to-fail and too-big-to-fail are not distinguished.⁵ Some specific regulation measures are proposed on restraining the interconnectedness of the well connected banks. For example, Single-Counterparty Credit Exposure Limits as part of the Dodd-Frank Acts, and the Basel Committee’s Large Exposures Standards limits the investment to a single counterparty.⁶

I treat such regulations as exogenous changes on the interbank lending network structures. The rules put a restriction on the interbank funding opportunities of the high- δ^I banks who are bigger and relies more on interbank funding. In order to separate out the effects of such a reduction of concentration, the change is specified as a mean-preserving concentration of the distribution of in-degrees. That is I assume each bank keeps the out-going connections (δ^O) fixed while it redirects the lending connections toward to the less connected (low- δ^I) banks. As a result, the high- δ^I big banks becomes smaller and less connected from interbank borrower, while the average degree μ stays unchanged.

5. In Bernanke (2010) the too-big-to-fail bank is defined as one whose size, complexity, interconnectedness, and critical functions are such that, should the firm go unexpectedly into liquidation, the rest of the financial system and the economy would face severe adverse consequences.

6. The proposed SCCL would require “covered companies” to limit their aggregate net credit exposure on a consolidated basis to any unaffiliated company to 25% of such covered company’s capital stock and surplus. A more stringent 10% limit applies to covered companies with \$500 billion in total consolidated assets for exposures

To ease notation, let the $(\theta; \tau)$ -contraction of a sequence $\{\delta_i\}_{i=1}^n$ denote an operation such that every element moves closer towards the center value τ at proportional rate θ .

DEFINITION 14 ($(\theta; \tau)$ -Contraction of a Sequence).

Let $(\theta; \tau)$ -contraction of a sequence $\{\delta_i\}_{i=1}^n$ be an operation such for any element δ_i is changed to $\delta_i\theta + \tau(1 - \theta)$.⁷

Formally, the regulations' effect on the network structure is specified as a mean-preserving $(\theta; \mu)$ -contraction on the in-degrees, with out-degrees unchanged. Suppose the original network supports a positive systemic liquidity equilibrium, I study how it and its fragility will change after the network structure change.

Consider a generic $(\theta; \tau)$ -contraction of in-degrees, then the mean degree (μ) is shifted towards τ and become $\theta\mu + (1 - \theta)\tau$. In order to keep the out-degree weights ($\delta_i^I/n\mu$) unchanged, while matching the change in the mean degree, let out-degrees have a $(\theta + (1 - \theta)\frac{\tau}{\mu}; 0)$ -contraction.⁸ Lemma 4 states the effect the transformation on the systemic response function. Here, $f^*(x; (\theta; \tau))$ denotes the systemic response function after the transformation; $f^*(x; (1; \tau))$ denotes the original systemic response function.

LEMMA 4 (Generic In-degree Distribution Contraction).

If the in-degrees have a $(\theta; \tau)$ -contraction, out-degrees have a $(\theta + (1 - \theta)\frac{\tau}{\mu}; 0)$ -contraction,

- For $x > \frac{y_l}{\delta_{min}^I}$,

$$S_h f^*(x; (1; \tau)) + (1 - S_h) f(y_h) = f^*\left(S_h x + (1 - S_h) \frac{y_h}{\tau}; (\theta; \tau)\right),$$

- Symmetrically, for $x < \frac{y_h}{\delta_{max}^I}$,

$$S_l f^*(x; (1; \tau)) + (1 - S_l) f(y_l) = f^*\left(S_l x + (1 - S_l) \frac{y_l}{\tau}; (\theta; \tau)\right),$$

7. I generally discuss cases where $\theta < 1$, otherwise it would be more properly called a spread rather than a contraction.

8. This should be more properly called an expansion when $\tau > \mu$ which means $\theta + (1 - \theta)\frac{\tau}{\mu} > 1$.

where $S_h = \frac{\theta y_h}{\theta y_h + (1-\theta)\tau x}$, $S_l = \frac{\theta y_l}{\theta y_l + (1-\theta)\tau x}$.⁹

In the following analysis, I impose the condition below, such that with enough distance between y_l, y_h , the two cases in Lemma 4 covers the entire domain $[0, \infty)$.

CONDITION 7 (No Interference Between the Two Kinks).

$$\frac{\delta_{max}^I}{\delta_{min}^I} \leq \frac{y_h}{y_l} \quad (5.3)$$

The transformation can be interpreted geometrically as scalings the f^* curve. In the higher section ($x > \frac{y_l}{\delta_{min}^I}$), the f^* curve scales towards the target point $(\frac{y_h}{\tau}, f(y_h))$, at the rate S_h . The similar can be stated for the lower section.

The lemma shows that W^* controls the general attitude of the f^* curve, while in-degree concentration controls the shape of the curve (rounded or kinked). W^* is the (δ^O -weighted) first moment of δ^O , whereas concentration is about the second moment. First study the case where the contraction target $\tau = W^*$, so that W^* is fixed after the $(\theta; W^*)$ -contraction. As shown in Figure 5.4, when W^* stays unchanged, the general attitude of the f^* curve does not change. The shape of the S-curve becomes more “kinked” with greater contraction (smaller θ). Specifically, as shown by the red dashed curve, for $x > \frac{y_l}{\delta_{min}^I}$, the f^* curve scales towards the upper kink point $(\frac{y_h}{W^*}, f(y_h))$. The lower portion scales to the lower kink point symmetrically. Notice if $\theta \in [0, 1]$, then $S_h, S_l \in [0, 1]$, and they are increasing in θ . In the extreme case of $\theta = 0$, all in-degrees become equalized at W^* , $S_h = S_l = 0$. The S-curve becomes piecewise linear, shown as the thin black line. Algebraically, $f^*(x; (0; W^*)) = f(W^*x)$. The systemic response function reduces back to the individual response function in a network with homogeneous δ^I .

In the general cases where $\tau \neq W^*$, the contraction not only changes the concentration of the in-degrees, but also changes the effective connectedness from W^* to $\theta W^* + (1-\theta)\tau$. If $\tau < W^*$, effective connectedness degrees. The scaling targets $(\frac{y_h}{\tau}, f(y_h))$, $(\frac{y_l}{\tau}, f(y_l))$ shift

9. If Condition 7 is satisfied, then the two cases covers the whole domain of f^* .

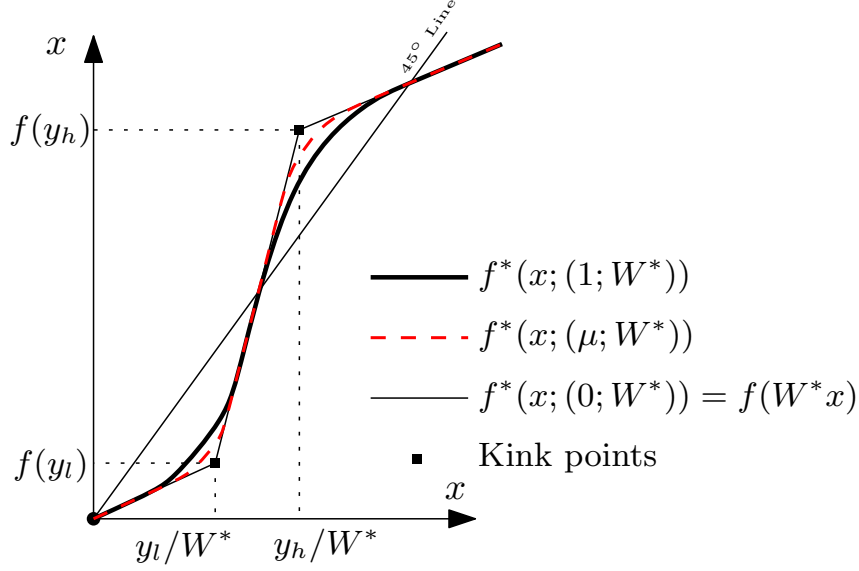


Figure 5.4: f^* after W^* -Preserving In-Degree Contractions

$f^*(x; (\mu; W^*))$ denotes the systemic response function after $(\theta; W^*)$ -contraction of in-degrees and $(\theta + (1 - \theta)\frac{W^*}{\mu}; 0)$ -contraction of out-degrees. The general attitude of the f^* curve does not change, but the shape of the S-curve becomes more “kinked”, and scales toward the piecewise linear limiting case in which $\mu = 0$.

to the right relative to the $\tau = W^*$ case targets (kink points in Figure 5.4). The general attitude of the S-curve stretches to the right, which decreases f^* .

With the analysis in Lemma 4, we can address the effects of the mean-preserving in-degree distribution contraction $(\theta; \mu)$. First focus on the case when in- and out-degrees are uncorrelated, i.e. $\text{Cov}(\delta^I, \delta^O) = 0$. Then according to equation (5.2), $W^* = \mu$. As a result, the effective connectedness is unchanged after the network change. The impact on f^* is the same as that in Figure 5.4. The concentration of funding opportunities increases f^* in the high interval, which is good for improving efficiency and reducing fragility.

PROPOSITION 11 (Mean-Preserving In-Degree Contraction (Uncorrelated In/Out-Degrees)).

Suppose $\text{Cov}(\delta^I, \delta^O) = 0$, Condition 7 is satisfied. Suppose the in-degrees have a mean-preserving $(\theta; \mu)$ -contraction, with out-degree unchanged. Then $\forall x \geq \frac{y_l}{\delta_{min}^I}$, $f^*(x)$ increases (or stays unchanged); the positive equilibrium systemic liquidity x^* and its efficiency increase (or both stay unchanged if $x^* > \frac{y_h}{\delta_{min}^I}$); financial fragility decreases.

Proof. See Appendix A.15. □

However, in reality, the in- and out-degrees are positively correlated. In other words, the banks with greater in-degree are also contributing more to the systemic liquidity on average. By concentrating the in-degree distribution, the high- δ^I banks that contribute more to systemic liquidity suffer disproportionately more reduction in funding opportunities, although the average in-degrees is not changed. Specifically, according to equation (5.2), W^* is decreasing in the in-degree's coefficient of variation, given the positive correlation. As a result, the effective connectedness decreases as the network structure changes. The decrease in effective connectedness has a negative impact on the systemic response function.

PROPOSITION 12 (In-degree Distribution Contraction (General Case)).

Suppose Condition 7 is satisfied. Suppose the in-degrees have a mean-preserving $(\theta; \mu)$ -contraction, with out-degree unchanged. Then financial fragility decreases if and only if

$$\frac{\text{Cov}(\delta^I, \delta^O)}{\mu^2} \leq \frac{y_h + d}{\Theta y_h} W^* - 1.$$

Proof. See Appendix A.16. □

In aggregate, a regulation that shrinks the spread of the in-degree distribution has two effects. The first makes the curve of the systemic response function more kinked, as illustrated in Proposition 11, which is beneficial to decreasing financial fragility. The second alters the general attitude of the curve via the change on W^* . If the in- and out-degrees are positively correlated, W^* is decreasing, which destabilizes the system. Proposition 12 shows that if the covariance between the in- and out-degrees is greater than a threshold level, the second effect dominates, and the net effect leads to a system with greater fragility. When the banks that are well connected to borrowers also take up a greater share in the contribution to systemic liquidity as a lender, putting a constraint on their interbank funding connections might outweigh giving support to the poorly funded banks.

CHAPTER 6

CONCLUSION

How can small and local insolvency shocks trigger a large and system-wide liquidity crunch in the interconnected financial system? Especially, this paper studies how the network structure affects the financial fragility, which measures how likely such a systemic liquidity crunch is to be triggered.

To answer these questions, I present a model of the systemic liquidity crisis with two new features. First, pairwise interbank lending exposures channel the bank-to-bank strategic interactions. The interactions are dispersed on a decentralized network with indirect connections. Second, the crisis is on the level of the whole financial system. It is modeled as the coordination failure among banks in the interbank lending sector.

The main result is a characterization of “interbank runs”, in which banks run on banks as they mutually reinforce each other to withdraw interbank liquidity. The key intuition and mechanism is an interplay between the bank-level threat of retail depositor run and the system-level interbank run. The bank level threat gives each bank an incentive to preemptively hoard cash. Although individually precautionary, the interconnected cash hoarding strategies cause system-wide instability. The model reflects the stylized facts observed during the 2007-2008 financial crises: interbank liquidity drops discontinuously across the financial system; real investments dip; the safe and liquid asset holding in the financial system expands. Moreover, when the interbank wholesale sector is stressed, the retail financing is relatively safe and inconspicuous.

Characterizing the equilibrium of the lending actions played by all banks in general networks is a hard problem. I apply the mean-field approximation method to make the complicated situation simple. The essence of method is a dimension reduction of the equilibrium condition that allows one to capture the systemic behavior from the aggregate network properties, while overlooking the exact local connection structures.

I constructed a random network model and justify the method by showing the approx-

imation error converges to zero in probability in large networks. I identify the weighted non-assortative matching as the key property that drives the approximation result. The characterization of systemic equilibrium can be applied to study the systemic behavior of other games played on network, such as the adoption of new technologies, peer effects of effort levels, and diffusion of information in social networks.

The characterization of the systemic liquidity equilibrium has immediate implications for policy, since central banks are interested, first and foremost, in systemic risks, and being able to detect when the system is at an elevated risk level. I also apply the model to two specific policy exercises. One is about the optimal bailout plan during the financial crisis. The other is about the proposed policies on restricting the connectedness of the too-interconnected-to-fail banks in reckoning the crisis.

This paper opens the door to new researches of the financial network and systemic risks. The mean-field approximation permits a concise measure of the complicated network, which paves the way for empirical and policy exercises that take financial fragility as an input. The analyses here also lay the foundation of several theoretical extensions. One potential aspect is the dynamic and endogenous evolution of the network structure. The one-dimensional summarization delivered in this paper allude to the possibility of such a dynamic model under approximation. Another interesting extension is restricting the banks to have limited information about the counterparties' connections. The insights from Sadler (2017), Caballero and Simsek (2013) can be valuable in such a framework.

APPENDIX A

PROOFS AND ADDITIONAL ALGEBRAIC DETAILS

A.1 Verifying the Conditional Expectation of Degrees

$$\delta_i^I = \sum_{j \neq i} \frac{1}{(n-1)\tilde{\mu}} \lambda_{i,j} \tilde{\delta}_i^I \tilde{\delta}_j^O \quad (\text{A.1})$$

$$\mathbb{E} \left[\delta_i^I \mid \tilde{\delta}_i^I \right] = \frac{1}{(n-1)\tilde{\mu}} \tilde{\delta}_i^I \sum_{j \neq i} \mathbb{E} \left[\lambda_{i,j} \tilde{\delta}_j^O \mid \tilde{\delta}_i^I \right] \quad (\text{A.2})$$

We have,

$$\mathbb{E} \left[\lambda_{i,j} \tilde{\delta}_j^O \mid \tilde{\delta}_i^I \right] = \mathbb{E} \left[\mathbb{E} \left[\lambda_{i,j} \tilde{\delta}_j^O \mid \tilde{\delta}_i^I, \tilde{\delta}_j^O \right] \mid \tilde{\delta}_i^I \right] = \mathbb{E} \left[\tilde{\delta}_j^O \mid \tilde{\delta}_i^I \right] = \tilde{\mu} \quad (\text{A.3})$$

The other two lines can be verified symmetrically.

A.2 Proof of Proposition 1

Suppose there are two different vectors $\{x^{[1]}\}, \{x^{[2]}\}$ that both satisfy equation (3.2). Then

$$x_i^{[1]} - x_i^{[2]} = f\left(\sum_j w_{i,j} x_j^{[1]}\right) - f\left(\sum_j w_{i,j} x_j^{[2]}\right), \quad \forall i. \quad (\text{A.4})$$

$$|x_i^{[1]} - x_i^{[2]}| = \left| f\left(\sum_j w_{i,j} x_j^{[1]}\right) - f\left(\sum_j w_{i,j} x_j^{[2]}\right) \right| \quad (\text{A.5})$$

$$\leq \left| \sum_j w_{i,j} x_j^{[1]} - \sum_j w_{i,j} x_j^{[2]} \right| \quad (\text{A.6})$$

$$= \left| \sum_j w_{i,j} (x_j^{[1]} - x_j^{[2]}) \right| \quad (\text{A.7})$$

$$\leq \sum_j w_{i,j} |x_j^{[1]} - x_j^{[2]}|, \quad \forall i. \quad (\text{A.8})$$

Take sum across i on both sides,

$$\sum_i |x_i^{[1]} - x_i^{[2]}| \leq \sum_j \delta_j^O |x_j^{[1]} - x_j^{[2]}|. \quad (\text{A.9})$$

Since $0 \leq \delta_j^O < 1, \forall j$, then there is an obvious contradiction. Therefore, there cannot be two distinct $\{x_i\}$ that both satisfy equation (3.2).

A.3 Proof of Proposition 2

The equilibrium condition is

$$x_{i+1} = f(y_{i+1}) = f(wx_i), \quad \forall i \quad (n+1 \text{ treated as } 1). \quad (\text{A.10})$$

Because f is increasing, the solution must be symmetric. Let x denote the symmetric equilibrium action. The equilibrium condition is reduced to the univariate equation $x = f(wx)$.

If $wx \geq \frac{1-\beta}{\beta}d + \frac{\gamma}{\beta}$, then $x = f(wx) = wx + d$. That implies, $x = \frac{d}{1-w}$ and $\frac{wd}{1-w} \geq \frac{1-\beta}{\beta}d + \frac{\gamma}{\beta}$. Plug in x , the inequity is equivalent to $w \in [1 - \frac{\beta}{1+\frac{\gamma}{d}}, 1)$.

It is easy to show that when $w < 1 - \frac{\beta}{1+\frac{\gamma}{d}}$, $x = 0$ is the only solution.

A.4 Proof of Lemma 1

$$\delta_i^I = \sum_j w_{i,j} = \frac{\tilde{\delta}_i^I}{(n-1)\tilde{\mu}} \sum_{j \neq i} \lambda_{i,j} \tilde{\delta}_j^O, \quad \forall i. \quad (\text{A.11})$$

For fixed i , $\lambda_{i,j} \tilde{\delta}_j^O$ is i.i.d. across $j \neq i$ with expectation $\mathbb{E}(\lambda_{i,j} \tilde{\delta}_j^O | \tilde{\delta}_i^I) = \mathbb{E}(\lambda_{i,j} | \tilde{\delta}_i^I) \mathbb{E}(\tilde{\delta}_j^O | \tilde{\delta}_i^I) =$

$\tilde{\mu}$. By the law of large numbers, its sample average converges to the expectation.

$$\delta_i^I = \tilde{\delta}_i^I \frac{1}{\tilde{\mu} n - 1} \sum_{j \neq i} \lambda_{i,j} \tilde{\delta}_j^O \xrightarrow{p} \tilde{\delta}_i^I, \quad n \rightarrow \infty, \forall i. \quad (\text{A.12})$$

Moreover, because $\lambda_{i,j} \tilde{\delta}_j^O$ is uniformly bounded (Condition 5), by CLT, the convergence rate is uniformly bounded. Therefore, across all i , δ_i^I uniformly converges to $\tilde{\delta}_i^I$ in probability.

That is $\forall \psi > 0$,

$$\max_i \Pr \left(\left| \delta_i^I - \tilde{\delta}_i^I \right| \geq \psi \right) \rightarrow 0, \quad n \rightarrow \infty, \forall i. \quad (\text{A.13})$$

Moreover, the convergence is faster than $1/n$. That is

$$\max_i \Pr \left(\left| \delta_i^I - \tilde{\delta}_i^I \right| \geq \psi \right) = o \left(\frac{1}{n} \right), \quad n \rightarrow \infty, \forall i. \quad (\text{A.14})$$

Then,

$$\Pr \left(\bigvee_i \left| \delta_i^I - \tilde{\delta}_i^I \right| \geq \psi \right) \leq n \max_i \Pr \left(\left| \delta_i^I - \tilde{\delta}_i^I \right| \geq \psi \right) \quad (\text{A.15})$$

$$\Pr \left(\left| \delta_i^I - \tilde{\delta}_i^I \right| < \psi, \forall i \right) \geq 1 - n \max_i \Pr \left(\left| \delta_i^I - \tilde{\delta}_i^I \right| \geq \psi \right) \quad (\text{A.16})$$

$$\Pr \left(\left| \delta_i^I - \tilde{\delta}_i^I \right| < \psi, \forall i \right) \rightarrow 1 \quad (\text{A.17})$$

The same result can be stated for out-degree as well.

$$\Pr \left(\left| \delta_i^O - \tilde{\delta}_i^O \right| < \psi, \forall i \right) \rightarrow 1 \quad (\text{A.18})$$

I.e. the probability convergence of sample degree is uniform across nodes.

Uniformly continuous ϕ means $\forall \epsilon, \exists \psi$ s.t. $\forall \{\delta_i^I, \delta_i^O\}$ satisfying $|\delta_i^I - \tilde{\delta}_i^I| + |\delta_i^O - \tilde{\delta}_i^O| < \psi$, we

have

$$\left| \phi \left(\delta_i^{\text{I}}, \delta_i^{\text{O}} \right) - \phi \left(\tilde{\delta}_i^{\text{I}}, \tilde{\delta}_i^{\text{O}} \right) \right| < \epsilon, \forall i. \quad (\text{A.19})$$

This implies the probability convergence of $\phi \left(\delta_i^{\text{I}}, \delta_i^{\text{O}} \right)$ is also uniform:

$$\Pr \left(\left| \phi \left(\delta_i^{\text{I}}, \delta_i^{\text{O}} \right) - \phi \left(\tilde{\delta}_i^{\text{I}}, \tilde{\delta}_i^{\text{O}} \right) \right| < \epsilon, \forall i \right) \rightarrow 1 \quad (\text{A.20})$$

Meanwhile, by LLN

$$\Pr \left(\left| \frac{1}{n} \sum_i \phi \left(\tilde{\delta}_i^{\text{I}}, \tilde{\delta}_i^{\text{O}} \right) - \mathbb{E} \phi \left(\tilde{\delta}_i^{\text{I}}, \tilde{\delta}_i^{\text{O}} \right) \right| < \epsilon \right) \rightarrow 1 \quad (\text{A.21})$$

Combined, by triangle inequality,

$$\Pr \left(\left| \frac{1}{n} \sum_i \phi \left(\delta_i^{\text{I}}, \delta_i^{\text{O}} \right) - \mathbb{E} \phi \left(\tilde{\delta}_i^{\text{I}}, \tilde{\delta}_i^{\text{O}} \right) \right| < 2\epsilon \right) \rightarrow 1. \quad (\text{A.22})$$

A.5 Proof of Proposition 3

Need to show

$$\text{plim}_{n \rightarrow \infty} \sum_j \frac{w_{i,j} \tilde{x}_j}{\delta_i^{\text{I}}} - \tilde{x}^* = 0, \quad \forall i \quad (\text{A.23})$$

First, the sample in-degree converges to the underlying in-degree, as proofed in the first steps of the proof of Lemma 1.

$$\delta_i^{\text{I}} \xrightarrow{p} \tilde{\delta}_i^{\text{I}}, \quad n \rightarrow \infty, \forall i. \quad (\text{A.24})$$

Second, according to the similar arguments as above, the in-neighborhood weighted av-

erage converges to its population counterpart.

$$\sum_j \frac{w_{i,j} \tilde{x}_j}{\delta_i^I} = \frac{\tilde{\delta}_i^I}{\delta_i^I} \frac{1}{(n-1)\tilde{\mu}} \sum_{j \neq i} \lambda_{i,j} \tilde{\delta}_j^O \tilde{x}_j \quad (\text{A.25})$$

For fixed i , $\lambda_{i,j} \tilde{\delta}_j^O \tilde{x}_j$ is i.i.d. across $j \neq i$ with expectation $\mathbb{E}[\tilde{\delta}^O \tilde{x}]$. By the law of large numbers, its sample average converges to the expectation. Therefore,

$$\sum_j \frac{w_{i,j} \tilde{x}_j}{\delta_i^I} \xrightarrow{p} \frac{\mathbb{E}[\tilde{\delta}^O \tilde{x}]}{\tilde{\mu}}, \quad n \rightarrow \infty, \forall i, \quad (\text{A.26})$$

Third, the aggregate \tilde{x}^* converges to the same population counterpart. As defined,

$$\tilde{x}^* = \frac{\sum_j \delta_j^O \tilde{x}_j}{\sum_j \delta_j^O}. \quad (\text{A.27})$$

In this expression, the denominator divided by n is $\frac{1}{n} \sum_j \delta_j^O$. By Lemma 1,

$$\frac{1}{n} \sum_j \delta_j^O \xrightarrow{p} \tilde{\mu}, \quad n \rightarrow \infty. \quad (\text{A.28})$$

The convergence of the denominator follows the same arguments, one can apply a trivariate version of Lemma 1 to show,

$$\frac{1}{n} \sum_j \delta_j^O \tilde{x}_j \xrightarrow{p} \mathbb{E}[\tilde{\delta}^O \tilde{x}], \quad n \rightarrow \infty. \quad (\text{A.29})$$

Hence, $\tilde{x}^* \xrightarrow{p} \mathbb{E}[\tilde{\delta}^O \tilde{x}]$ too. As a result, the proposition is proved.

A.6 Proof of Lemma 2

Apply Lemma 1, we have $\mu \xrightarrow{p} \tilde{\mu}$, and

$$\frac{1}{n} \sum_i \delta_i^{\text{O}} f(\delta_i^{\text{I}} x) \xrightarrow{p} \mathbb{E}[\tilde{\delta}^{\text{O}} f(\tilde{\delta}^{\text{I}} x)], \quad n \rightarrow \infty \quad (\text{A.30})$$

Therefore, the convergence of systemic response function (equation 4.9) is proven.

A.7 Proof of Proposition 4

For the second result, if $\tilde{x}^* = 0$, then it must be $f^*(0) = 0$. Then $\hat{x}^{*[n]} = 0, \forall n$ satisfies.

Then, focus on the case that $\tilde{x}^* > 0$. $\forall \epsilon > 0$ sufficiently small, local stability of \tilde{x}^* implies

$$\tilde{f}^*(\tilde{x}^* - \epsilon) > \tilde{x}^* - \epsilon \quad (\text{A.31})$$

$$\tilde{f}^*(\tilde{x}^* + \epsilon) < \tilde{x}^* + \epsilon \quad (\text{A.32})$$

By equation (4.9)

$$\Pr \left[f^{*[n]}(\tilde{x}^* - \epsilon) > \tilde{x}^* - \epsilon \right] \rightarrow 1, \quad n \rightarrow \infty \quad (\text{A.33})$$

$$\Pr \left[f^{*[n]}(\tilde{x}^* + \epsilon) < \tilde{x}^* + \epsilon \right] \rightarrow 1, \quad n \rightarrow \infty \quad (\text{A.34})$$

For each n , $f^{*[n]}$ is continuous. If $f^{*[n]}(\tilde{x}^* - \epsilon) > \tilde{x}^* - \epsilon$ and $f^{*[n]}(\tilde{x}^* + \epsilon) < \tilde{x}^* + \epsilon$, by contraction mapping, $\exists \hat{x}^{*[n]} \in (\tilde{x}^* - \epsilon, \tilde{x}^* + \epsilon)$ such that $\hat{x}^{*[n]} = f^{*[n]}(\hat{x}^{*[n]})$. This implies,

$$\Pr \left[\hat{x}^{*[n]} \in (\tilde{x}^* - \epsilon, \tilde{x}^* + \epsilon) \right] \rightarrow 1, \quad n \rightarrow \infty$$

A.8 Proof of Proposition 5

$$f \left(\sum_j w_{i,j} \tilde{x}_j^{[n]} \right) = f \left(\frac{\tilde{\delta}_i^{\text{I}}}{\tilde{\mu}} \frac{1}{n-1} \sum_j \lambda_{i,j} \tilde{\delta}_j^{\text{O}} f \left(\tilde{\delta}_j^{\text{I}} \tilde{x}^* \right) \right) \quad (\text{A.35})$$

This equation is seen in the proof of Proposition 3. Similarly, by WLLN, the iid average term converges to the expectation in probability.

$$\frac{1}{n-1} \sum_j \lambda_{i,j} \tilde{\delta}_j^{\text{O}} f \left(\tilde{\delta}_j^{\text{I}} \tilde{x}^* \right) \xrightarrow{p} \mathbb{E} \lambda_{i,j} \tilde{\delta}_j^{\text{O}} f \left(\tilde{\delta}_j^{\text{I}} \tilde{x}^* \right) = \mathbb{E} \left[\mathbb{E} \left[\lambda_{i,j} | \tilde{\delta}_j^{\text{I}}, \tilde{\delta}_j^{\text{O}} \right] \tilde{\delta}_j^{\text{O}} f \left(\tilde{\delta}_j^{\text{I}} \tilde{x}^* \right) \right] \quad (\text{A.36})$$

$$= \mathbb{E} \left[\tilde{\delta}_j^{\text{O}} f \left(\tilde{\delta}_j^{\text{I}} \tilde{x}^* \right) \right] \quad (\text{A.37})$$

By continuous mapping theorem, plug this back,

$$f \left(\frac{\tilde{\delta}_i^{\text{I}}}{\tilde{\mu}} \mathbb{E} \left[\tilde{\delta}_j^{\text{O}} f \left(\tilde{\delta}_j^{\text{I}} \tilde{x}^* \right) \right] \right) - f \left(\sum_j w_{i,j} \tilde{x}_j^{[n]} \right) \xrightarrow{p} 0, \quad n \rightarrow \infty \quad (\text{A.38})$$

Notice \tilde{x}^* is the fixed point of \tilde{f}^* . The first term is simplified as:

$$f \left(\frac{\tilde{\delta}_i^{\text{I}}}{\tilde{\mu}} \mathbb{E} \left[\tilde{\delta}_j^{\text{O}} f \left(\tilde{\delta}_j^{\text{I}} \tilde{x}^* \right) \right] \right) = f \left(\frac{\tilde{\delta}_i^{\text{I}}}{\tilde{\mu}} \tilde{f}^* \left(\tilde{x}^* \right) \right) = f \left(\tilde{\delta}_i^{\text{I}} \tilde{x}^* \right) = \tilde{x}_i^{[n]} \quad (\text{A.39})$$

In summary, that is to say,

$$\tilde{x}_i^{[n]} - f \left(\sum_j w_{i,j} \tilde{x}_j^{[n]} \right) \xrightarrow{p} 0, \quad n \rightarrow \infty \quad (\text{A.40})$$

$\forall \epsilon > 0,$

$$\Pr \left(\left| \tilde{x}_i^{[n]} - f \left(\sum_j w_{i,j} \tilde{x}_j^{[n]} \right) \right| < \epsilon, \forall i \right) \rightarrow 1, \quad n \rightarrow \infty \quad (\text{A.41})$$

This requires simply reexamining the proof of Proposition 5. In the first plim operation in

equation (A.46), the summand term $\lambda_{i,j} \tilde{\delta}_j^{\text{O}} f\left(\tilde{\delta}_j^{\text{I}} \tilde{x}^*\right)$ is uniformly bounded across i according to Condition 5. Therefore,

$$\Pr \left(\left| \frac{1}{n-1} \sum_j \lambda_{i,j} \tilde{\delta}_j^{\text{O}} f\left(\tilde{\delta}_j^{\text{I}} \tilde{x}^*\right) - \mathbb{E} \left[\tilde{\delta}_j^{\text{O}} f\left(\tilde{\delta}_j^{\text{I}} \tilde{x}^*\right) \right] \right| < \epsilon, \forall i \right) \quad (\text{A.42})$$

In the second plim operation in equation (A.47), it is noted that f is uniformly continuous and $\tilde{\delta}^{\text{I}}$ is bounded. Therefore, apply $f\left(\frac{\tilde{\delta}_i^{\text{I}}}{\tilde{\mu}} \cdot\right)$ to the two terms inside equation (A.51), we have $\forall \epsilon'$

$$\Pr \left(\left| f\left(\frac{\tilde{\delta}_i^{\text{I}}}{\tilde{\mu}} \frac{1}{n-1} \sum_j \lambda_{i,j} \tilde{\delta}_j^{\text{O}} f\left(\tilde{\delta}_j^{\text{I}} \tilde{x}^*\right)\right) - f\left(\frac{\tilde{\delta}_i^{\text{I}}}{\tilde{\mu}} \mathbb{E} \left[\tilde{\delta}_j^{\text{O}} f\left(\tilde{\delta}_j^{\text{I}} \tilde{x}^*\right) \right] \right) \right| < \epsilon', \forall i \right) \quad (\text{A.43})$$

The same manipulations as in the previous proof leads to the required uniform convergence in probability result.

$$f\left(\sum_j w_{i,j} \tilde{x}_j^{[n]}\right) = f\left(\frac{\tilde{\delta}_i^{\text{I}}}{\tilde{\mu}} \frac{1}{n-1} \sum_j \lambda_{i,j} \tilde{\delta}_j^{\text{O}} f\left(\tilde{\delta}_j^{\text{I}} \tilde{x}^*\right)\right) \quad (\text{A.44})$$

This equation is seen in the proof of Proposition 3. Similarly, by WLLN, the iid average term converges to the expectation in probability.

$$\frac{1}{n-1} \sum_j \lambda_{i,j} \tilde{\delta}_j^{\text{O}} f\left(\tilde{\delta}_j^{\text{I}} \tilde{x}^*\right) \xrightarrow{p} \mathbb{E} \lambda_{i,j} \tilde{\delta}_j^{\text{O}} f\left(\tilde{\delta}_j^{\text{I}} \tilde{x}^*\right) = \mathbb{E} \left[\mathbb{E} \left[\lambda_{i,j} | \tilde{\delta}_j^{\text{I}}, \tilde{\delta}_j^{\text{O}} \right] \tilde{\delta}_j^{\text{O}} f\left(\tilde{\delta}_j^{\text{I}} \tilde{x}^*\right) \right] \quad (\text{A.45})$$

$$= \mathbb{E} \left[\tilde{\delta}_j^{\text{O}} f\left(\tilde{\delta}_j^{\text{I}} \tilde{x}^*\right) \right] \quad (\text{A.46})$$

By continuous mapping theorem, plug this back,

$$f\left(\frac{\tilde{\delta}_i^{\text{I}}}{\tilde{\mu}} \mathbb{E} \left[\tilde{\delta}_j^{\text{O}} f\left(\tilde{\delta}_j^{\text{I}} \tilde{x}^*\right) \right] \right) - f\left(\sum_j w_{i,j} \tilde{x}_j^{[n]}\right) \xrightarrow{p} 0, \quad n \rightarrow \infty \quad (\text{A.47})$$

Notice \tilde{x}^* is the fixed point of \tilde{f}^* . The first term is simplified as:

$$f\left(\tilde{\delta}_i^{\text{I}} \frac{1}{\tilde{\mu}} \mathbb{E}\left[\tilde{\delta}_j^{\text{O}} f\left(\tilde{\delta}_j^{\text{I}} \tilde{x}^*\right)\right]\right) = f\left(\tilde{\delta}_i^{\text{I}} \tilde{f}^*(\tilde{x}^*)\right) = f\left(\tilde{\delta}_i^{\text{I}} \tilde{x}^*\right) = \tilde{x}_i^{[n]} \quad (\text{A.48})$$

In summary, that is to say,

$$\tilde{x}_i^{[n]} - f\left(\sum_j w_{i,j} \tilde{x}_j^{[n]}\right) \xrightarrow{p} 0, \quad n \rightarrow \infty \quad (\text{A.49})$$

$\forall \epsilon > 0$,

$$\Pr\left(\left|\tilde{x}_i^{[n]} - f\left(\sum_j w_{i,j} \tilde{x}_j^{[n]}\right)\right| < \epsilon, \forall i\right) \rightarrow 1, \quad n \rightarrow \infty \quad (\text{A.50})$$

This requires simply reexamining the proof of Proposition 5. In the first plim operation in equation (A.46), the summand term $\lambda_{i,j} \tilde{\delta}_j^{\text{O}} f\left(\tilde{\delta}_j^{\text{I}} \tilde{x}^*\right)$ is uniformly bounded across i according to Condition 5. Therefore,

$$\Pr\left(\left|\frac{1}{n-1} \sum_j \lambda_{i,j} \tilde{\delta}_j^{\text{O}} f\left(\tilde{\delta}_j^{\text{I}} \tilde{x}^*\right) - \mathbb{E}\left[\tilde{\delta}_j^{\text{O}} f\left(\tilde{\delta}_j^{\text{I}} \tilde{x}^*\right)\right]\right| < \epsilon, \forall i\right) \quad (\text{A.51})$$

In the second plim operation in equation (A.47), it is noted that f is uniformly continuous and $\tilde{\delta}^{\text{I}}$ is bounded. Therefore, apply $f\left(\frac{\tilde{\delta}_i^{\text{I}}}{\tilde{\mu}} \cdot\right)$ to the two terms inside equation (A.51), we have $\forall \epsilon'$

$$\Pr\left(\left|f\left(\frac{\tilde{\delta}_i^{\text{I}}}{\tilde{\mu}} \frac{1}{n-1} \sum_j \lambda_{i,j} \tilde{\delta}_j^{\text{O}} f\left(\tilde{\delta}_j^{\text{I}} \tilde{x}^*\right)\right) - f\left(\frac{\tilde{\delta}_i^{\text{I}}}{\tilde{\mu}} \mathbb{E}\left[\tilde{\delta}_j^{\text{O}} f\left(\tilde{\delta}_j^{\text{I}} \tilde{x}^*\right)\right]\right)\right| < \epsilon', \forall i\right) \quad (\text{A.52})$$

The same manipulations as in the previous proof leads to the required uniform convergence in probability result.

A.9 Proof of Proposition 6

First step, construct a compact convex set $\mathbb{S} \in \mathbb{R}^n$ to apply the Brouwer fixed-point theorem with.

For each realization and given an $\epsilon > 0$, make the following constructions:

Define vector $\mathbf{v}^{[1]} = \epsilon \frac{\tilde{\mu}}{\mathbb{E}(\tilde{\delta}^O)^2} \tilde{\boldsymbol{\delta}}^O$.

Define set

$$\mathbb{S}^{\text{preimage}} = \left\{ \mathbf{e} \mid e_i = f\left(\tilde{\delta}_i^I(\tilde{x}^* + \epsilon')\right) - f\left(\tilde{\delta}_i^I(\tilde{x}^*)\right), \frac{1}{n\tilde{\mu}} \tilde{\boldsymbol{\delta}}^O \cdot \mathbf{e} \in [-\epsilon, \epsilon] \right\}. \quad (\text{A.53})$$

Define set \mathbb{S}^{res} as the convex hull of the projection residual of $\mathbb{S}^{\text{preimage}}$ onto $\mathbf{v}^{[1]}$.

Define set $\mathbb{S} = \left\{ \mathbf{x} \mid \mathbf{x} = \tilde{\mathbf{x}}^{[n]} + \mathbf{e} \right\}$ for any vectors \mathbf{e} with the following orthogonal decomposition: $\mathbf{e} = \mathbf{e}^{[1]} + \left(\mathbf{e}^{[2]} + \mathbf{e}^{[3]} \right)$, such that the three components are any $\mathbf{e}^{[1]} = b^{[1]} \mathbf{v}^{[1]}$, where $|b^{[1]}| \leq 1$; $\mathbf{e}^{[2]} \in \mathbb{S}^{\text{res}}$; $\mathbf{e}^{[3]} \perp \mathbf{v}^{[1]}$, and $|\mathbf{e}^{[3]}| \leq \sqrt{n-1}\epsilon$. Notice the sets are dependents of the underlying degrees $\tilde{\boldsymbol{\delta}}^I, \tilde{\boldsymbol{\delta}}^O$, and hence random. We will verify they are infinitesimal as ϵ goes to zero. For the moment, it is noted that \mathbb{S} is compact and convex. If $\mathcal{M}(\mathbb{S}) \subseteq \mathbb{S}$, then one can apply the Brouwer fixed-point theorem.

Second step, show that

$$\Pr(\mathcal{M}(\mathbb{S}) \subseteq \mathbb{S}) \rightarrow 1, \quad n \rightarrow \infty. \quad (\text{A.54})$$

For any $\mathbf{x} \in \mathbb{S}$ with the associated \mathbf{e} and decomposition $\mathbf{e} = \mathbf{e}^{[1]} + \mathbf{e}^{[2]} + \mathbf{e}^{[3]}$ defined as above,

$$\mathcal{M}_i(\mathbf{x}) = f\left(\sum_j w_{i,j} \left(\tilde{x}_j^{[n]} + e_j\right)\right), \quad (\text{A.55})$$

in which

$$\sum_j w_{i,j} \left(\tilde{x}_j^{[n]} + e_j \right) = \frac{\tilde{\delta}_i^{\text{I}}}{(n-1)\tilde{\mu}} \left[\sum_j \lambda_{i,j} \tilde{\delta}_j^{\text{O}} f \left(\tilde{\delta}_j^{\text{I}} \tilde{x}^* \right) + \sum_j \lambda_{i,j} \tilde{\delta}_j^{\text{O}} \left(e_j^{[1]} + e_j^{[2]} + e_j^{[3]} \right) \right]. \quad (\text{A.56})$$

The first term is familiar, it uniformly converges to $\tilde{\delta}_i^{\text{I}} \tilde{x}^*$ in probability according to Lemma Proposition 5. The second term:

$$\frac{\tilde{\delta}_i^{\text{I}}}{(n-1)\tilde{\mu}} \left[\sum_j \lambda_{i,j} \tilde{\delta}_j^{\text{O}} \left(e_j^{[1]} + e_j^{[2]} + e_j^{[3]} \right) \right] \quad (\text{A.57})$$

$$\xrightarrow{p} \frac{\tilde{\delta}_i^{\text{I}}}{\tilde{\mu}} \mathbb{E} \left[\mathbb{E} \left[\lambda_{i,j} | \tilde{\delta}_j^{\text{O}} \right] \tilde{\delta}_j^{\text{O}} \left(e_j^{[1]} + e_j^{[2]} + e_j^{[3]} \right) \right] \quad (\text{A.58})$$

$$= \frac{\tilde{\delta}_i^{\text{I}}}{\tilde{\mu}} \mathbb{E} \left[\tilde{\delta}_j^{\text{O}} \left(e_j^{[1]} + e_j^{[2]} + e_j^{[3]} \right) \right] \quad (\text{A.59})$$

$$= \frac{\tilde{\delta}_i^{\text{I}}}{\tilde{\mu}} \mathbb{E} \left[\tilde{\delta}_j^{\text{O}} e_j^{[1]} + 0 + 0 \right] \quad (\text{A.60})$$

$$= \tilde{\delta}_i^{\text{I}} b^{[1]} \epsilon \quad (\text{A.61})$$

Plug this back to equation (A.55)

$$\mathcal{M}_i(\mathbf{x}) - f \left(\tilde{\delta}_i^{\text{I}} (\tilde{x}^* + b^{[1]} \epsilon) \right) \xrightarrow{p} 0 \quad (\text{A.62})$$

Next, we argue that $f \left(\tilde{\delta}_i^{\text{I}} (\tilde{x}_i^{[n]} + b^{[1]} \epsilon) \right)$ is well contained in \mathbb{S} with a positive margin. Therefore, even with the asymptotic error, $\mathcal{M}(\mathbb{S}) \subseteq \mathbb{S}$ at converging probability.

$$\text{Define } \mathbb{S}^{\text{image}} = \left\{ f \left(\tilde{\delta}_i^{\text{I}} (\tilde{x}^* + b^{[1]} \epsilon) \right) - f \left(\tilde{\delta}_i^{\text{I}} \tilde{x}^* \right) \mid b^{[1]} \in [-1, 1] \right\}.$$

For any $\mathbf{e} \in \mathbb{S}^{\text{image}}$, assess it with respect to the definition of $\mathbb{S}^{\text{preimage}}$:

$$\frac{1}{n\tilde{\mu}} \tilde{\boldsymbol{\delta}}^{\text{O}} \cdot \mathbf{e} \xrightarrow{p} \tilde{f}^* \left(\tilde{x}^* + b^{[1]} \epsilon \right) - \tilde{f}^* \left(\tilde{x}^* \right). \quad (\text{A.63})$$

Because \tilde{x}^* is a locally stable equilibrium of \tilde{f}^* ,

$$\left| \tilde{f}^* \left(\tilde{x}^* + b^{[1]}\epsilon \right) - \tilde{f}^* \left(\tilde{x}^* \right) \right| < \epsilon \quad (\text{A.64})$$

That is to say the probability limit of this \mathbf{e} is in $\mathbb{S}^{\text{preimage}}$.

In fact, \tilde{f}^* around \tilde{x}^* have Lipschitz coefficient $\tilde{f}^{*p} < 1$, we have

$$\Pr \left(\frac{1}{\tilde{f}^{*p}} \mathbf{e} \in \mathbb{S}^{\text{preimage}} \right) \rightarrow 1. \quad (\text{A.65})$$

Plug this back

$$\mathcal{M}_i(\mathbf{x}) = f \left(\tilde{\delta}_i^{\text{I}}(\tilde{x}^* + b^{[1]}\epsilon) \right) + \left[\mathcal{M}_i(\mathbf{x}) - f \left(\tilde{\delta}_i^{\text{I}}(\tilde{x}^* + b^{[1]}\epsilon) \right) \right] \quad (\text{A.66})$$

With converging probability, the first term is well contained in $\mathbb{S}^{\text{preimage}}$ with a positive margin, the second term is uniformly converging to zero. $\mathbb{S}^{\text{preimage}}$ is in turn contained in \mathbb{S} with margin of at least $\epsilon^{[3]}$. Combined, we achieved the goal of the second step: equation (A.54).

Third and final step, apply Brouwer's fixed point theorem:

$$\Pr (\exists \mathbf{x} \in \mathbb{S}, \text{ s.t. } \mathbf{x} = \mathcal{M}(\mathbf{x})) \rightarrow 1, \quad n \rightarrow \infty. \quad (\text{A.67})$$

Remind in the first step, S is controlled by ϵ , which can be infinitesimal. Especially the first component controls the systemic averages of the vectors in the set. $\forall \mathbf{x} \in \mathbb{S}$, its systemic average is

$$x^* = \frac{1}{n\mu} \sum_i \delta_i^{\text{O}} x_i \xrightarrow{p} \tilde{x}^* + b^{[1]}\epsilon \quad n \rightarrow \infty. \quad (\text{A.68})$$

All combined, that is to say $\forall \epsilon > 0$, the probability that there exist an original equilibrium $\mathbf{x}^{[n]}$ whose systemic average is within $\tilde{x}^* \pm \epsilon$ converges to one as n goes to infinity.

A.10 Proof of Proposition 7

Combine Proposition 4 and Proposition 6.

A.11 Proof of Lemma 3

Proof.

$$h^{*'}(x) = \sum_i \frac{\delta_i^O \delta_i^I}{n\mu} h'(\delta_i^I x) \quad (\text{A.69})$$

$$\text{plim}_{n \rightarrow \infty} h^{*'}(x) = \text{plim}_{n \rightarrow \infty} \frac{1}{n} \sum_i \frac{\delta_i^O \delta_i^I}{\mu} h'(\delta_i^I x) \quad (\text{A.70})$$

$$= \frac{1}{\tilde{\mu}} \mathbb{E} \delta^O \delta^I h'(\delta^I x) \quad (\text{A.71})$$

$$= \frac{1}{\tilde{\mu}} \iint h'(\delta^I x) \delta^O \delta^I \Pi(\delta^I, \delta^O) d\delta^I d\delta^O \quad (\text{A.72})$$

$$= \frac{\iint \delta^O \delta^I \Pi(\delta^I, \delta^O) d\delta^O d\delta^I}{\tilde{\mu}} \int h'(\delta^I x) \frac{\int \delta^O \delta^I \Pi(\delta^I, \delta^O) d\delta^O}{\iint \delta^O \delta^I \Pi(\delta^I, \delta^O) d\delta^O d\delta^I} d\delta^I \quad (\text{A.73})$$

$$= \tilde{W}^* \int h'(\delta^I x) \pi^t(\delta^I) d\delta^I. \quad (\text{A.74})$$

In this expression, \tilde{W}^* is defined as

$$\tilde{W}^* = \frac{1}{\tilde{\mu}} \iint \delta^O \delta^I \Pi(\delta^I, \delta^O) d\delta^O d\delta^I. \quad (\text{A.75})$$

Notice it is the population counterpart of sample W^* , $\text{plim}_{n \rightarrow \infty} W^* = \tilde{W}^*$.

And $\pi^t(\delta^I)$ is the transformed marginal probability density function of δ^I , such that the Radon-Nikodym derivative with respect to the natural probability π is proportional to $\delta^O \delta^I$.

Specifically, it is,

$$\pi^t(\delta^I) = \frac{\int \delta^O \delta^I \Pi(\delta^I, \delta^O) d\delta^O}{\iint \delta^O \delta^I \Pi(\delta^I, \delta^O) d\delta^O d\delta^I}. \quad (\text{A.76})$$

Moreover the denominator of $\pi^t(\delta^{\text{I}})$ further decompose to,

$$\pi^t(\delta^{\text{I}}) = \frac{\delta^{\text{I}}\pi(\delta^{\text{I}}) \int \delta^{\text{O}} \frac{\Pi(\delta^{\text{I}}, \delta^{\text{O}})}{\pi(\delta^{\text{I}})} d\delta^{\text{O}}}{\mathbb{E}\delta^{\text{O}}\delta^{\text{I}}} \quad (\text{A.77})$$

$$\pi^t(\delta^{\text{I}}) = \frac{\delta^{\text{I}}\pi(\delta^{\text{I}})\mathbb{E}[\delta^{\text{O}}|\delta^{\text{I}}]}{\mathbb{E}\delta^{\text{O}}\delta^{\text{I}}} \quad (\text{A.78})$$

□

A.12 Proof of Proposition 8

Proof. From equation (4.11),

$$\tilde{h}^{*'}(x) = \tilde{W}^* \int_0^{+\infty} h'(\delta^{\text{I}}x)\pi^t(\delta^{\text{I}}) d\delta^{\text{I}} \quad (\text{A.79})$$

$$= \tilde{W}^* \int_{-\infty}^{+\infty} h'(\log \delta^{\text{I}} + \log x) \frac{\mathbb{E}[\delta^{\text{O}}|\delta^{\text{I}}]}{\mathbb{E}[\delta^{\text{O}}\delta^{\text{I}}]} \pi(\delta^{\text{I}}) d \log \delta^{\text{I}} \quad (\text{A.80})$$

$$= \frac{u}{\tilde{\mu}} \int_{-\infty}^{+\infty} \mathbb{1}_{(\log y_l, \log y_h)}(\log \delta^{\text{I}} + \log x) \mathbb{E}[\delta^{\text{O}}|\delta^{\text{I}}] \pi(\delta^{\text{I}}) d \log \delta^{\text{I}} \quad (\text{A.81})$$

The integral takes the form of convolution with respect to $\log \delta^{\text{I}}$.

$$x \frac{d\tilde{h}^{*'}(x)}{dx} = \frac{d\tilde{h}^{*'}(x)}{d \log x} = \frac{u}{\tilde{\mu}} \left(\mathbb{E}[\delta^{\text{O}}|\frac{y_l}{x}] \pi(\frac{y_l}{x}) - \mathbb{E}[\delta^{\text{O}}|\frac{y_h}{x}] \pi(\frac{y_h}{x}) \right) \quad (\text{A.82})$$

Since $\mathbb{E}[\delta^{\text{O}}|\delta^{\text{I}}] \pi(\delta^{\text{I}})$ is unimodal, $\left(\mathbb{E}[\delta^{\text{O}}|\frac{y_l}{x}] \pi(\frac{y_l}{x}) - \mathbb{E}[\delta^{\text{O}}|\frac{y_h}{x}] \pi(\frac{y_h}{x}) \right)$ must cross only once. Therefore, $\frac{d\tilde{h}^{*'}(x)}{dx}$ is composed of a positive region followed by a negative region. As a result, $\tilde{h}^{*'}$ is unimodal.

Then, the integral \tilde{h}^* is composed of a convex interval followed by a concave interval, separated by an inflection point. Since $\tilde{f}^*(x) = \tilde{h}^*(x) + \tilde{W}^*x$, \tilde{f}^* takes the same convexity situation. It is also composed of a convex interval followed by a concave interval, separated by an inflection point.

Suppose there are three locally stable equilibria for $x^* = \tilde{f}^*(x^*)$, then there are at least

two that fall in the same convexity region. At these two points $\tilde{f}^{*'}(x^*) < 1$. In between them, $\tilde{f}^{*'}$ is monotonic, therefore $\tilde{f}^{*'} < 1$ for all points in between. Then, $x^* = \tilde{f}^*(x^*)$ at the two points is a violation of contraction mapping theorem. \square

A.13 Proof of Proposition 9

Both the in- and out-degrees scales down at the rate of θ . Simply apply the definition of the systemic response function (Definition 8) delivers the desired result.

A.14 Proof of Proposition 10

The proof can be accomplished in two steps. First, at the optimal government injection plan, systemic response function evaluated at the critical level of systemic liquidity ($f^*(\Theta x_c; \{z_i\})$) must be maximized. To show by contradiction, suppose there exist another government injection plan $\{z'_i\}$ that achieves a higher level of $f^*(\Theta x_c; \{z'_i\}) > f^*(\Theta x_c; \{z_i\})$. Then there must exist a $\Theta' > \Theta$ such that $f^*(\Theta' x_c; \{z'_i\}) > x_c$. This would imply the contradiction that the fragility associated with $\{z'_i\}$ is at least Θ' , which is strictly greater than Θ .

Second, to maximize $f^*(\Theta x_c)$, $\frac{z_i}{Z}$ must be a (weakly) increasing function of $\delta_i^O f'(\delta_i^I \Theta x_c)$. This step can be easily shown as the first order condition of the contained optimization problem. Fixing Θ at the optimal level,

$$\begin{aligned} \max_{z_i} \sum_i \frac{\delta_i^O}{n\mu} f(\delta_i^I \Theta x_c + z_i) \\ \text{s.t. } \sum_i (z_i + \zeta(\frac{z_i}{Z})) = Z \end{aligned}$$

Then, the first order conditions are,

$$\frac{\delta_i^O}{n\mu} f'(\delta_i^I \Theta x_c + z_i) = \lambda_A \left(1 + \frac{1}{Z} \zeta'(\frac{z_i}{Z})\right)$$

Evaluated at the limit of $(Z \rightarrow 0^+)$, the result is shown as required.

A.15 Proof of Proposition 11

Proposition 11 is a special case of Proposition 12. When in- and out-degrees are uncorrelated, $W^* = \mu$. As a result, $\Theta \leq \frac{y_h+d}{y_h/W^*}$. Therefore, financial fragility decreases.

A.16 Proof of Proposition 12

First, $\frac{\text{Cov}(\delta^I, \delta^O)}{\mu^2} \leq \frac{y_h+d}{\Theta y_h} W^* - 1$ is equivalent to $\Theta \leq \frac{y_h+d}{y_h/\mu}$. Notice the upper kink point of the $(\theta; \mu)$ -contraction is $(y_h/\mu, y_h + d)$. Therefore, $\Theta \leq \frac{y_h+d}{y_h/\mu}$ means the focal point of the $(\theta; \mu)$ -scale transformation is to the upper left of the tangent line as in Figure 5.1 (b) whose slope is Θ .

Next, I need to show if and only if the focal point is to the upper left, then Θ will decrease.

“If”: according to Lemma 4, evaluate the tangent point $(\Theta x_c, x_c)$,

$$S_h x_c + (1 - S_h)(y_h + d) = f^* \left(S_h x + (1 - S_h) \frac{y_h}{\tau}; (\theta; \tau) \right),$$

In addition, point $(S_h x + (1 - S_h) \frac{y_h}{\tau}, S_h x_c + (1 - S_h)(y_h + d))$ is also to the upper left of the tangent line. Therefore, it must support a financial fragility that is lower than Θ .

“Only If”: Given financial fragility decreases to Θ' . Then there is a new tangent point $(\Theta' x'_c, x'_c)$ that lies to the upper-left of the original tangent line. Lemma 4 implies that the focal points $(y_h/\mu, y_h + d)$ lies to the upper left of the tangent line as well. As discussed, this implies that $\frac{\text{Cov}(\delta^I, \delta^O)}{\mu^2} \leq \frac{y_h+d}{\Theta y_h} W^* - 1$.

A.17 Optimized Bank Profit Function

The optimized bank profit function given interbank funding y_i is

$$profit(y_i) = \begin{cases} 0 & y_i \in [0, \frac{\gamma}{\beta}) \\ (R-1)(\frac{\beta}{1-\beta}y_i - \frac{\gamma}{1-\beta}) & y_i \in [\frac{\gamma}{\beta}, \frac{1-\beta}{\beta}d + \frac{\gamma}{\beta}) \\ (R-1)d & y_i \in [\frac{1-\beta}{\beta}d + \frac{\gamma}{\beta}, +\infty) \end{cases}$$

APPENDIX B

ADDITIONAL FIGURES

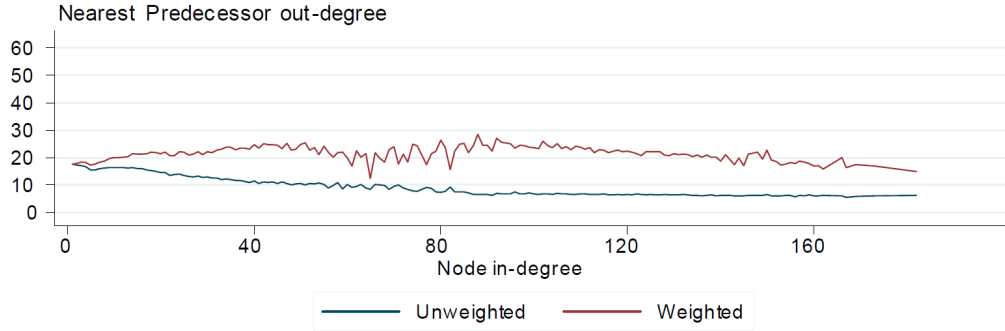


Figure B.1: Weighted non-assortative matching in the federal funds market
Fig. 16. of Bech and Atalay (2010): “The relationship between node in-(out-)degree and the average out-(in-)degree of the nearest predecessor (successor).”

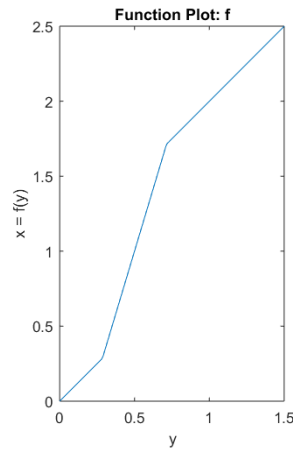
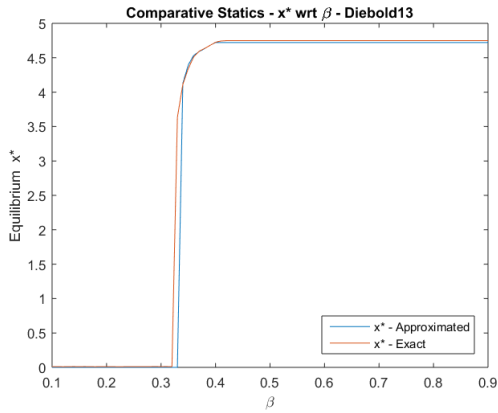
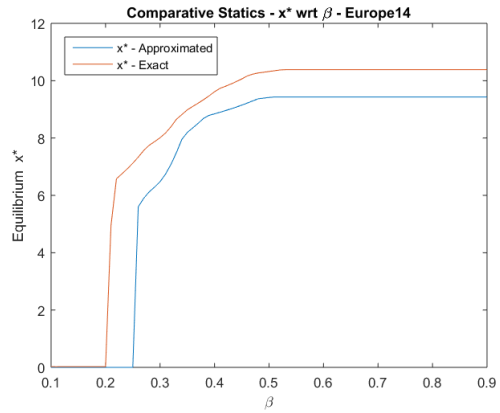


Figure B.2: Numerical Individual Response Function used in Subsection 4.7
Function f is constructed according to the definition in equation (3.1), by assigning the primitives as $d = 1, \gamma = 0.05, \beta = 0.9$.



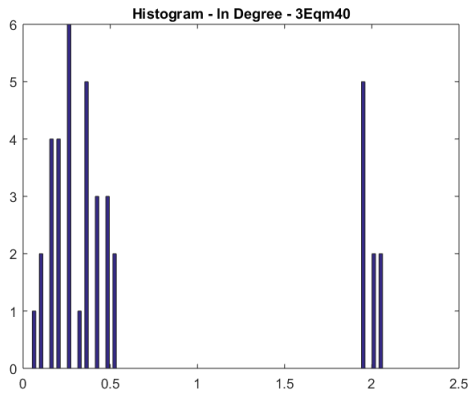
(a) Diebold13



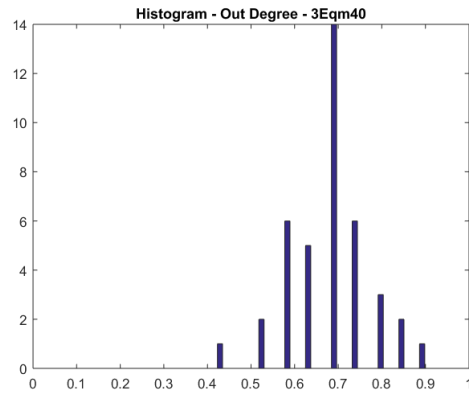
(b) Europe14

Figure B.3: Numerical Comparative Statics with respect to β

The plots are calculated under the same construction as Figure 4.2, but with changing β at the horizontal axis. The red and blue curves plot the highest systemic liquidity (x^*) calculated for the exact equilibrium and the systemic liquidity equilibrium respectively.



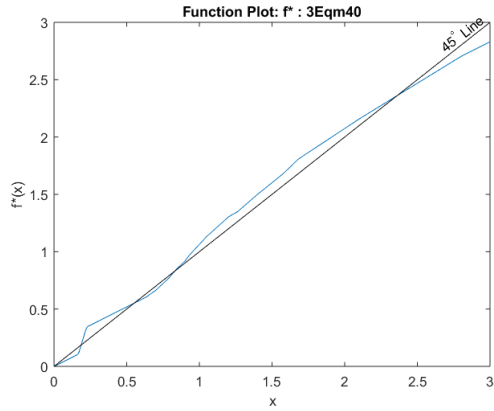
(a) In-Degree Distribution



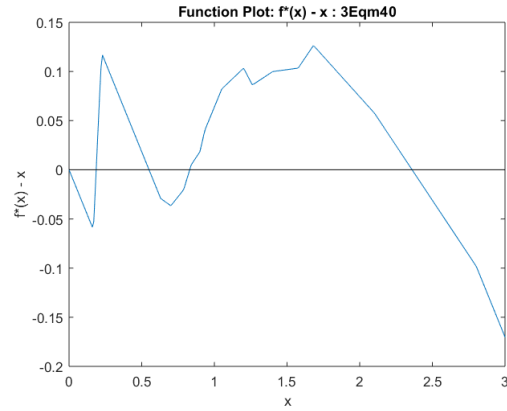
(b) Out-Degree Distribution

Figure B.4: Degree Distributions of 3Eqm40 in Figure 4.4

In-degree distribution is binomial, the necessary condition for more than two equilibria.

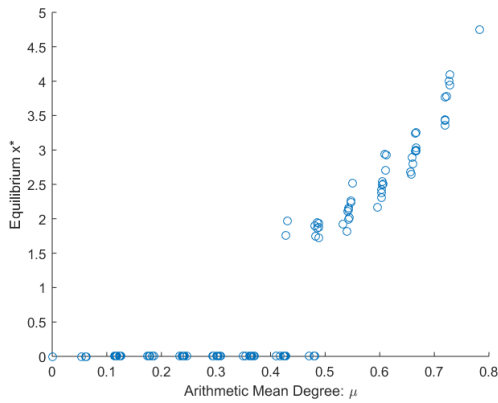


(a) Function Plot: $f^*(x)$

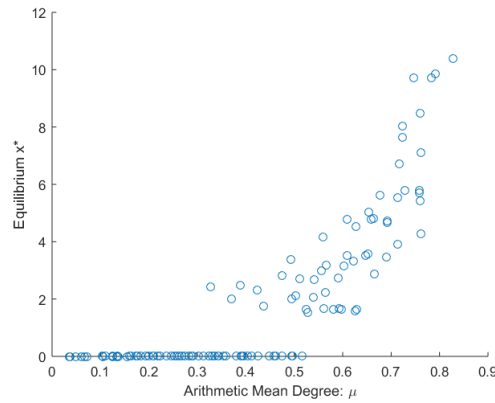


(b) Function Plot: $f^*(x) - x$

Figure B.5: Systemic Response Function f^* of 3Eqm40as in Figure 4.4
 Panel (a) shows $f^*(x)$ has two consecutive S-shaped regions. Panel (b) zooms in to the difference with x to show how $f^*(x)$ crosses the 40° line several times, constituting three stable equilibria.



(a) Diebold13



(b) Europe14

Figure B.6: μ and equilibrium systemic liquidity in Stress Testing
 Each marker represents one stress testing scenario. The vertical position is the equilibrium systemic liquidity, as calculated in Figure 5.2. The horizontal position is the average degree (μ) of the remaining set \mathcal{R} .

REFERENCES

- Acemoglu, Daron, Asuman Ozdaglar, and Alireza Tahbaz-Salehi, 2015a, Networks, shocks, and systemic risk, Technical report, National Bureau of Economic Research.
- Acemoglu, Daron, Asuman Ozdaglar, and Alireza Tahbaz-Salehi, 2015b, Systemic risk and stability in financial networks, *The american economic review* 105, 564–608.
- Allen, Franklin, and Douglas Gale, 2000, Financial Contagion, *Journal of Political Economy* 108, 1–33.
- Ballester, Coralio, Antoni Calvó-Armengol, and Yves Zenou, 2006, Who’s who in networks. Wanted: The key player, *Econometrica* 74, 1403–1417.
- Bebchuk, Lucian A., and Itay Goldstein, 2011, Self-fulfilling Credit Market Freezes, *Review of Financial Studies* 24, 3519–3555.
- Bech, Morten L., and Enghin Atalay, 2010, The topology of the federal funds market, *Physica A: Statistical Mechanics and its Applications* 389, 5223–5246.
- Bech, Morten Linnemann, and Kirsten Bonde Rørdam, 2008, The topology of danish inter-bank money flows, Technical report, Danmarks Nationalbank Working Papers.
- Benmelech, Efraim, and Nittai K. Bergman, 2012, Credit traps, *The American Economic Review* 102, 3004–3032.
- Bernanke, Ben, 2010, Statement by Ben S. Bernanke, chairman, Board of Governors of the Federal Reserve System, before the Financial Crisis Inquiry Commission. Washington, DC.
- Bernardo, Antonio E., and Ivo Welch, 2004, Liquidity and financial market runs, *The Quarterly Journal of Economics* 119, 135–158.
- Bramoullé, Yann, and Rachel Kranton, 2015, Games played on networks .
- Bramoullé, Yann, Rachel Kranton, and Martin D’Amours, 2014, Strategic Interaction and Networks, *American Economic Review* 104, 898–930.
- Brunnermeier, Markus K., 2009, Deciphering the liquidity and credit crunch 2007–2008, *The Journal of economic perspectives* 23, 77–100.
- Brunnermeier, Markus K., and Lasse Heje Pedersen, 2009, Market Liquidity and Funding Liquidity, *Review of Financial Studies* 22, 2201–2238.
- Caballero, Ricardo J., and Alp Simsek, 2013, Fire Sales in a Model of Complexity: Fire Sales in a Model of Complexity, *The Journal of Finance* 68, 2549–2587.
- Chung, Fan, and Linyuan Lu, 2002, The average distances in random graphs with given expected degrees, *Proceedings of the National Academy of Sciences* 99, 15879–15882.
- Chung, Fan R. K., and Linyuan Lu, 2006, *Complex Graphs and Networks* (American Mathematical Soc.).

- Craig, Ben, and Goetz von Peter, 2014, Interbank tiering and money center banks, *Journal of Financial Intermediation* 23, 322–347.
- Denbee, Edward, Christian Julliard, Ye Li, and Kathy Yuan, 2017, Network Risk and Key Players: A Structural Analysis of Interbank Liquidity, SSRN Scholarly Paper ID 2884461, Social Science Research Network, Rochester, NY.
- Diamond, Douglas W., and Philip H. Dybvig, 1983, Bank runs, deposit insurance, and liquidity, *Journal of political economy* 91, 401–419.
- Diamond, Douglas W., and Raghuram G. Rajan, 2005, Liquidity shortages and banking crises, *The Journal of finance* 60, 615–647.
- Diebold, Francis X., and Kamil Yilmaz, 2011, On the Network Topology of Variance Decompositions: Measuring the Connectedness of Financial Firms, Working Paper 17490, National Bureau of Economic Research, DOI: 10.3386/w17490.
- Eisenberg, Larry, and Thomas H. Noe, 2001, Systemic Risk in Financial Systems, *Management Science* 47, 236–249.
- Elliott, Matthew, Benjamin Golub, and Matthew O. Jackson, 2014, Financial Networks and Contagion, *American Economic Review* 104, 3115–3153.
- Ennis, Huberto M., and Todd Keister, 2006, Bank runs and investment decisions revisited, *Journal of Monetary Economics* 53, 217–232.
- Gai, P., and S. Kapadia, 2010, Contagion in financial networks, *Proceedings of the Royal Society A: Mathematical, Physical and Engineering Sciences* 466, 2401–2423.
- Gai, Prasanna, Andrew Haldane, and Sujit Kapadia, 2011, Complexity, concentration and contagion, *Journal of Monetary Economics* 58, 453–470.
- Galeotti, Andrea, Sanjeev Goyal, Matthew O. Jackson, Fernando Vega-Redondo, and Leet Yariv, 2009, Network Games, *Review of Economic Studies* 77, 218–244.
- Gao, Jianxi, Baruch Barzel, and Albert-LászlóBarabási, 2016, Universal resilience patterns in complex networks, *Nature* 530, 307–312.
- Glasserman, Paul, and H. Peyton Young, 2016, Contagion in Financial Networks, *Journal of Economic Literature* 54, 779–831.
- Gofman, Michael, 2017, Efficiency and stability of a financial architecture with too-interconnected-to-fail institutions, *Journal of Financial Economics* 124, 113–146.
- Haldane, Andrew G., and Robert M. May, 2011, Systemic risk in banking ecosystems, *Nature* 469, 351–355.
- He, Zhiguo, and Wei Xiong, 2012, Dynamic Debt Runs, *The Review of Financial Studies* 25, 1799–1843.

- Jackson, Matthew O., and Leeat Yariv, 2007, Diffusion of Behavior and Equilibrium Properties in Network Games, *American Economic Review* 97, 92–98.
- Jackson, Matthew O., and Yves Zenou, 2014, Games on networks .
- Kelly, Bryan, Hanno Lustig, and Stijn Van Nieuwerburgh, 2013, Firm Volatility in Granular Networks, Working Paper 19466, National Bureau of Economic Research, DOI: 10.3386/w19466.
- Liu, Xuewen, 2016, Interbank Market Freezes and Creditor Runs, *Review of Financial Studies* 29, 1860–1910.
- Morris, Stephen, and Hyun Song Shin, 1998, Unique equilibrium in a model of self-fulfilling currency attacks, *American Economic Review* 587–597.
- Nash, John Gerard Francis, 2016, *Liquidity Sharing and Financial Contagion*, Ph.D. thesis, University of Chicago.
- Paddrik, Mark E., Haelim Park, and Jessie Jiayu Wang, 2016, Bank networks and systemic risk: Evidence from the national banking acts .
- Sadler, Evan, 2017, Diffusion Games, SSRN Scholarly Paper ID 2624865, Social Science Research Network, Rochester, NY.
- Scott, Hal S., 2016, *Connectedness and Contagion: Protecting the Financial System from Panics* (MIT Press).
- Shin, Hyun Song, 2009, Reflections on Northern Rock: The bank run that heralded the global financial crisis, *The Journal of Economic Perspectives* 23, 101–119.
- Soramäki, Kimmo, Morten L. Bech, Jeffrey Arnold, Robert J. Glass, and Walter E. Beyeler, 2006, Staff Reports .
- Volcker, Paul, 2012, Unfinished Business in Financial Reform, *International Finance* 15, 125–135.